

JAERI-Review

96-004



ANNUAL REPORT OF JMTR, 1994

(April 1, 1994 – March 31, 1995)

March 1996

Department of JMTR Project

日本原子力研究所
Japan Atomic Energy Research Institute

本レポートは、日本原子力研究所が不定期に公刊している研究報告書です。

入手の間合わせは、日本原子力研究所技術情報部情報資料課（〒319-11 茨城県那珂郡東海村）あて、お申し込みください。なお、このほかに財団法人原子力弘済会資料センター（〒319-11 茨城県那珂郡東海村日本原子力研究所内）で複写による実費領布をおこなっております。

This reports are issued irregularly.

Inquiries about availability of the reports should be addressed to Information Division Department of Technical Information, Japan Atomic Energy Research Institute, Tokaimura, Naka-gun, Ibaraki-ken 319-11, Japan.

© Japan Atomic Energy Research Institute, 1996

編集兼発行 日本原子力研究所
印刷 ニッセイエプロ株式会社

Annual Report of JMTR, 1994
(April 1, 1994-March 31, 1995)

Department of JMTR Project

Oarai Research Establishment
Japan Atomic Energy Research Institute
Oarai-machi, Higashiibaraki-gun, Ibaraki-ken

(Received February 6, 1996)

In FY1994, JMTR was in operation during 4 operation cycles with low enriched Uranium(LEU,20%) fuel for irradiation study of nuclear fuels and materials and for radioisotope production.

Irradiation studies were carried out using capsules, Oarai Gas Loop-1(OGL-1), Oarai Shraud Facility(OSF-1) and hydraulic rabbits irradiation facilities in support of LWR, FBR, HTTR and thermonuclear reactor. Irradiation studies on blanket materials were intensively carried out. Power ramping tests were carried out and the future program is under consideration. For R&D works, neutron spectrum evaluation technology, re-instrumentation technique for irradiation fuel rod, remote controlled SEM apparatus and examination technique with miniaturized specimens were successfully developed.

Keywords : JMTR, Annual Report, Research Reactor, Irradiation, Post Irradiation Examination, Reactor Operation, Maintenance

Editorial group of the Annual Report of JMTR

KONDO Ikuo(Chief), NAMIKI Shinji, TSUCHIDA Noboru, YOKOKAWA Makoto,
NIIMI Motoji, SAITO Haruo, USUI Takeshi, ISHIZUKA Etsuo, MITADERA Masayoshi

1994年度 材料試験炉部年報

日本原子力研究所大洗研究所
材料試験炉部

(1996年2月6日受理)

1994年、JMTRは全サイクルに亘って濃縮度20%を下まわる燃料(LEU燃料)のみで運転した。照射試験は、キャプセル、ガスループ(OGL-1)、シュラウド(OSF-1)及びラビットで行い、軽水炉、高速増殖炉、高温ガス炉及び核融合の開発に利用された。水力ラビットを除く照射利用では、大学基礎研究、核融合炉開発、照射技術開発、軽水炉関連、R I生産が各15~20%を占めた。また高温ガス炉、所内基礎研究、高速炉関係が各3~6%であった。技術開発では、照射需要に応じて更に精度を上げるための中性子スペクトル調整法、出力急昇時の燃料ふるまいを解明する目的で中心温度とFPガス圧を共に計測する多重計装等の開発を進めた。核融合ブランケット関連では、中性子増倍材のトリチウム放出挙動その他の解明を進めた。

大洗研究所：〒311-13 茨城県東茨城郡大洗町成田町新堀3607

年報編集委員会

近藤 育朗(委員長)、並木 伸爾、土田 昇、横川 誠、新見 素二、斎藤 春雄、
薄井 洸、石塚 悦男、三田寺 正義

Message from the Director

The Japan Materials Testing Reactor (JMTR) can provide a wide variety of irradiation under controlled environmental conditions. JMTR has been used to perform engineering tests on nuclear fuels and materials and to produce radioisotopes since 1970.


The report contains facility descriptions of JMTR and of the JMTR Hot Laboratory and their activities in FY 1994.

For more than 20 years, JMTR has contributed to R & D as regards nuclear fuels and materials of light water reactor (LWR), High Temperature Engineering Test Reactor (HTTR), fast breeder reactor (FBR) and Advanced Thermal Reactor(ATR). Recently, blanket irradiation tests have been carried out for the International Thermonuclear Experimental Reactor (ITER). Significant progress has been made in the post irradiation examination technique in the Hot Laboratory.

Contributing to the world's nonproliferation, a reduced enrichment program at JAERI had been started since 1979 with close international collaboration. In 1994, JMTR was in operation with fully converted low enriched uranium (LEU, 20%) fuel from medium enriched uranium fuel.

In the Department of JMTR project, irradiation services are widely open to researchers inside JAERI and outside JAERI including overseas. We are willing to further increase our cooperation in sharing our wide experience of irradiation tests with our users and make technological upgrades for R&D regarding irradiation techniques.

November 1995
Department of JMTR project
Director



NIIHO Toshisada

Contents

1. Introduction.....	1
2. Facilities.....	6
2.1 Japan Materials Testing Reactor.....	8
2.2 Irradiation Facilities	16
2.3 Hot Laboratory	26
3. Activities in FY1994.....	36
3.1 Reactor Operation	36
3.2 Irradiations in the Reactor.....	39
3.3 Utilization of Hot Laboratory	44
3.4 Design of Capsules and Irradiation Facilities.....	47
3.5 Technological Development for a Fusion Reactor Blanket	53
3.6 Experimental Study on Advanced Irradiation Field	59
4. R&D and Major Achievements in Recent Years.....	61
4.1 Present Situation and Future Plans for the LWR Fuel Tests.....	61
4.2 Irradiation Effect of Stainless Steel at a High Exposure by Neutrons.....	63
4.3 Re-instrumentation Technique for Irradiated Fuel Rod	69
4.4 Remote Controlled Scanning Electron Microscope(SEM).....	74
4.5 Examination Technology with Miniaturized Specimens	76
4.6 New PIE Facilities for the Fusion Reactor Development.....	78
4.7 Development of High Temperature Shape Memory Alloys.....	82
5. Summary	87
6. Publications.....	88
7. Organization.....	89

目 次

1. 概 要	1
2. 施 設	6
2.1 材料試験炉	8
2.2 照射設備	16
2.3 ホットラボ	26
3. 1994年度の活動	36
3.1 原子炉の運転管理	36
3.2 照射施設の運転管理	39
3.3 ホットラボの運転管理	44
3.4 キャプセル及び照射施設の設計	47
3.5 核融合ブランケットの技術開発	53
3.6 高性能照射場の開発	59
4. 近年の技術開発	61
4.1 軽水炉燃料照射技術	61
4.2 ステンレス鋼の高中性子による照射効果	63
4.3 燃料棒再計装技術	69
4.4 遠隔操作型走査電子顕微鏡	74
4.5 微小試験片技術	76
4.6 核融合ブランケット開発用照射後試験施設	78
4.7 形状記憶合金継手の開発	82
5. まとめ	87
6. 刊行物	88
7. 組 織	89

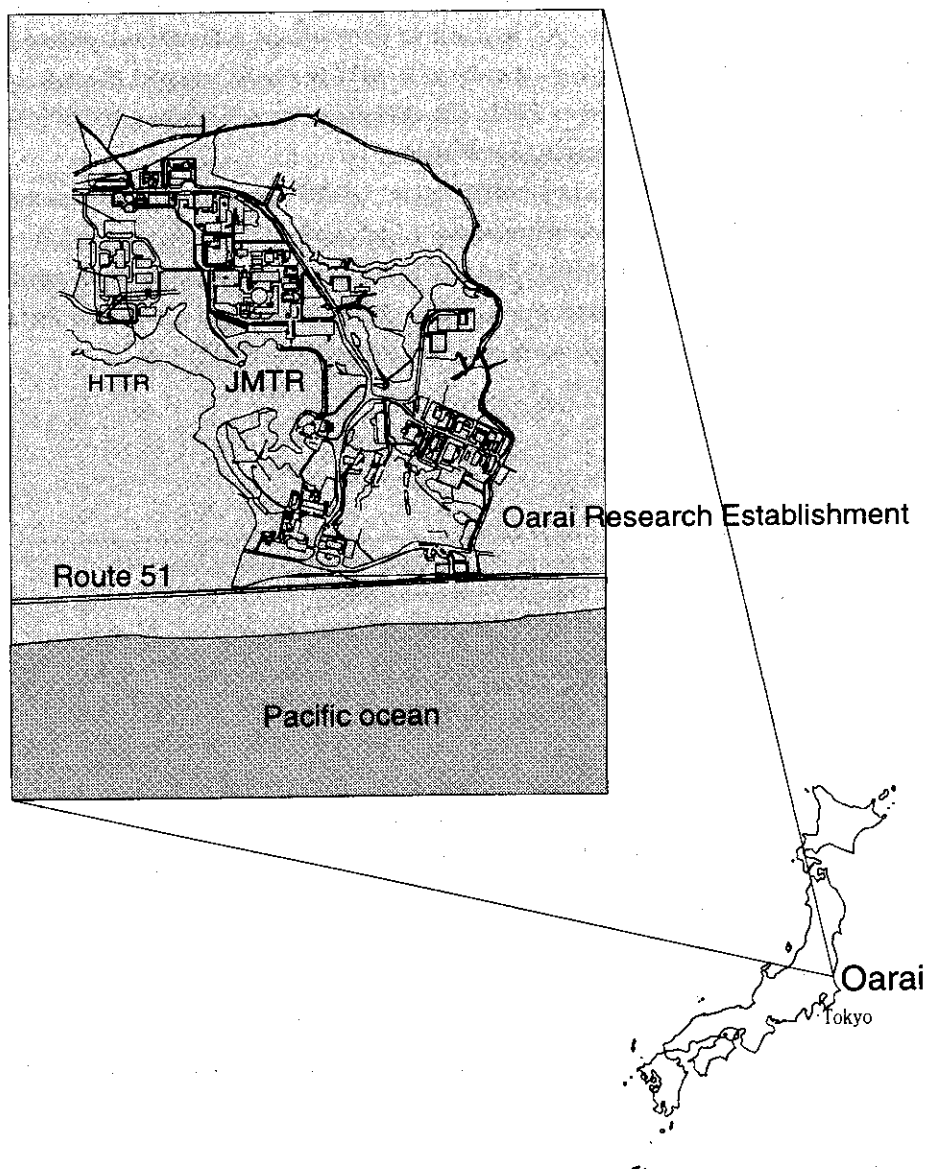
1. Introduction

Location of JMTR

The Japan Materials Testing Reactor (JMTR) is situated in the Oarai Research Establishment, one of the five research establishments of the Japan Atomic Energy Research Institute (JAERI), 100 km north of Tokyo (Fig. 1.1).

In the Oarai Research Establishment, the High-Temperature Engineering Test Reactor (HTTR) is under construction, with initial criticality expected in 1997.

Fig. 1.1
Oarai Research Establishment



Historical Background

In late 1950's, industries requested construction of a material testing reactor for irradiation tests for nuclear fuels and structural materials and for radioisotope production in Japan. The Japan Atomic Energy Commission (JAEC) decided to construct a material testing reactor at JAERI. JAERI started the design study of a material testing reactor in April 1965.

In the design concept, the main characteristics of JMTR were:

- (1) flexibility of the core configuration for irradiation tests, and
- (2) adoption of the proven technology which had long experience in ETR, ORR and other high flux reactors for safety and economical reasons.

The construction of JMTR started in April 1965.

JMTR achieved the first criticality in March 1968. JMTR started the first two operation cycles in December 1969 as a testing program and achieved full power of 50 MW in January 1970. The operation cycle at 30 MW begun in August 1970 and started the 50 MW operation in October 1971. The cumulative power reached 100,000 MWd during the 108th operation cycle in March 1994.

To contribute the world's non-proliferation, JAERI started a reduced enrichment program from 1979 with close international collaboration. The core conversion to the Medium Enriched Uranium (MEU) fuel was fully completed during the 75th operation cycle in July 1986. The core conversion to Low Enriched Uranium (LEU) fuel was fully completed during the 108th operation cycle in January 1994. (Table 1.1)

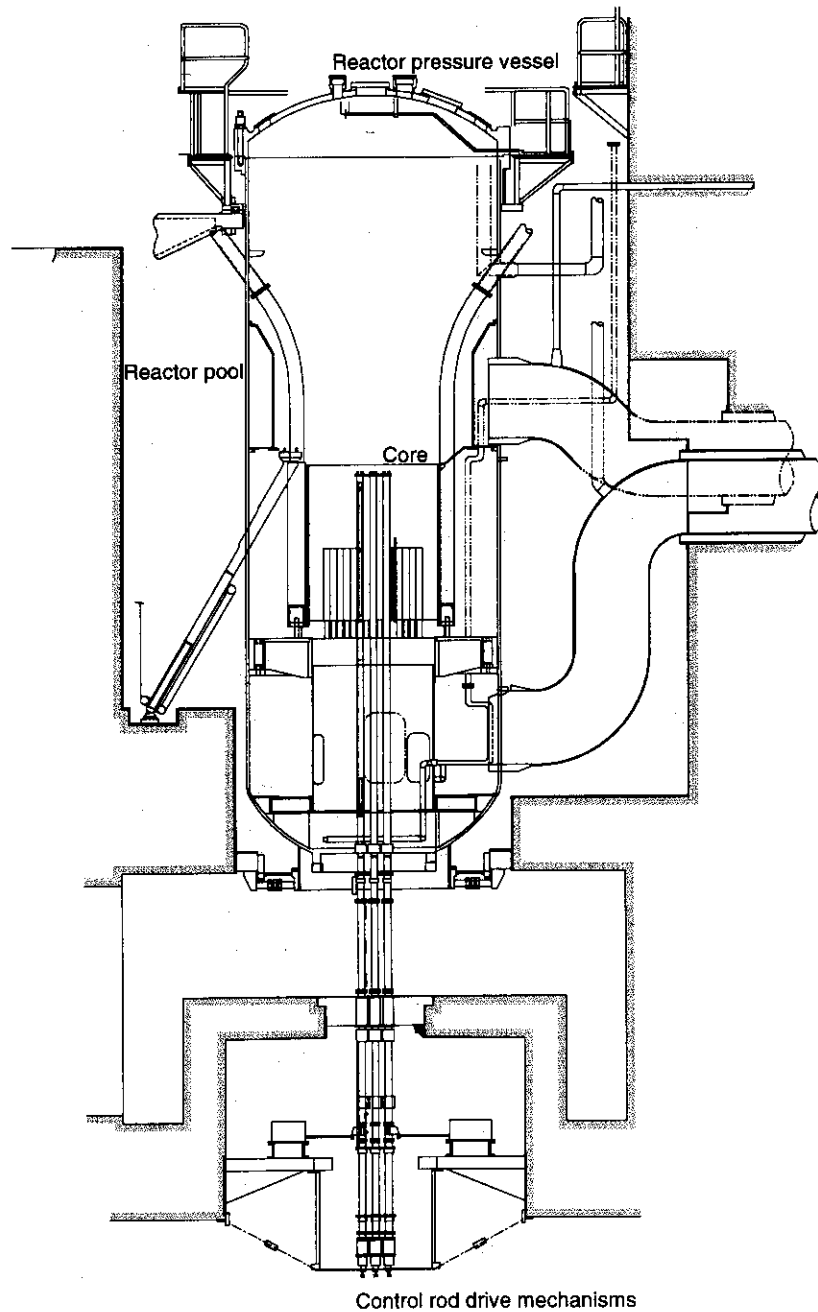
Table 1.1
History of JMTR

Aug.	1963	Construction of JMTR in Oarai was approved by Japan Atomic Energy Commission (JAEC)
Mar.	1967	Construction of the Hot Laboratory
Apr.	1967	Foundation of Oarai Research Establishment
Mar.	1968	JMTR achieved initial criticality
Jan.	1969	Completion of the Hot Laboratory
Apr.	1972	Completion of Oarai Water Loop -2(OWL-2)
Oct.	1972	Completion of Hydraulic Rabbit Irradiation Facility (HR-2)
Jan.	1977	Completion of Oarai Gas Loop (OGL-1)
Jan.	1983	Cumulative power reached 50,000 MWd
Jan.	1984	Completion of Oarai Shroud Irradiation Facility (OSF-1)
Jul.	1986	Enrichment of fuel was reduced to 45 %(MEU)
Jan.	1989	Replacement of OSF-1 in-pile tube of stainless steel with zircaloy tube
Mar.	1992	JMTR achieved 100 operation cycles
Jan.	1994	Enrichment of fuel was reduced to 20 %(LEU)
Mar.	1994	Cumulative power reached 100,000 MWd

Reactor

JMTR is a tank-in-pool type reactor cooled and moderated by light water with thermal power of 50 MW. JMTR operates a regular 26-days cycle and five cycles a year. Figure 1.2 shows a cross-section of the reactor.

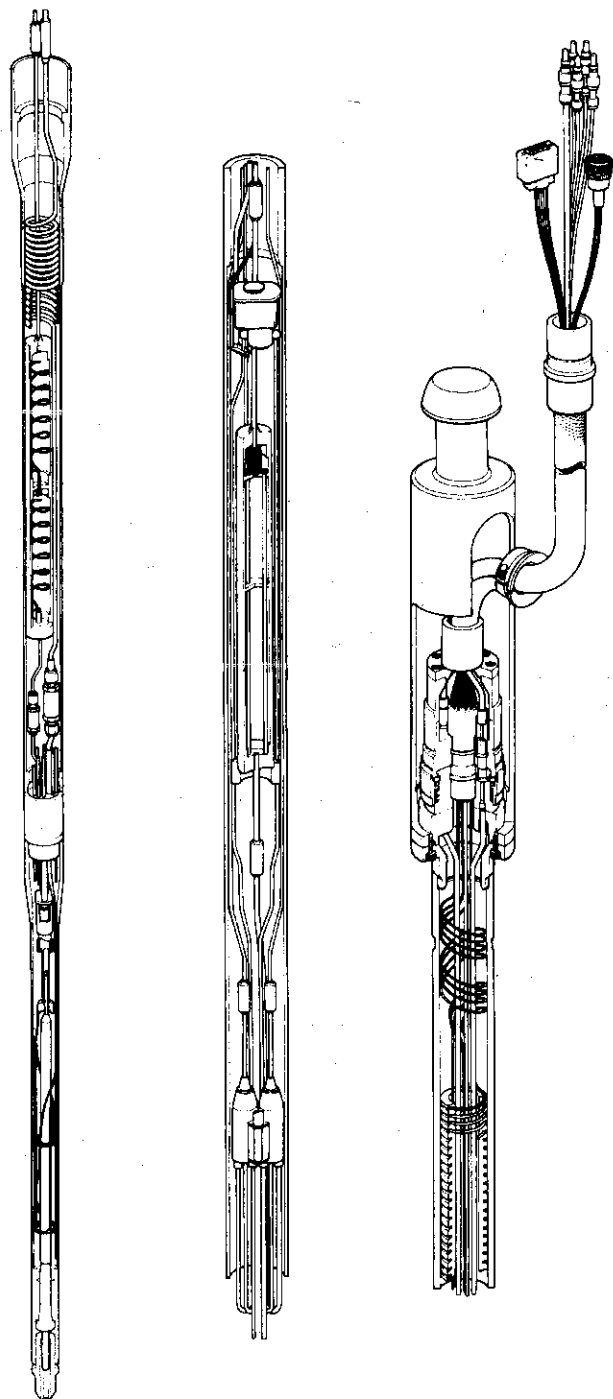
Fig. 1.2
Cross-section of JMTR



Irradiation facilities

To meet the requirements of irradiation test for a fundamental study, development of nuclear fuels and materials and radioisotope production, JMTR is provided with a variety of irradiation facilities such as capsule irradiation facilities (Fig 1.3), hydraulic rabbit irradiation facilities, in-pile loops and a shroud irradiation facility.

Fig. 1.3
Boiling Water Capsule (BOCA)

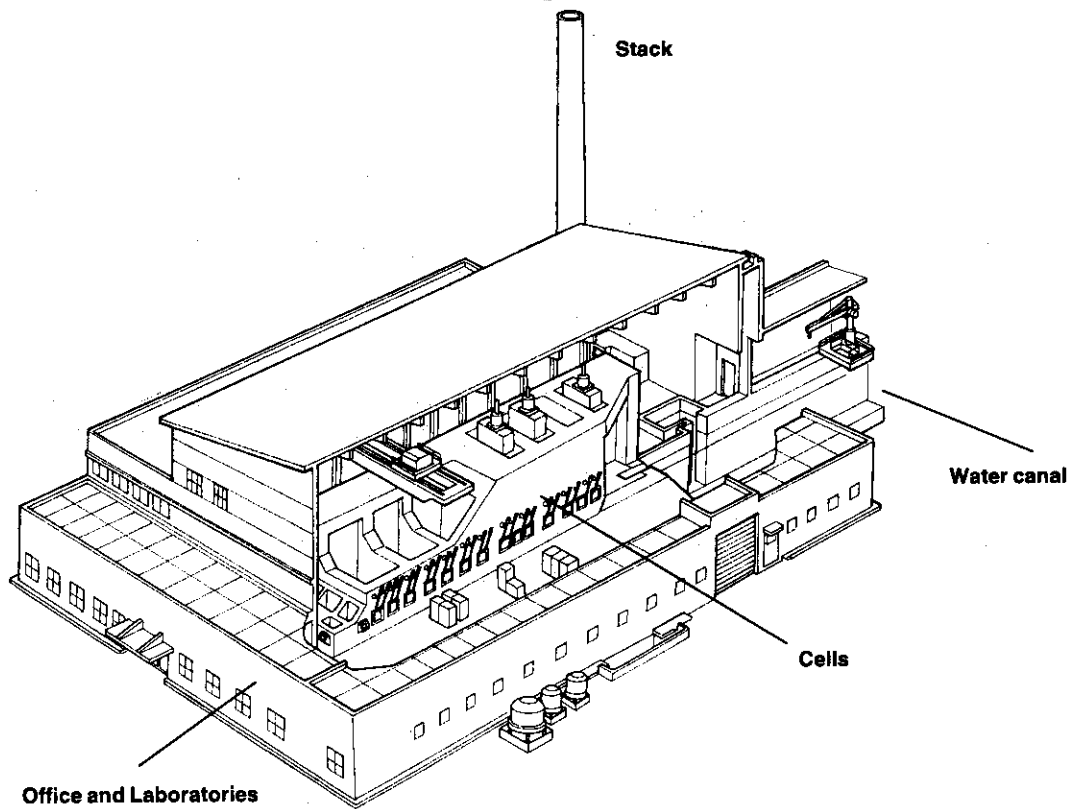


Hot laboratory

Irradiated specimens are transferred to the Hot Laboratory(Fig. 1.4) for post irradiation examination (PIE). The Hot Laboratory is connected to the reactor through water canal.

The Hot laboratory started its construction in 1967 and services in 1971. The steel cells were installed in the Hot Laboratory in 1982.

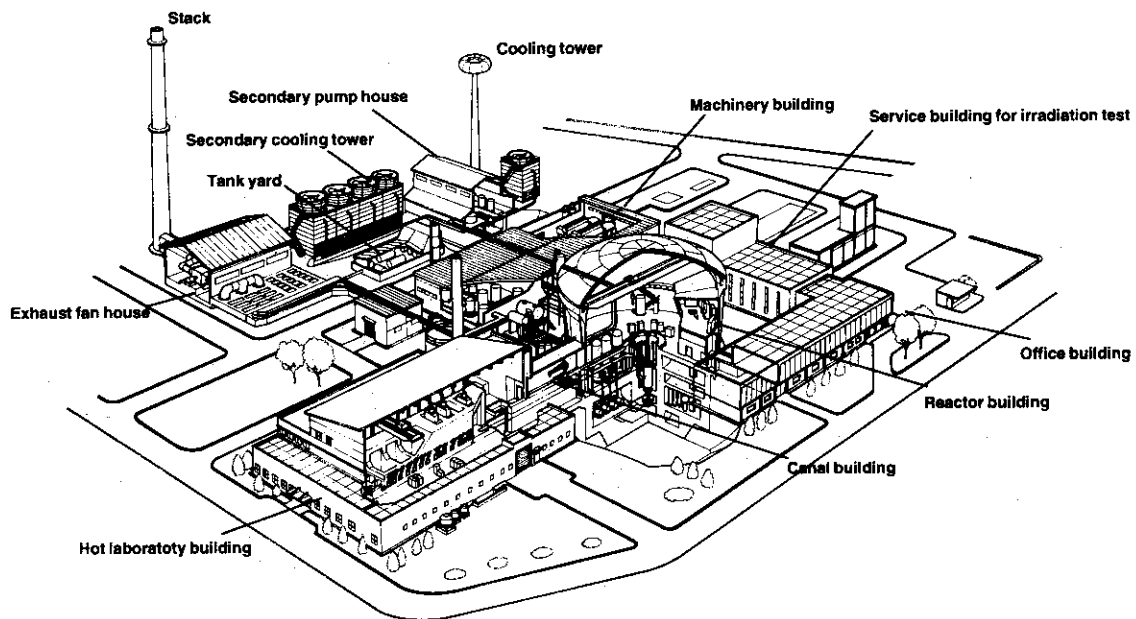
Fig. 1.4
Hot Laboratory building



2. Facilities

JMTR buildings consist of a reactor building, machinery building, secondary pump house, secondary cooling tower, exhaust fan house, tank yard, cooling water tower, stack, service building for irradiation tests, canal building, hot laboratory building and an office building. The buildings are placed around the reactor building in the center (Fig. 2.1).

Fig. 2.1
Arrangement of the buildings

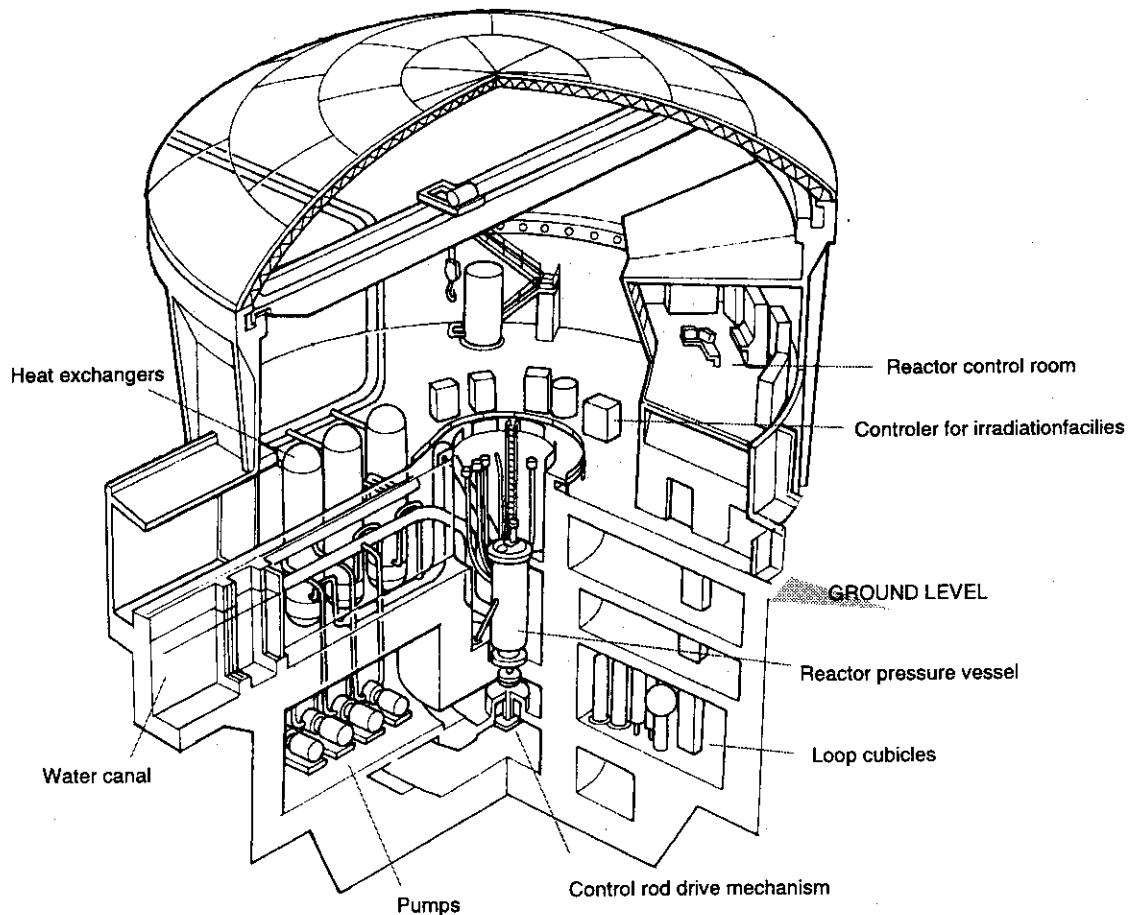


The reactor building is of a reinforced concrete structure. Its dimensions are 41.1 m in diameter 20.4 m in height above grade and 23.5 m deep below the ground level. The reactor is placed in the reactor pool near the center of the reactor building (Fig. 2.2).

The reactor building houses the reactor control room and control room for the irradiation facilities.

The hot laboratory is connected to the reactor building through a water canal. The irradiated specimens are transferred to the hot laboratory without any shielding devices for a post irradiation examination.

Fig. 2.2
Reactor building



2.1. Japan Materials Testing Reactor

JMTR is a multipurpose, material testing, high flux, tank-in-pool type reactor cooled and moderated by light water. The engineering specifications of JMTR are described in Table 2.1.1. The reactor can be seen in Fig. 2.1.1.

Pressure vessel

The pressure vessel, 9.5 m in height, 3 m in diameter and 34 mm thick, is made of stainless steel and is designed to withstand an internal pressure of 1.8 MPa. The pressure

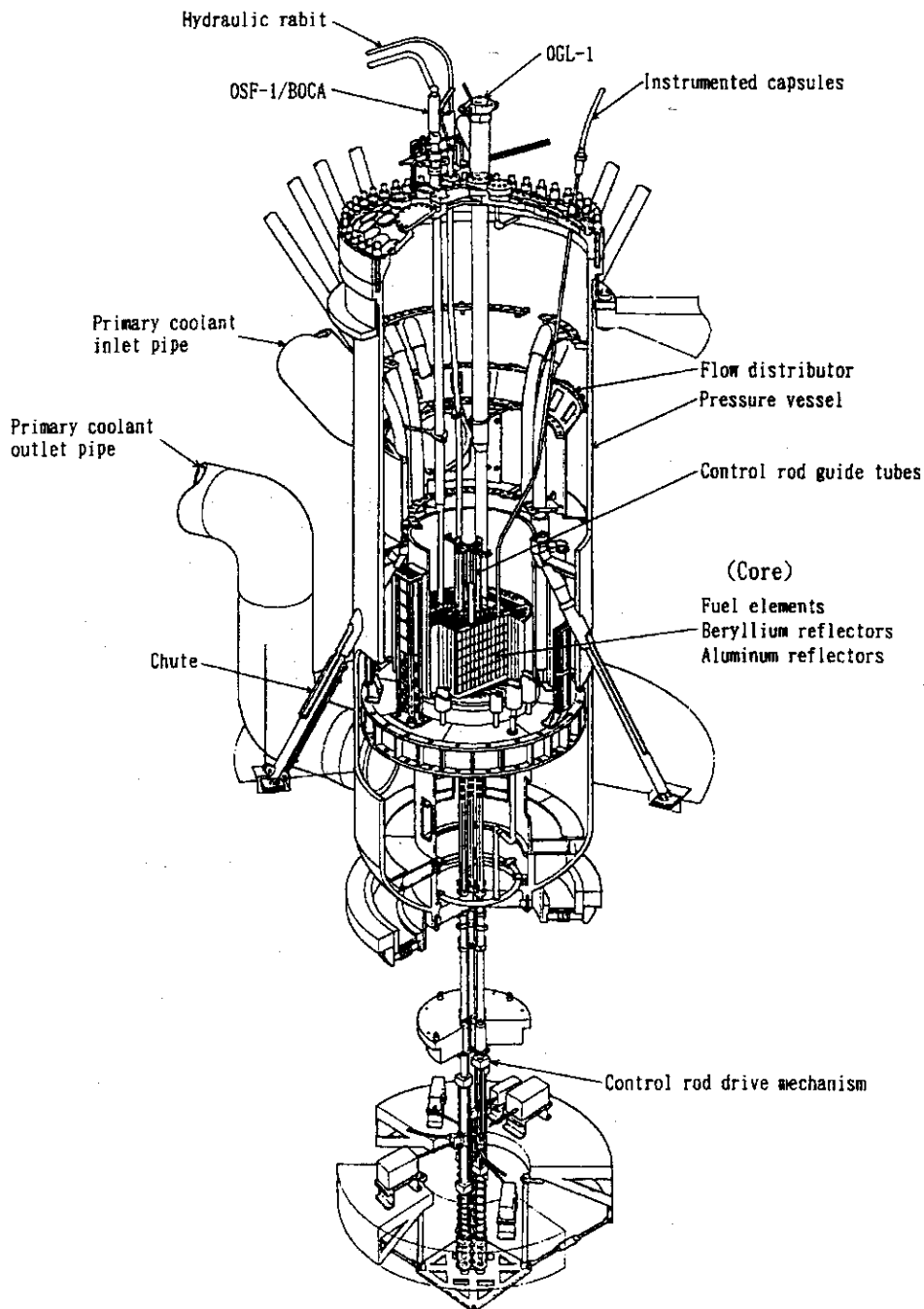


Fig.2.1.1
Reactor

Table 2.1.1
Engineering specifications
of JMTR

Thermal power		50 [MW]			
Neutron flux	Fuel region	$\phi_{th}(<0.68\text{eV})$ $\phi_f(>1\text{MeV})$	Max. 4×10^{14} [n/(cm ² -s)] Max. 4×10^{14} [n/(cm ² -s)]		
	Reflector region	$\phi_{th}(<0.68\text{eV})$ $\phi_f(>1\text{MeV})$	Max. 4×10^{14} [n/(cm ² -s)] Max. 1×10^{14} [n/(cm ² -s)]		
Power density	Core average	Approx. 500 [kW/t]			
	Average heat flux	120 [W/cm ²]			
Pressure vessel	Material	Stainless steel			
	Height	9.5 [m]			
	Diameter	3 [m]			
	Thickness	34 [mm]			
Core	Structure material	Stainless steel			
	Effective height	750 [mm]			
	Equivalent diameter	416 [mm]			
	Core loading (²³⁵ U)	Max. 11 [kg]			
Core component Fuel	Core loaded number	Standard fuel element	22	Fuel follower	5
		Type	Flat	Flat	
	Dimension	76.2 × 1,200 [mm]		63.6 × 890 [mm]	
	Fuel plate	Number	19 per element	16 per element	
		Thickness	1.27 [mm]	1.27 [mm]	
		Length	778 [mm]	769 [mm]	
		Cladding thickness	0.38 [mm]	0.38 [mm]	
		Cladding material	Aluminum alloy	Aluminum alloy	
		Thickness	0.51 [mm]	0.51 [mm]	
		Length	780 [mm]	750 [mm]	
	Meat	Width	61.6 [mm]	49.7 [mm]	
	²³⁵ U Content	Per element	Approx. 410 [g]	Approx. 275 [g]	
	Enrichment		Approx. 20 [%]	Approx. 20 [%]	
	Burnable absorber	Number of Cadmium wires	18 (φ0.3)	16 (φ0.3)	
	Burn up		Max. 50 [%]	Max. 50 [%]	
Control rod	Type	Top entry bottom mounted with follower			
	Number	5			
	Absorber	Material	Hafnium		
Dimension		63.5 X 800 [mm]			
Reflector	Material	Reflector element	Beryllium Aluminum		
		H-shaped frame	Beryllium		
	Grid plate	Material	Stainless steel		
Reactivity effect	Max. Excess reactivity	15 [%Δk/k]			
	Shutdown margin	≤ 0.9 [Keff]			
Primary coolant	Inlet temperature	Max. 49 [°C]			
	Outlet temperature	Approx. 56 [°C]			
	Fuel surface temp	Max. 186 [°C]			
	Fuel channel velocity	10 [m/s]			
	Fuel channel flow rate	125 [m ³ /h]			
	Total flow rate	6,000 [m ³ /h]			
	Core inlet pressure	1.4 [MPa]			
Differential pressure between inlet/outlet	0.32 [MPa]				

vessel is installed in the reactor pool which is 13 m in depth. The pressure vessel contains the reactor core, irradiation facilities ,etc. The top closure head of the pressure vessel provides many nozzles for in-pile loops, instrumented capsule irradiation facilities and hydraulic rabbit irradiation facilities. Two chutes are attached on the side wall of the pressure vessel to remove the spent fuel and reflectors from the core to the reactor pool. The primary coolant, entering through the primary coolant inlet pipe, flows downwards through the reactor core for heat removal, passes the lower plenum and exits through the primary coolant outlet pipe.

Reactor core

The reactor core, 1,560 mm in diameter and 750 mm in effective height, is made up fuel elements, control rods, reflectors and an H-shaped beryllium frame as shown in Fig.2.1.2. The H-shaped beryllium frame separates the core into four regions. The reactor core consists of a 204 lattice position, 77.2 mm square each, arranged in a square matrix. The 22 standard fuel elements and 5 control rods are loaded in the lattice positions.

The H-shaped beryllium frame and beryllium and aluminum elements are equipped with irradiation holes. The irradiation holes are filled with solid plugs of the same material as the elements when they are not loaded with the capsules.

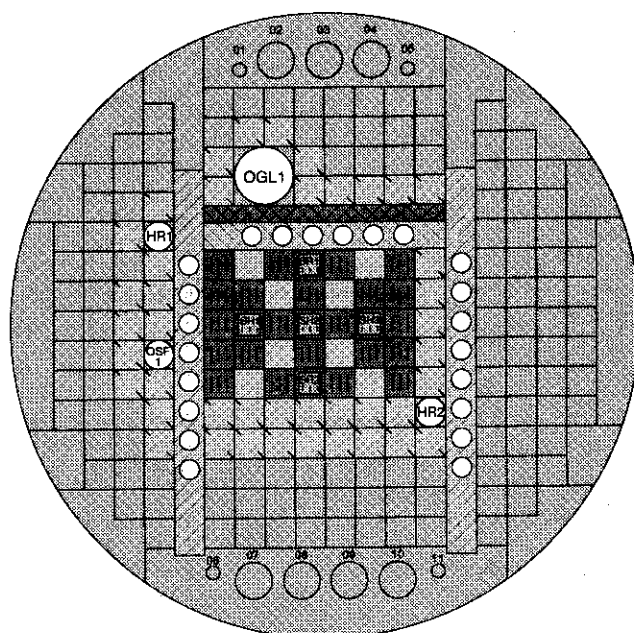








Fig. 2.1.2
Core configuration

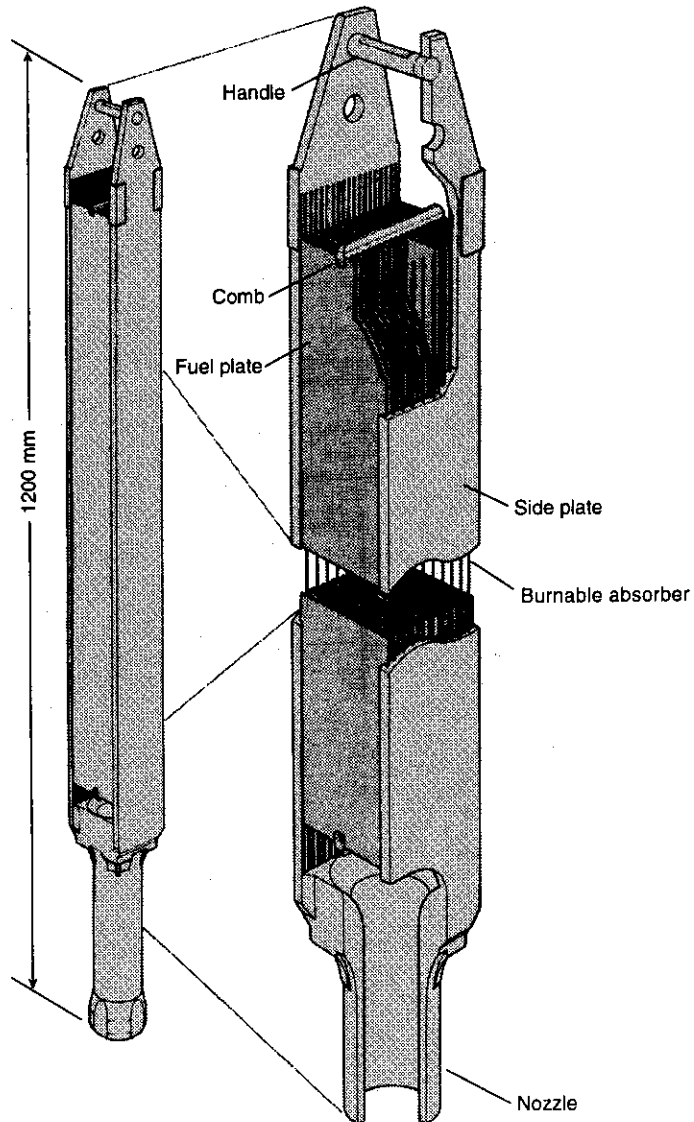
-  Fuel element
-  Beryllium reflector
-  Beryllium frame
-  Control rod with fuel follower
-  Aluminum holder
-  Gamma ray shield plate

Fuel elements

The fuel elements are of the modified ETR type with flat-plate assemblies. They are classified into standard fuel elements and fuel followers.

Each standard fuel element consists of 19 fuel plates which are 1.27 mm thick, 70.5 mm wide, and 780 mm long (Fig.2.1.3). The fuel plates are attached to the aluminum alloy side plates using a "roll-swagging" technique. Cadmium wires clad with aluminum as burnable absorbers are inserted into grooves where fuel plates are attached. A fuel plate consists of a layer of uranium-silicon-aluminum fuel (U_3Si_2-Al), 0.5 mm thick, which is covered with aluminum cladding.

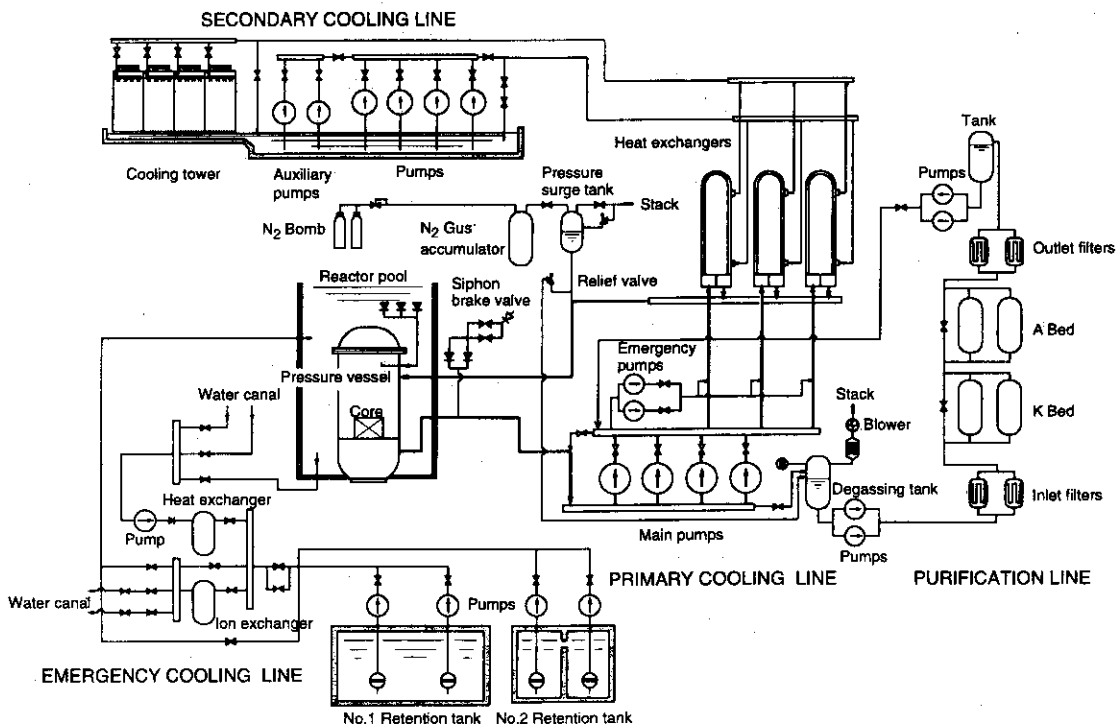
Fig. 2.1.3
A fuel element
(standard element)



Cooling systems

The diagram of the reactor cooling system is shown in Fig.2.1.4. The primary cooling system consists of 4 main pumps, 2 emergency pumps, an emergency cooling system and 3 heat exchangers. The three main pumps and an emergency pump operate during the normal operation. For abnormal reactor conditions such as LOCA and coast down of the primary coolant flow, one of the main pumps and the emergency pump powered by a diesel engine generator operate for decay heat removal. The coolant flows downward through the reactor core at the flow rate of 6,000 m³/h. Maximum coolant inlet temperature is 49°C and the corresponding outlet temperature is 56°C. The generated reactor heat is transferred to the secondary coolant in the heat exchangers and is dissipated into the atmosphere by way of the cooling tower. (Table 2.1.1)

**Fig. 2.1.4
Cooling systems**



Instrumentation and control system

The nuclear instrumentation consists of start-up, log-power and liner-power systems. Each system consists of 3 channels. Mean value of the 3 channels is used for controlling and for measuring nuclear power level and period. The trip signals are taken through the 2-out-of-3 circuits.

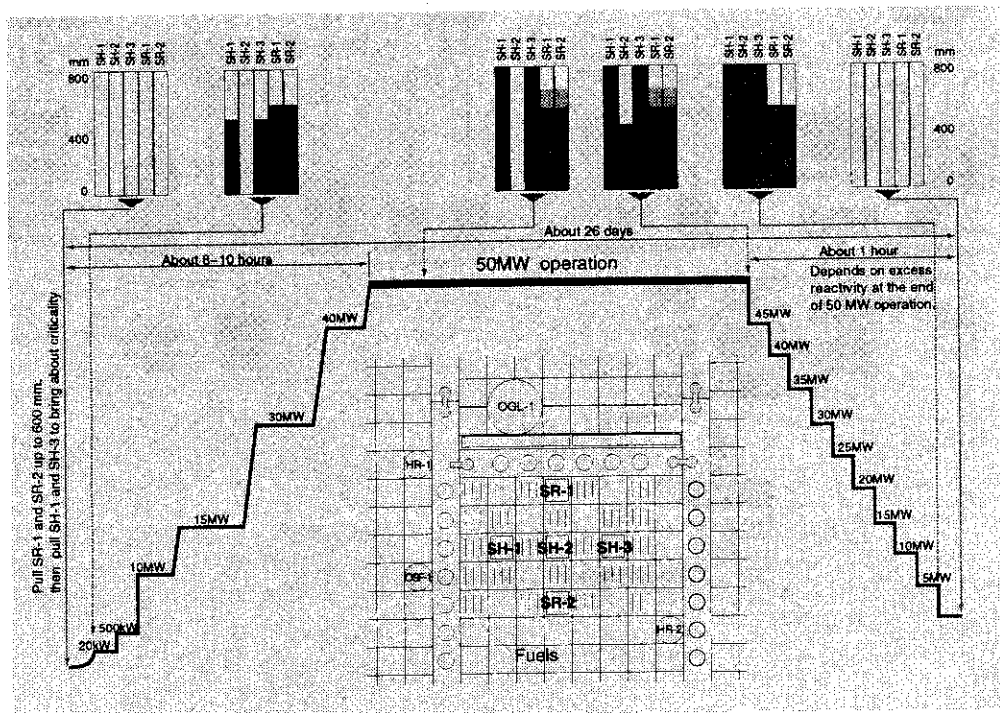
There are 5 control rods: 3 are used for shim control and the other 2 are used for regulating. One of the regulating control rods is used for automatic control of the reactor power.

Each rod consists of a box-type hafnium absorber and a fuel follower under the hafnium absorber. The drive mechanisms are installed on the bottom of the pressure vessel. The control rods are moved vertically along the guide tubes. When a control rod is withdrawn upwards, the fuel follower moves upwards in the core displacing the hafnium absorber of the control rod.

Operation procedure

Operation procedure of the reactor is shown in Fig.2.1.5. It takes about 8 hr from the start-up to the 50 MW full power. The reactor power is increased stepwise up to 50 MW with safety of the reactor facilities and irradiation experiments constantly being checked.

Fig. 2.1.5
Operation pattern and position of control rods during operation



Operation support system: ARGUS

Two computer systems are developed to support the operation of the reactor and of the irradiation facilities. ARGUS is the computer system of the reactor and has the following functions:

- (1) monitoring the state of the feedback control circuits
- (2) logging the major process data and indicating trend
- (3) checking the data over/under limited value
- (4) displaying the result of monitoring sequence control under abnormal conditions
- (5) making of diagnosis unusual status and indicating the results
- (6) indicating operation guidance

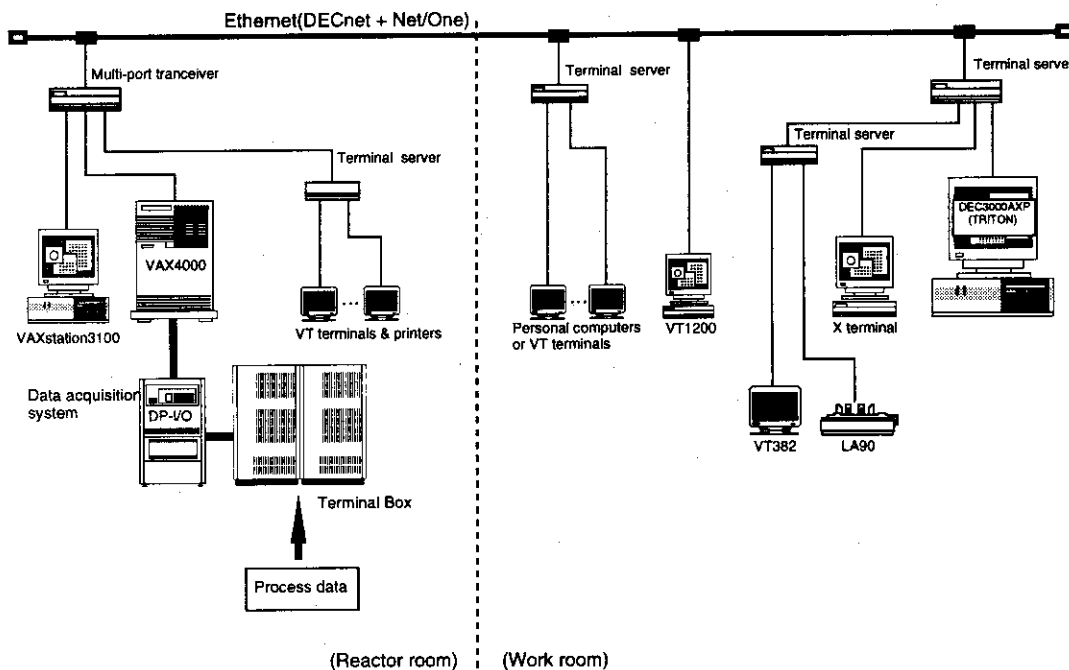
ARGUS is also used for the following calculations.

- (1) calculation of neutron fluence and irradiation deformation of core components
- (2) calculation of volume of the primary coolant leakage
- (3) calculation of possible restart time after a scram

The schematic diagram of ARGUS is shown in Fig. 2.1.6.

The support system of the irradiation facilities(LOOCAS, IDASS) is described in Chapter 2.2.

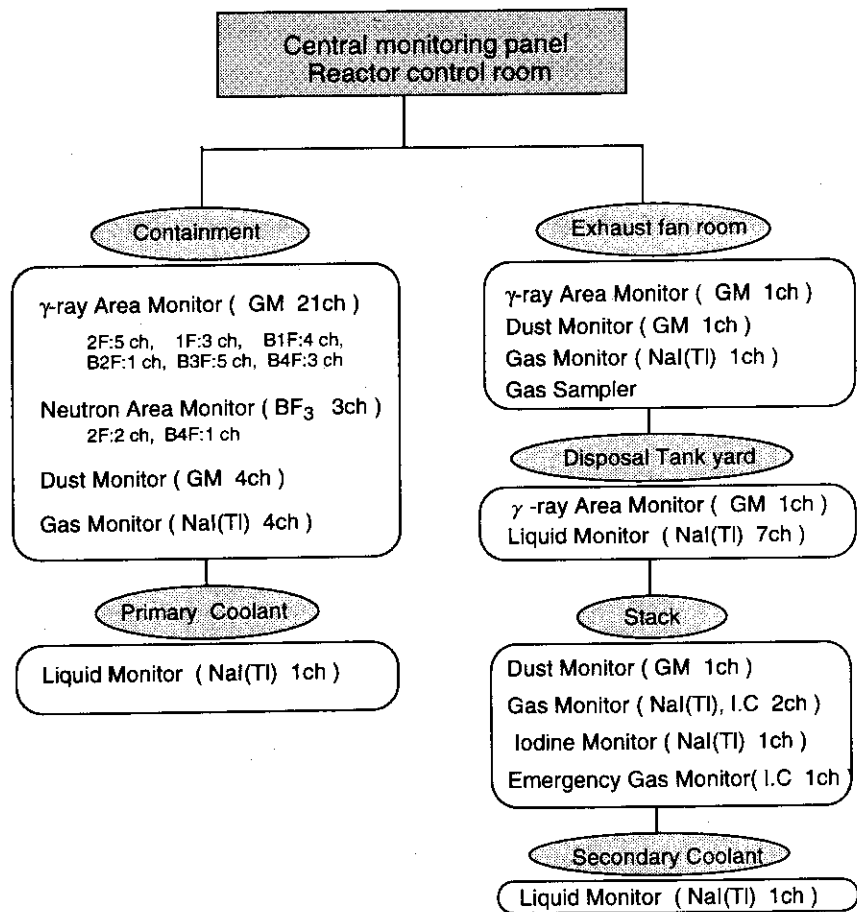
**Fig. 2.1.6
Operation Support
system: ARGUS**



Radiation monitoring system

Radiation monitoring in JMTR is carried out continuously through the radiation monitoring systems as shown in Fig. 2.1.7. The central monitoring panel of this system is located in the reactor control room at JMTR.

Fig. 2.1.7
Radiation monitoring system



2.2. Irradiation Facilities

JMTR provides a wide variety of irradiation facilities for irradiation tests of nuclear fuels and materials and radioisotope production.

The capsules are inserted into suitable irradiation holes in the reactor core according to the required irradiation conditions. The two Hydraulic Rabbit irradiation facilities (HR-1 and 2), the Oarai Gas Loop-1 irradiation facilities (OGL-1) and the power ramping test facility are installed into fixed position in the reactor core.

The Oarai Water Loop-1 and 2 (OWL-1,2) and the Neutron Control Facility (NCF) have completed their irradiation tests and were removed.

Capsule irradiation facilities

The capsule irradiation facilities are installed for a irradiation tests of nuclear fuels and materials and radioisotope production. The capsules are classified into three types:

- (1) non-instrumented capsule,
- (2) instrumented capsule, and
- (3) advanced capsule.

The capsules are cooled by a reactor primary coolant. Up to 60 capsules can be loaded in the reactor core, of which 20 capsules are instrumented capsules. The characteristics of the capsules can be seen in Table 2.2. 1. The types of the capsules are shown in Fig. 2.2.1 and Table 2.2.2.

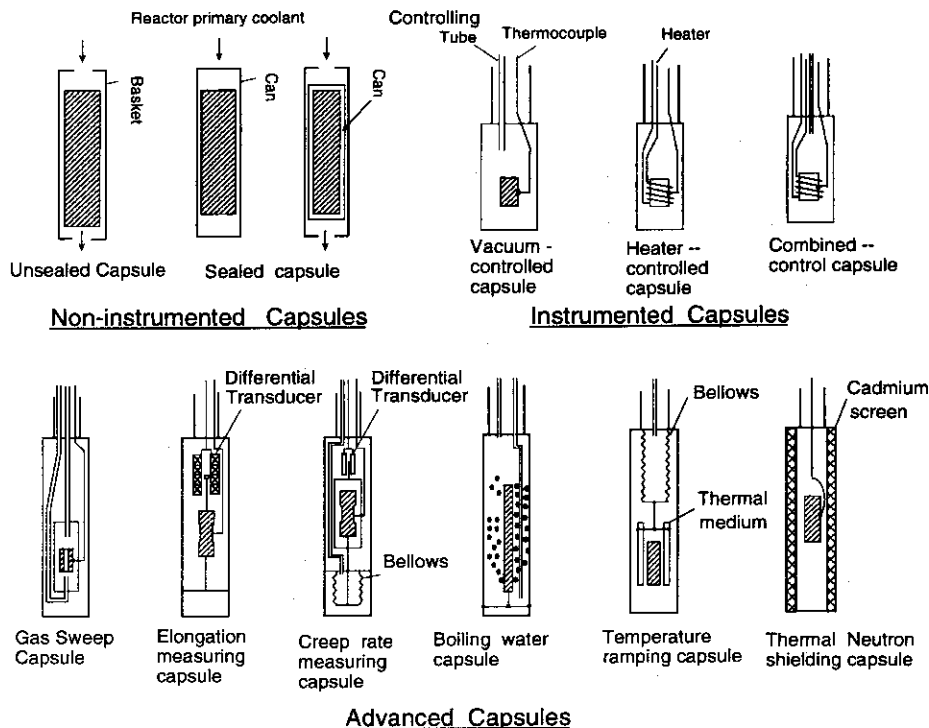


Fig. 2.2.1
Capsule structure

Table 2.2.1
Characteristics of
capsule irradiation facilities

Thermal neutron flux	$1.0 \times 10^{13} \sim 3.0 \times 10^{14} \text{ n}/(\text{cm}^2 \cdot \text{s})$
Fast neutron flux (>1MeV)	$1.0 \times 10^{13} \sim 2.0 \times 10^{14} \text{ n}/(\text{cm}^2 \cdot \text{s})$
γ heat rate	0.5 ~ 10 W/g
Heat generation	Max. 100 kW

Table 2.2.2
Types of Capsules

Types of capsule	Structure and function
Non-instrumented Capsule	
Unsealed capsule	Test specimens are held in an open-type basket, and are directly cooled by the reactor primary coolant.
Sealed capsule	Test specimens are contained in a sealed vessel and cooled by the reactor primary coolant.
Instrumented Capsule	
Non-control capsule	Temperature of test specimens is not controlled. The temperature and/or neutron fluence around the specimens are measured by thermocouples and self-powered neutron detectors (SPND) or fluence monitors (FM).
Vacuum-control capsule	Temperature of test specimens is controlled by adjusting the thermal conductivity which depends on helium gas pressure between the inner and outer vessels.
Heater-control capsule	Temperature of test specimens is controlled by electric heaters wound around the specimens.
Combined-control capsule	Temperature of test specimens is controlled by combination of the vacuum-control and the heater-control which have been mentioned above.
Advanced capsule	
Fission gas sweep capsule	This capsule is designed for measuring the activity of FP gas released from coated particle fuels for HTTR fuel. FP gas is swept out to the sweep gas measuring equipment by carrier gas.
Elongation measuring capsule	Elongation of the specimen is measured by a differential transducer or a helium gas micrometer.
Creep rate measuring capsule	Test specimens are stressed by pressurized bellows and its creep rate is measured by a differential transducer.
Boiling water capsule	Surface temperature of specimens is controlled by the pressure of boiling water which surrounds the test specimens.
Temperature ramping capsule	The temperature of test specimens is rapidly increased by removing the solid thermal medium which has high thermal conductivity and surrounds the test specimens.
Thermal neutron shielding capsule.	Test specimens are surrounded by a thermal neutron absorber such as cadmium or hafnium for cutting thermal neutrons.

(1) *Non-instrumented capsules*

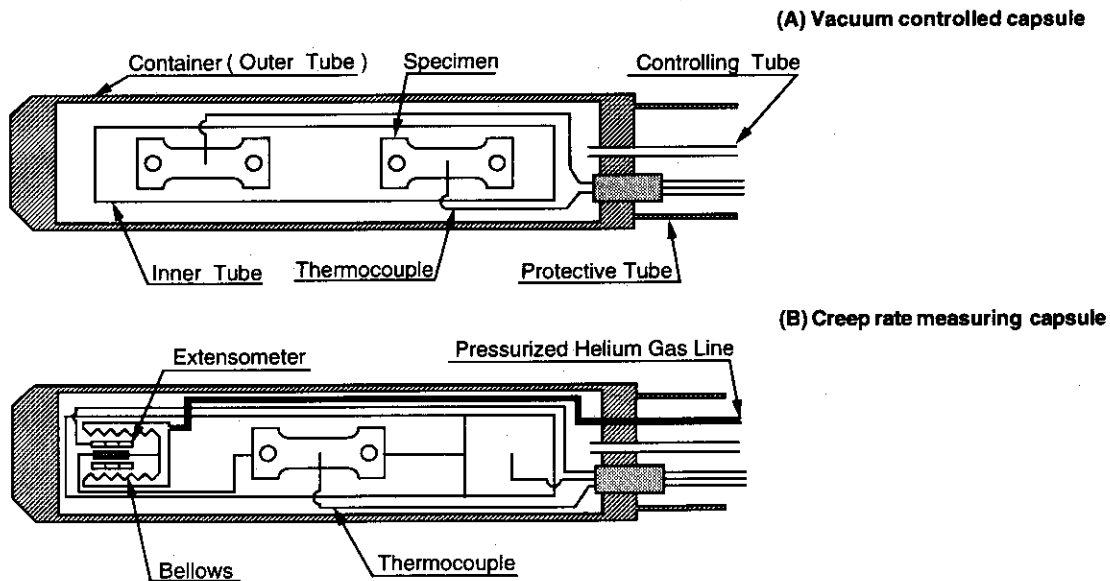
In an unsealed capsule, the reactor primary coolant flows between specimens and the outer tube. In a sealed capsule, specimens are held in an aluminum or stainless steel can.

(2) *Instrumented capsule irradiation facilities*

An instrumented capsule irradiation facility can measure and control temperature of specimens and pressure. The instrumented capsule irradiation facility consists of a capsule, a protective tube, a guide tube, a connection box and a control panel. The structure of a typical instrumented capsule is shown in Fig. 2.2.2(A).

The control system is shown in Fig. 2.2.3. The capsule consists of a container (outer tube) which is made of stainless steel, an inner tube for holding specimens, a protective tube and a guide tube including the vacuum control tubes and instrument cables. The guide tube is joined to the connection box around the reactor pool. The vacuum control

Fig. 2.2.2
Vacuum-controlled capsule
and creep rate capsule



tubes and the instrument cables are joined to the control panel through the connection box.

To control the temperature of a specimen during irradiation, three methods are available.

1) Vacuum-controlled method

Thermal conductivity is altered by changing the helium gas pressure between the inner and outer tubes in a capsule so as to control temperature. The helium gas pressure in the annular space is controlled from 1.33×10^2 to 1.37×10^5 Pa. In this method, the one of the measuring points in the capsule is controlled.

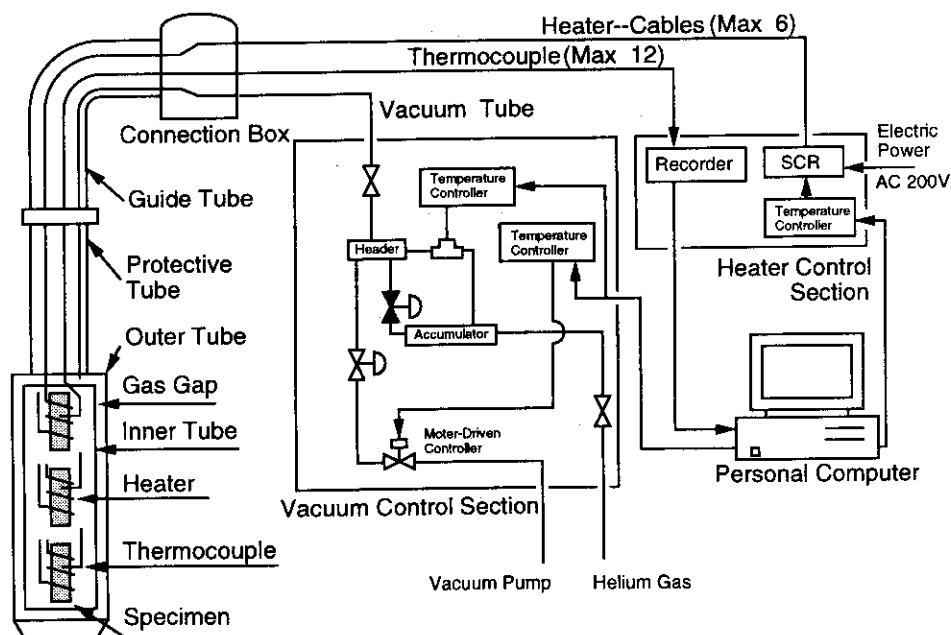
2) Heater-controlled method

The temperature of specimens is individually controlled by electric heaters around specimens.

3) Combined-control method

The temperature of the specimen is controlled using the combination of the two methods mentioned above. This method is available for fine control of the temperature of the specimen.

Fig. 2.2.3
Capsule control system



(3) Advanced capsule irradiation facilities

Due to required irradiation conditions, advanced capsules have been developed.(Fig. 2.2.1 and Table 2.2.2)

The specifications and system for the Fission Gas Sweep (FGS) capsule as a representative of advanced capsules are shown in Table 2.2.3 and Fig. 2.2.4.

Table 2.2.3
Characteristics of Fission Gas Sweep Capsule

Type of fuel	Coated particle fuel
Diameter of coated particle fuel	Approx. 920 μm
Amount of ²³⁵ U	Max. 6 g
Thermal neutron flux	1.0 x 10 ¹³ ~ 3.0 x 10 ¹⁴ n/(cm ² ·s)
Fast neutron flux (>1MeV)	1.0 x 10 ¹² ~ 2.0 x 10 ¹⁴ n/(cm ² ·s)
Heat generation	Max. 41.2 kW
Temperature of the specimen	Max. 1600 °C
Flow rate of helium gas	Max. 1 l/min
Pressure of helium gas	Max. 0.3 MPa

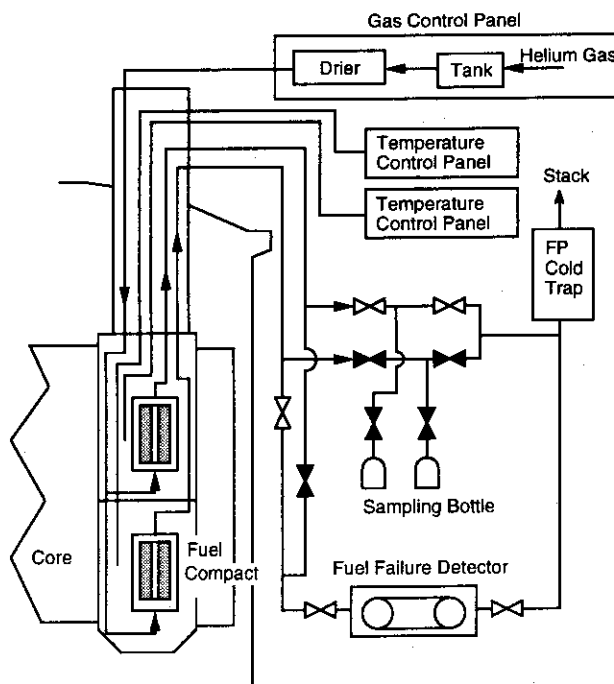


Fig. 2.2.4
Fission Gas Sweep Capsule

Hydraulic rabbit irradiation facilities

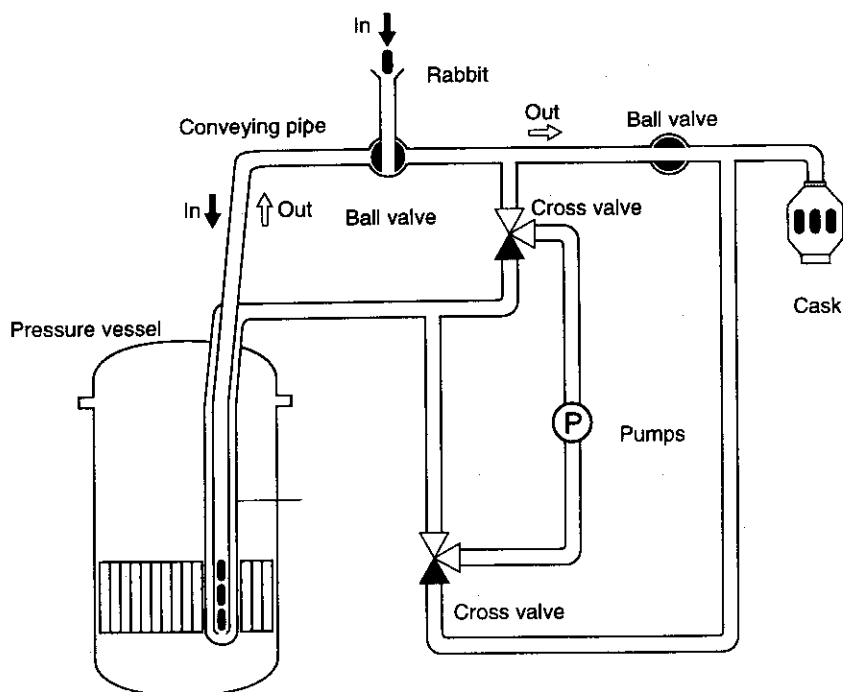
Two hydraulic rabbit irradiation facilities (HR-1 and HR-2) have been installed for short-term irradiation for radioisotope production and fundamental research. A diagram of the facilities is shown in Fig. 2.2.5. The major specifications are shown in Table 2.2.4.

The specimen is put in a holder which is called rabbit. Each facility consists of an in-pile tube, two pumps, a loading station and an unloading station. The rabbit can be transferred into the reactor core and be withdrawn from the core during reactor operation by changing the direction of the cooling water.

Table 2.2.4
Major specifications of two Hydraulic rabbit irradiation facilities

	HR-1	HR-2
Location in the core	D - 5	M - 11
Thermal neutron flux	$1.1 \times 10^{14} \text{ n}/(\text{cm}^2 \cdot \text{s})$	$1.3 \times 10^{14} \text{ n}/(\text{cm}^2 \cdot \text{s})$
Fast neutron flux (>1MeV)	$8.8 \times 10^{12} \text{ n}/(\text{cm}^2 \cdot \text{s})$	$2.1 \times 10^{13} \text{ n}/(\text{cm}^2 \cdot \text{s})$
γ heat rate	1.1 W/g	2.2 W/g
Coolant	Light Water	Light Water
Temperature of the coolant	Max. 50 °C	Max. 50 °C
Pressure of the coolant	Max. 2.0 M Pa	Max. 2.0 M Pa
Flow rate of the coolant	11.0 m ³ /h	8.4 m ³ /h
Dimension of the holder	$\phi 32 \times 150 \text{ mm}$	$\phi 32 \times 150 \text{ mm}$
Dimension of the specimen	$\phi 26 \times 120 \text{ mm}$	$\phi 26 \times 120 \text{ mm}$
Number of charged rabbits	Max. 3	Max. 3
Time of irradiation	Min. 1 min	Min. 1 min

Fig. 2.2.5
Hydraulic rabbit irradiation facility



OGL-1 irradiation facility

The OGL-1 irradiation facility was installed for the irradiation test of coated particle fuels, heat-resisting metals and graphite materials for HTTR. When fuels are irradiated in the in-pile tube, the average outlet temperature of cooling gas of the specimen is designed up to 1000°C. OGL-1 consists of a primary cooling system, a secondary cooling system and a coolant purification system. The diagram of OGL-1 can be seen in Fig. 2.2.6. Major specifications are shown in Table 2.2.5.

Helium gas is used in the primary cooling system as the same coolant as in HTTR. Primary cooling system consists of an in-pile tube, two gas circulators, a heater and a heat exchanger.

The coolant in the secondary cooling system is air. The secondary cooling system consists of a secondary heat exchanger, two air blowers and dampers.

The coolant purification system consists of a pre-charcoal trap, a molecular sieve trap, a cold charcoal trap and a titanium sponge trap. The gas in the coolant purification system flows from the outlet of the gas circulator and then flows into the inlet of the gas circulator for purification of the primary coolant gas and for measurement of the impurities.

Table 2.2.5
Major specifications of OGL-1

Location in the core	G,H-3,4
Thermal neutron flux	Max. 5.5×10^{13} n/(cm ² ·s)
Fast neutron flux (>1MeV)	Max. 1.1×10^{13} n/(cm ² ·s)
γ heat rate	Max. 1.0 W/g
Flow rate of the coolant	6 kg/min.
Temperature of the coolant	Max. 1000 °C
Pressure of the coolant	3.0 MPa
Dimensions of a fuel rod	φ 82x750 mm
Heat generation	Max. 135 kW

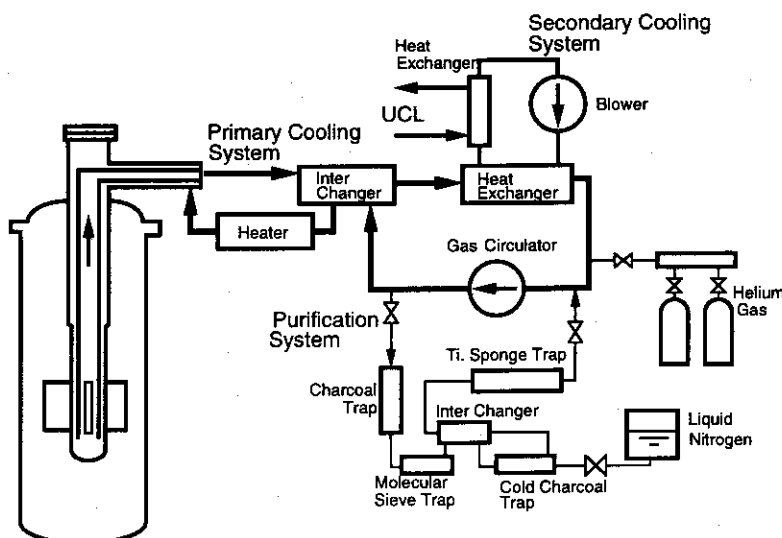


Fig. 2.2.6
Oarai Gas Loop-1 (OGL-1)

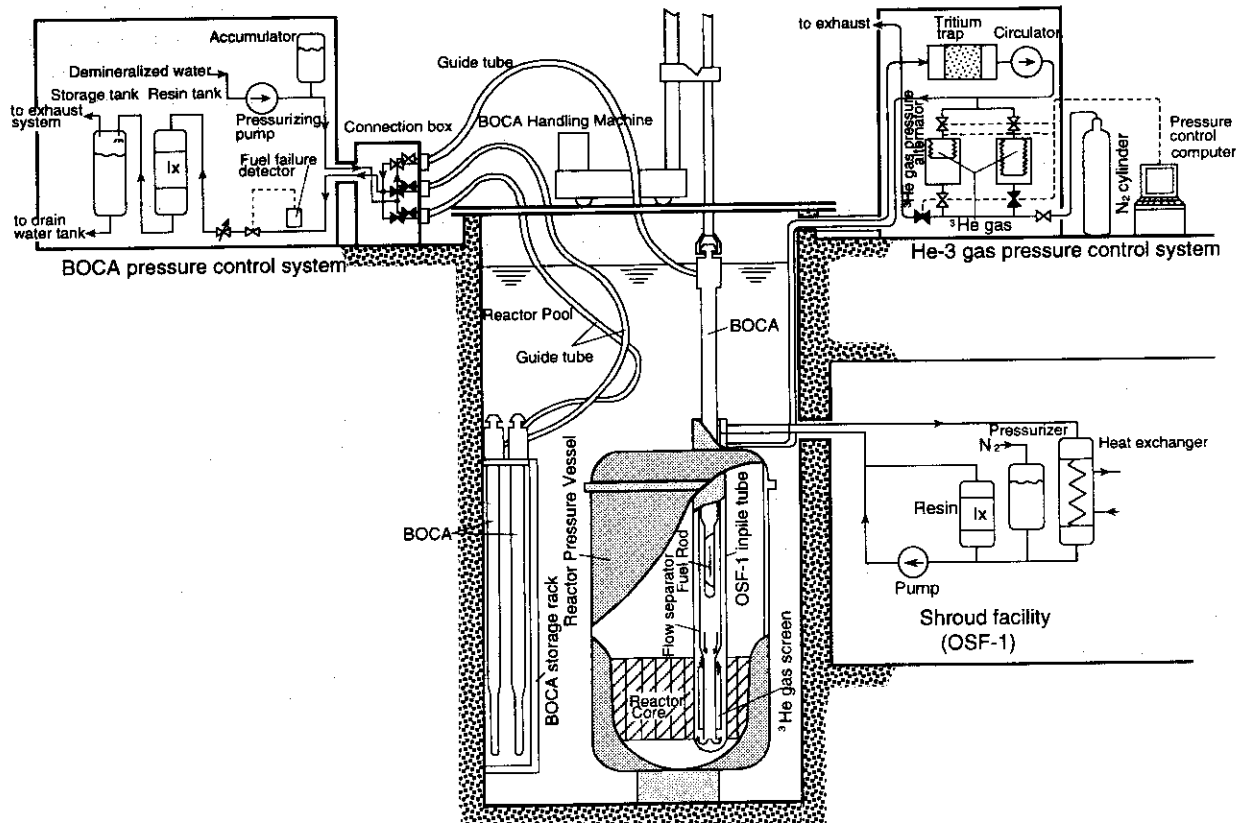
Power ramping test facility

The power ramping test facility consists of Boiling Water Capsules (BOCA), the Oarai Shroud Facility-1 (OSF-1), a pressure control system, a He-3 gas pressure control system and a BOCA handling machine. These are shown in Fig.2.2.7. Major specifications are shown in Table 2.2.6.

Table 2.2.6
Major specifications of
the power ramping test facility

BOCA	Coolant	Light water
	Press. of the coolant	7.3 MPa
	Flow rate of the coolant	1.0 cm ³ /sec
	Linear heat rate	Max. 60 kW/m
	Thermal neutron flux	Max. 2.6 x 10 ¹⁴ n/(cm ² ·s)
	Fast neutron flux (>1MeV)	Max. 2.2 x 10 ¹³ n/(cm ² ·s)
OSF-1	Location in the core	D-9
	Coolant	Light water
	Pressure of the coolant	0.4 MPa
	Flow rate of the coolant	1.9 m ³ /h
	Temp. of the coolant	Max. 90 °C
	γ heat rate	Max. 2.5 W/g

Fig. 2.2.7
Power ramping test facility



The BOCA with a fuel rod to be tested is connected to the BOCA pressure control system through a connection box, and water surrounding the fuel rod is pressurized at 7.3 MPa. Four BOCA's are connected to the box, and, of these, a BOCA is inserted into the in-pile tube of the OSF-1 by a BOCA handling machine.

The BOCA is a stainless steel, cylindrical tube, 800 cm long and 6.9 cm in maximum diameter. Its inside structure is shown in Fig. 2.2.8.

The cylindrical in-pile tube of the OSF-1 has an opening on the top of the pressure vessel through which a BOCA is inserted into the reactor core. The OSF-1 allows a BOCA to be replaced with another one while the reactor is in operation.

OSF-1 has a cooling system to remove heat generated out of BOCA and the heat is estimated using a calorimetric method by calculating from temperature difference between the inlet and outlet of the coolant and from its flow rate. At the reactor core zone of the in-pile tube, an aluminium cylindrical He-3 gas screen is installed. The thermal power of a fuel rod is altered by changing the gas pressure with the He-3 gas pressure control system. The relation of the He-3 pressure, linear heat rate of a fuel rod and surface temperature of a fuel rod can be seen in Fig. 2.2.9.

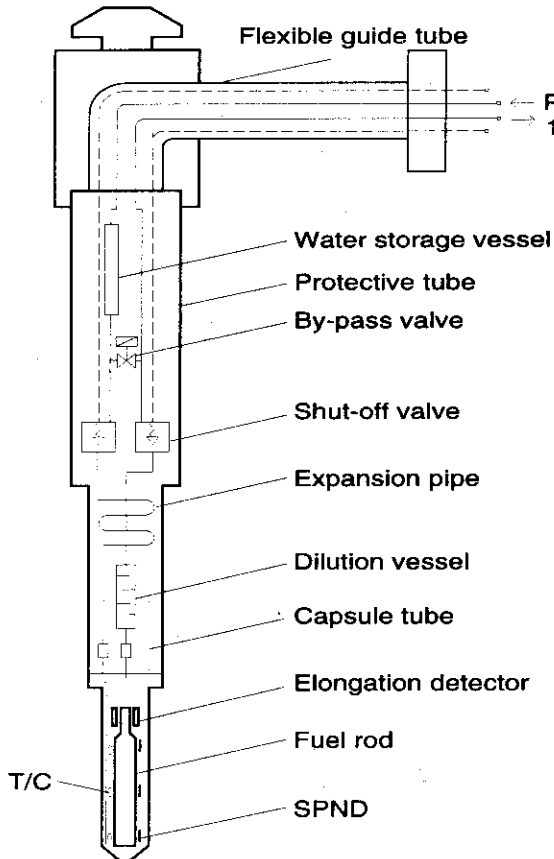
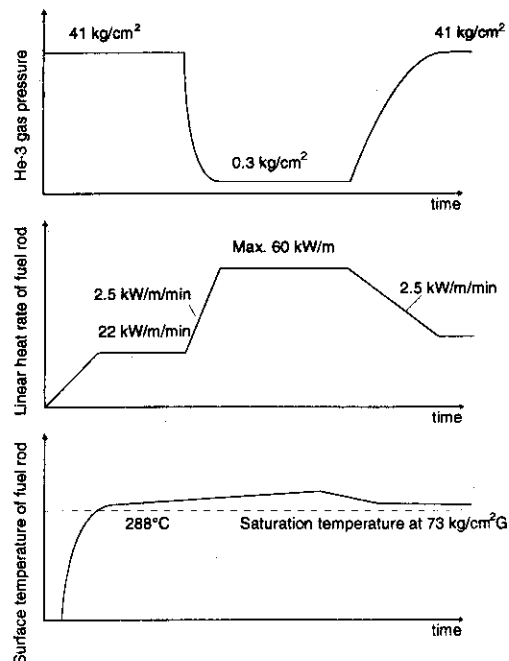


Fig. 2.2.8 (left)
Boiling water capsule
(BOCA)

Fig. 2.2.9(Lower right)
Relation of the He-3 pressure,
linear heat rate of a fuel rod
and surface temperature of a
fuel rod



Data acquisition system: LOOCAS

The data acquisition system monitors the operation data of all the irradiation facilities and collects irradiation data. A schematic drawing of the data acquisition system is shown in Fig. 2.2.10.

The data acquisition system is connected to all irradiation facilities and the reactor to obtain many important signals and monitor the state of all the irradiation facilities.

The system acquires a lot of data of the specimens irradiated in the core, for example, temperatures and pressures. The acquired data in the system are saved at intervals of 10 sec, 3 min and 30 min according to the nature of the data. The irradiation reports are printed out in table form and plotted in graphical form using the data acquisition system and are offered to customers.

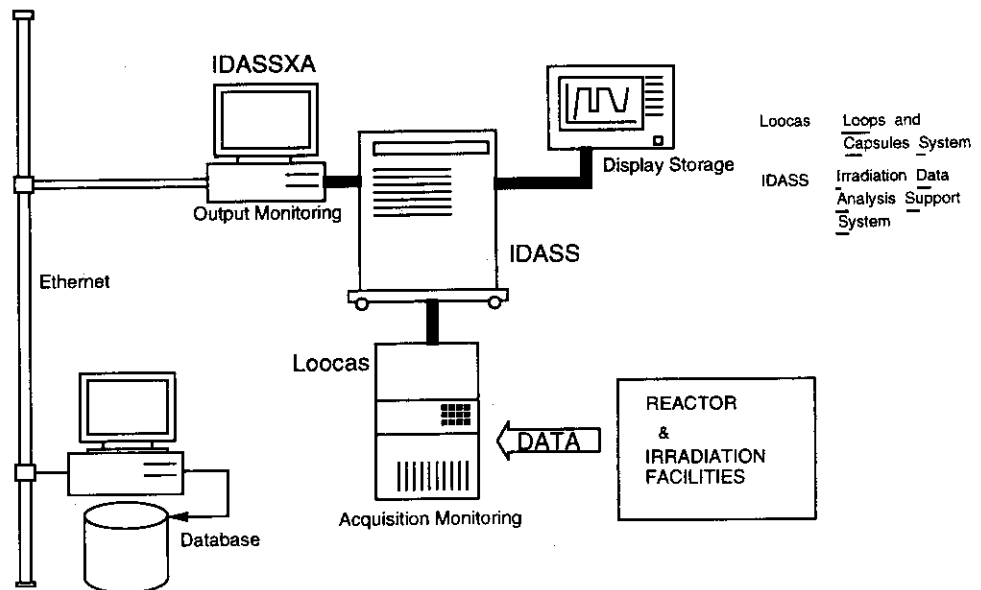
Removed irradiation facilities

OWL-1 was installed as an experimental irradiation facility for testing fuels and structural materials of BWR and of PWR. The OWL-2 was built for the irradiation tests of fuels and materials for PWR, BWR and Advanced Thermal Reactor (ATR). The irradiation facilities can simulate PWR, BWR or ATR conditions.

NCF was constructed to control the total neutron flux or the temperature of a specimen by moving the capsule vertically.

These irradiation facilities were removed after completion of the irradiation tests.

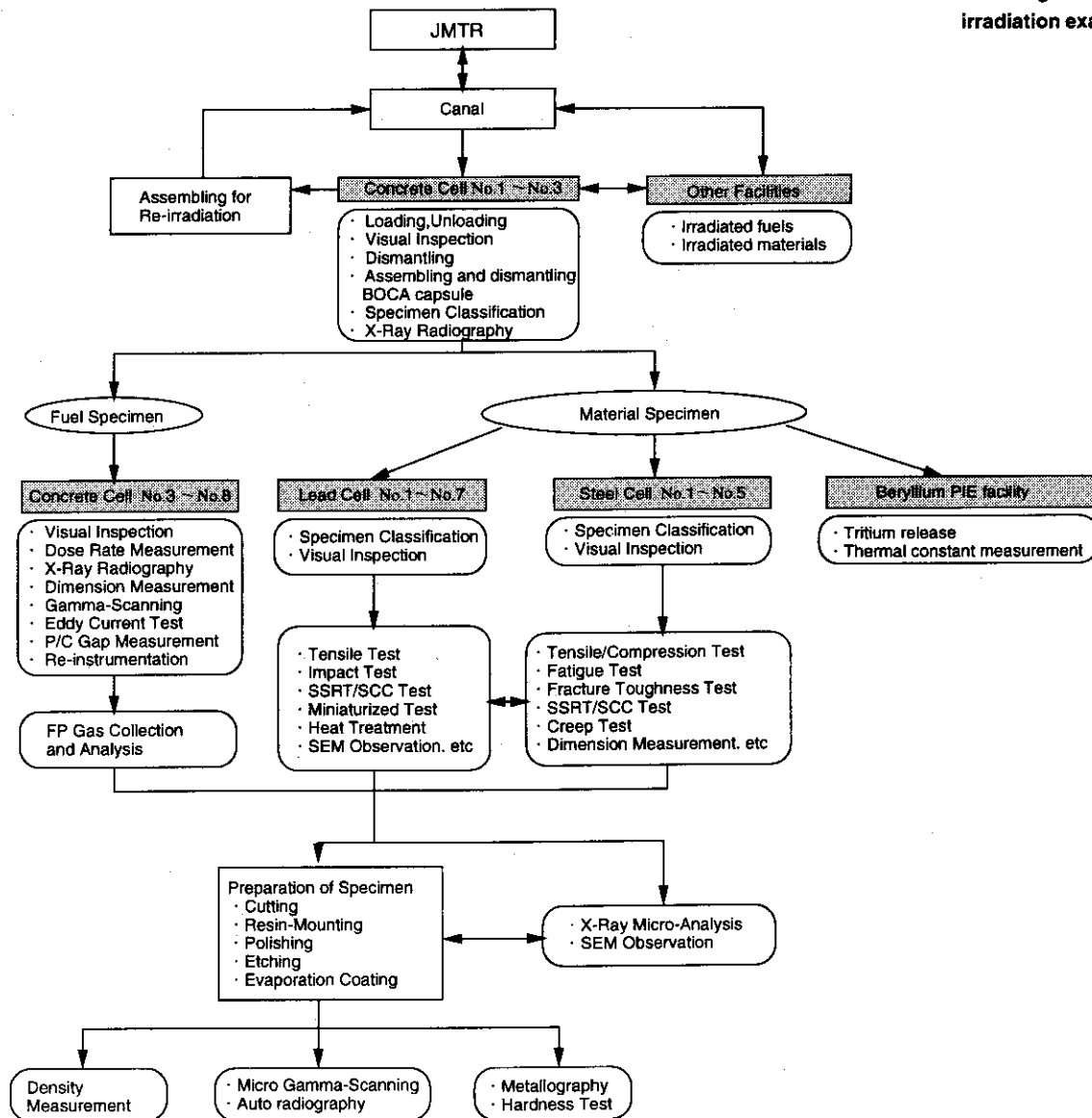
Fig. 2.2.10
Data acquisition system



2.3. Hot Laboratory

The Hot Laboratory provides the data for post irradiation examinations (PIE) on irradiated fuels and materials in JMTR and other reactors. Concrete cells, lead cells and steel cells are installed in the Hot Laboratory. After preparatory work for the post irradiation examination in the C-1 through C-3 cells of the concrete cells, nondestructive examinations and destructive examinations for irradiated fuel specimens are carried out in the concrete cells. A mechanical property test on irradiated material specimens are carried out in the lead cells and steel cells. A flow diagram of the post irradiation examinations in the Hot Laboratory is shown in Fig. 2.3.1.

Fig. 2.3.1
Flow diagram of a post irradiation examination



Arrangement of Hot Laboratory

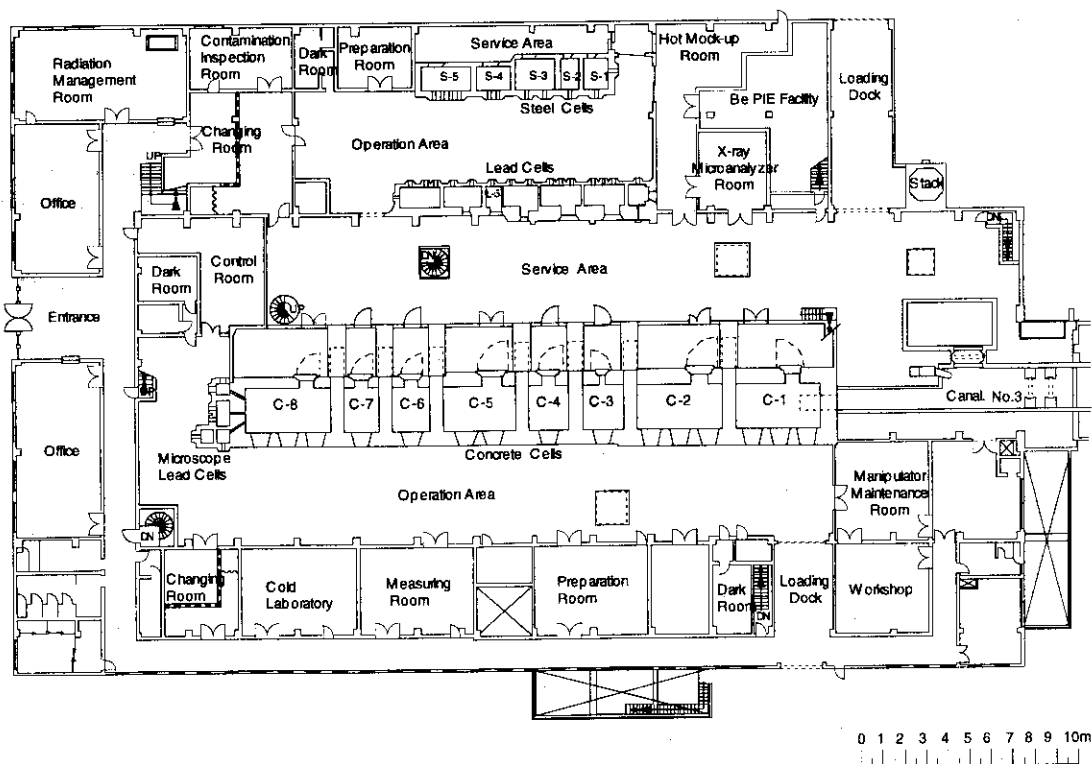
The Hot Laboratory is connected to JMTR through a water canal to transfer irradiated capsules from JMTR and to JMTR for re-irradiation. The building houses the concrete cells with the microscope lead cells, lead cells and steel cells. Each cell is designed as β - γ cell. Figure 2.3.2 shows the ground floor of the Hot Laboratory. Auxiliary facilities such as the ventilation system, the power supply system and the liquid waste disposal system are located in the basement.

Concrete cells and microscope lead cell

The concrete cells consist of 8 concrete cells and 4 microscope lead cells. The following work can be carried out in the concrete cells:

- (1) loading and unloading capsules
- (2) dismantling the irradiated capsules
- (3) re-capsuling
- (4) re-instrumentations of the specimens
- (5) nondestructive examinations of the fuel specimens
- (6) destructive examinations of the fuel specimens

Fig. 2.3.2
Hot Laboratory



The maximum length of the fuel specimens is about 1 m. The irradiated capsules in JMTR are transferred into the C-1 cell from the canal after cooling. The irradiated capsules in the other reactors are transported by the transport casks and are loaded into the C-1 cell through the posting port installed on the ceiling. The re-instrumentations of the fuel specimens are carried out in the C-7 cell, then the re-instrumented fuel specimens are loaded into the Boiling Water Capsule (BOCA) in the C-1 cell.

In the concrete cells, the following items of post irradiation examination are carried out:

(1) for nondestructive examination (NDE);

visual inspection, X-ray radiography, dimensional measurement, gamma scanning, eddy current test, pellet/ cladding (P/C) gap measurement

(2) for destructive examination (DE);

fission gas collection and analysis, density measurement of fuel specimens and specimen preparation for metallography .

Metallography, hardness measurements, autoradiography and micro-gamma scanning for fuels and materials are carried out in the microscope lead cells attached to the concrete cells. Preparatory work for composition analysis and fractography with the X-ray Micro-Analyzer (XMA) installed in another room are carried out in the concrete cells.

The wall of the concrete cells is constructed of the high-density magnetite concrete and its thickness is 1 m or 1.1 m. The shielding windows (dry-type) with an equivalent shield thickness to the wall are installed on the wall. In the microscope lead cells, lead bricks with a thickness of 17.8 cm and shield windows were built on the wall. Table 2.3.1 shows the specifications of the concrete cells and the microscope lead cells. Figure 2.3.3

Table 2.3.1
Specifications of concrete cells
and microscope lead cells

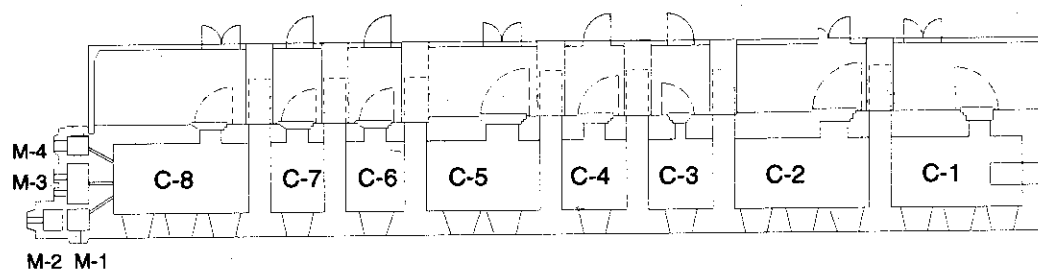
Cell No.	Inside dimension	Shielding wall		Number of windows	Maximum activity (1MeV)
	W x D x H	thickness	density		
C-1	6 x 3 x 5.5 m	1.1 m	>3.8	3	33 pBq
C-2	6 x 3 x 5.5 m	1.1 m	>3.8	3	33 pBq
C-3	3 x 3 x 5.5 m	1.0 m	>3.8	1	3.7 pBq
C-4	3 x 3 x 4.5 m	1.0 m	>3.8	1	1.1 pBq
C-5	5 x 3 x 4.5 m	1.0 m	>3.8	2	1.1 pBq
C-6	2.5 x 3 x 4.5 m	1.0 m	>3.1	1	85 TBq
C-7	2.5 x 3 x 4.5 m	1.0 m	>3.1	1	85 TBq
C-8	6 x 3 x 5.5 m	1.0 m	>3.1	3	85 TBq

(A) Concrete cells

Cell No.	Inside dimension	Shielding wall	Number of windows	Maximum activity (1MeV)
	W x D x H	thickness		
M-1	1 x 1 x 1.1 m	17.8 cm	1	3.7 TBq
M-2	1 x 0.85 x 1.1 m	17.8 cm	1	3.7 TBq
M-3	1.59 x 1 x 1.1 m	17.8 cm	2	3.7 TBq
M-4	1.5 x 1 x 0.95 m	17.8 cm	2	3.7 TBq

(B) Microscope lead cells

Fig. 2.3.3
Functions and major apparatuses
of the concrete cells



Cell no.	Functions	Main Apparatuses & specifications	Cell no.	Functions	Main Apparatuses & specifications
C-1	Lifting up irradiated capsules from water canal Irradiated specimens loading and unloading BOCA capsule assembling and dismantling Visual inspection Dose measurement	Loading lift Capacity:500kg Loading cask Shielding wall Pb 150mm End-plug tightener Torque:7kg · m Periscope Mag. ×10 Dose measuring device 3mR ~ 10,000R, 0.1mR/min, 35keV ~ 1.2MeV 0mR ~ 1000R, 0.1mR/min, 40keV ~ 3MeV	(C-5)	Leak test of fuel rod Welding for re-fabrication Machining of the end plug	Leak locator Size: φ 50 ~ φ 20, 100 ~ 800mm Medium:White spirit ρ=0.794 Size: φ 9 ~ φ 40 Remote welding machine Size: φ 9 ~ φ 40 Welding method:Tig welding End plug machining device Size: φ 8 ~ φ 20±0.05mm, 100~800mm
C-2	Dismantling of capsule Cutting of capsule Processing after reweld for irradiated test piece	Diamond cutter Size:Max. φ 60, Blade width 1.0mm Guillotin cutter Size: φ 120 × 5t Power:Max.200ton Milling machine		Weight measurement Density measurement Electromotive force measurement	Mettler balance Cap:Max. 160g ±0.0001g Max.1200g ±0.01g Densimeter Cap:Max. 150g ±0.01g/cc Medium:Metaxylene Electromotive force measuring apparatus Furnace size: φ 40, 150mm Temp. range:100~1000°C in Inert gas
C-3	X-ray radiography Gamma scanning	X-ray radiography system Cap:150kVp, 300kVp, Film size 140×990 Gamma scanning system Scanning speed:5,10,20,40mm/s. Collimator:0.2×20,1×15, φ 0.75, φ 1.5	C-6	Electron beam heating facility	Beam power Max.50kW Beam current Max.1.7A
C-4	Eddy current test Pellet/Clad gap measurement Dismantling of NaK capsule	Eddy current testing machine Size: φ 4 ~ φ 17, 100 ~ 1000mm Feed speed: 5 ~ 30mm/s Gap measuring apparatus Size: φ 6 ~ φ 18, 50 ~ 1000mm Gap range:1mm ± 5 μm NaK capsule dismantling machine Size: φ 15 ~ φ 50, 150 ~ 800mm Medium:Kerosen (Max. Nak 200cc)	C-7	Making center hole of UO2 pellets to insert thermocouple	Drilling machin Size: φ 2.0, 54mm Frozen CO ₂ (-78°C) machining:-160°C
C-5	Dimensional measurement FP gas volume and pressure measurement FP gas analysis Preparation for XMA sample	Dimension measuring apparatus Diameter: φ 5 ~ φ 30 ±0.005mm Bowling : ±3.0mm ±0.02mm Length : 0 ~ 1000mm ±0.02mm Puncturing device and gas collector Size: φ 6.0 ~ φ 17, 30 ~ 1000mm Mass spectrometer Detection limit:Kr,Xe,H ₂ ,He,Ar,CH ₄ ,O ₂ , O ₂ ,N ₂ +CO,CO ₂ 0.01v% Vacuum evaporator Size: φ 30×30H Vacuum (3×10 ⁻⁴ Pa)	C-8	Preparation for metallography	Micro-cutter(Diamond cutter) Test piece: Max. φ 30, Cutting width 1mm Grinding polisher: Abrasive paper #180 ~ #100 Ultrasonic cleaner:100W, 28kHz Resin impregnating machine:Vacuum(10 ⁻² P) Periscope: Magnification ×4.5 ~ ×45
			M-1	Metallography	Magnification: x 50~900
			M-2	Metallography	Magnification: x 50~900
			M-3	Metallography Hardness test	Magnification: x 5~10(zoom) Load: 50, 100, 200, 500, 1,000 g Measuring mag. : x 400
			M-4	Micro-gamma scanning	Step scanning: 0.1 mm Collimater : φ 0.2~0.5 Detector: Ge-Nal anticoincidence Ge 50cc, 2.5 keV

shows the major apparatuses and functions of the concrete cells and the microscope lead cells.

Master-slave manipulators, power manipulators and in-cell hoists are installed in the concrete cells. Ball socket manipulators are installed in the microscope lead cells.

An isolation room is attached to the each concrete cell to prevent radioactivity splashing from the concrete cell to the service area. The isolation rooms are lined with steel plates on the floor and the lower part of wall for easier decontamination. Each cell provides a shielding access door. The access door is of the hinge type and manually opened with a mild steel shielding wall in the rear side and used for entrance and exit of personnel for decontamination and maintenance work on the cells.

Lead cells

The lead cells consist of 7 cells for post irradiation examinations for the material specimens. The irradiated specimens to be examined are brought in/out through a wall-type posting port installed at the rear wall of the L-1 cell. The L-1 cell is used for relatively long-term storage of the specimens for the post irradiation examinations.

Major items of the post irradiation examinations carried out in the lead cells are tensile tests, SCC (Stress Corrosion Cracking) tests, instrumented impact tests, visual inspection and dimensional measurements.

The post irradiation examinations on miniaturized specimen for studying fusion reactor materials, including the development of testing techniques, are carried out in the lead cells.

The wall of the each cell in front of the operation area is built up with the lead bricks with a thickness of 15 cm or 20 cm and the shielding windows (dry-type) which have an equivalent shield thickness to the wall. Table 2.3.2 shows the specifications of the lead

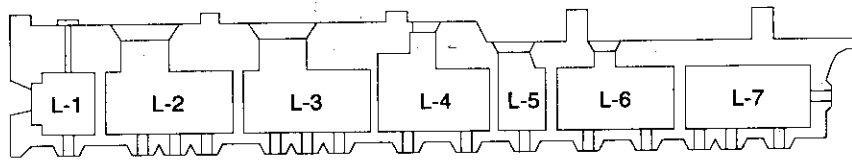
Table 2.3.2
Specifications of lead cells

Cell No.	Inside dimension W x D x H	Shielding wall thickness	Number of windows	Maximum activity (1MeV)
L-1	1.5 x 1.3 x 1.95 m	20 cm	1	1.2 TBq
L-2	2.9 x 1.75 x 2.25 m	15 cm	3	37 GBq
L-3	2.9 x 1.75 x 2.25 m	15 cm	3	37 GBq
L-4	1.2 x 1.75 x 1.8 m 1.2 x 1.25 x 1.8 m	15 cm	2	37 GBq
L-5	1.2 x 1.25 x 1.8 m	15 cm	1	37 GBq
L-6	2.8 x 1.25 x 1.8 m	15 cm	2	37 GBq
L-7	2.75 x 1.25 x 1 m	15 cm	4	37 GBq

cells. Figure 2.3.4 shows the major apparatuses and functions of the lead cells. Each lead cell is provided with a pair of master-slave (M/S) manipulators and some of them are provided with ball socket manipulators.

The rear wall of the each cell is constructed with the ordinary concrete with a necessary shielding thickness. Each cell is provided with a shielding access door and a

Fig. 2.3.4
Functions and major apparatuses
of the lead cells



Cell no.	Functions	Main Apparatuses	Specifications
L-1	Specimen identification	Periscope	Mag.:x10
	Specimen storage	Storage pits	60 pits
L-2	SSRT/SCC test	SSRT/SCC testing machine	Capacity: 30kN Test temp.: -320 Atmospher: Purified water, Inert gas
	Visual inspection	Periscope	Mag.: x10
L-3	Tensile test	Tensile testing machine (Instron-type)	Capacity: 10kN Test temp.: Max.1500 Atmospher: Vacuum
	Charpy impact test	Instrumented Charpy impact testing machine	Capacity: 300J Test temp.: -120~200°C
	Visual inspection	Periscope	Mag.: x10
L-4	Miniaturized specimen test	Small punch testing machine	Capacity: 5kN Test temp.: -160 ~750 °C Atmospher: Vacuum
	Heat treatment	Heat treatment furnace	Test piece volume:Max. φ30x100l Atmospher: Vacuum or Ar gas Test temp.: Max.1000°C
	Visual inspection	Periscope	Mag.: x10
L-5	Miniaturized specimen machining	Electrical discharge machining device	Atmospher: Oil
L-6	Miniaturized specimen test	High-speed punch testing machine	Capacity: 1kN Test temp.: -150°C Atmospher: Vacuum
	Miniaturized specimen handling	Micro-manipulator	
L-7	Fractography	Scanning electron microscope	Mag.: x15~200,000 Resolving power:0.5~3kV 5~30kV 40nm

transfer port for the transportation of specimens to the next hot cell. The access door is of the hinge-type and manually opened with mild steel shielding wall in the rear side. The doors are used for entrance and exit of personnel for decontamination and maintenance work regarding the cells.

Steel cells

The steel cells consist of 5 cells which are mainly used for testing the properties of the material specimens. Major items of the post irradiation examinations carried out in the cells are high temperature tensile/compression tests, fracture toughness tests, creep tests, fatigue tests, SCC tests, visual inspections and dimensional measurements.

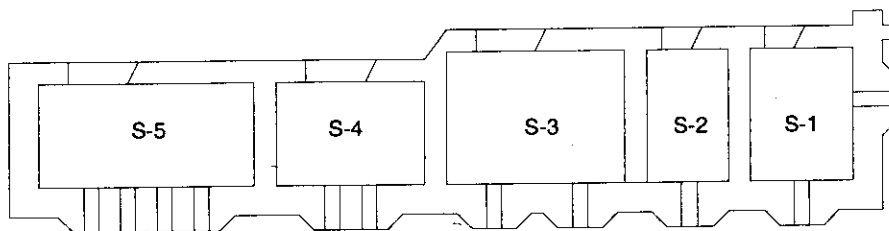
Each cell wall of the operation side is built of mild steel with a thickness of 35 cm or 40 cm and the shielding windows (dry-type) which have an equivalent shield thickness to the wall. Table 2.3.3 shows the specifications of the steel cells. Figure 2.3.5 shows the apparatuses and functions of the steel cells.

A pair of master-slave (M/S) manipulators are installed in each cell. Each cell has a shielding access door made of mild steel. The access doors are of the hinge type built in the rear side of the shielding wall and are used for entrance and exit of personnel for decontamination and maintenance work in the cell. Transfer ports installed on the partition walls of the cells are used for the transfer of specimens to the adjacent hot cells.

Table 2.3.3
Specifications of steel cells

Cell No.	Inside dimension W x D x H	Shielding wall thickness	Number of windows	Maximum activity (1MeV)
S-1	2 x 1.7 x 2.4 m	35 cm	2	66 GBq
S-2	1.3 x 1.6 x 2.35 m	40 cm	1	5.9 TBq
S-3	3.2 x 1.7 x 2.4 m	35 cm	2	66 GBq
S-4	2.2 x 1.25 x 2.4 m	35 cm	2	66 GBq
S-5	4 x 1.25 x 2.4 m	35 cm	4	66 GBq

Fig. 2.3.5
Functions and major apparatuses
of the steel cells



Cell no.	Functions	Main apparatuses	Specifications
S-1	Low cycle fatigue test	Fatigue testing machine	Capacity: 100kN Atmospher: Vacuum Test temp.: -900°C Cyclic speed: Max 100Hz
	Dimensional measurement	Dimensional measuring device	Max. Length: 100mm Precision: +10μ m
S-2	Specimen storage	Storage pits	42 pits
	Visual inspection	TV Monitor	
S-3	Tensile/compression test	Tensile/compression testing machine	Capacity : 50kN (Instron type) Atmospher : Air or Ar gas Test temp.: -150-900°C
	Fracture toughness test	Fracture toughness testing machine	Capacity : 63kN Atmospher : Air Test temp.: -150-500°C
	Visual inspection	Periscope	Mag.: X 10
S-4	SSRT/SCC test	SSRT/SCC testing machine	Capacity : 20kN Atmospher : Purified water or Ar gas Test temp.: ~320°C
	SCC test	UCL/SCC testing machine	Capacity : 5kN Atmospher : Purified water or Ar gas Test temp.: ~320°C
S-5	Creep rupture test	Creep rupture testing machines(3)	Capacity : 10kN Atmospher : Vacuum or Ar gas Test temp.: Max:1000°C
	Creep deformation test	Creep testing machine	Capacity : 5kN Atmospher : Vacuum or Ar gas Test temp.: Max:1000°C

SSRT: Slow Strain Rate Tensile
 SCC: Stress Corrosion Cracking
 UCL: Uni-axial Constant Load

X-ray Micro-Analyzer

The X-ray Micro-Analyzer (XMA) consists of a sample chamber, an electron gun, an EDS cooling system, a gate valve and a transportation cask (Fig. 2.3.6). The sample chamber is surrounded with a tungsten shielding wall for protection from radiation.

The XMA is used for element analysis of micro-spheres on the specimens and observation of the dispersion situation on the specified elements, observing the surface situation by a secondary electron, backscattered electron and absorbed electron.

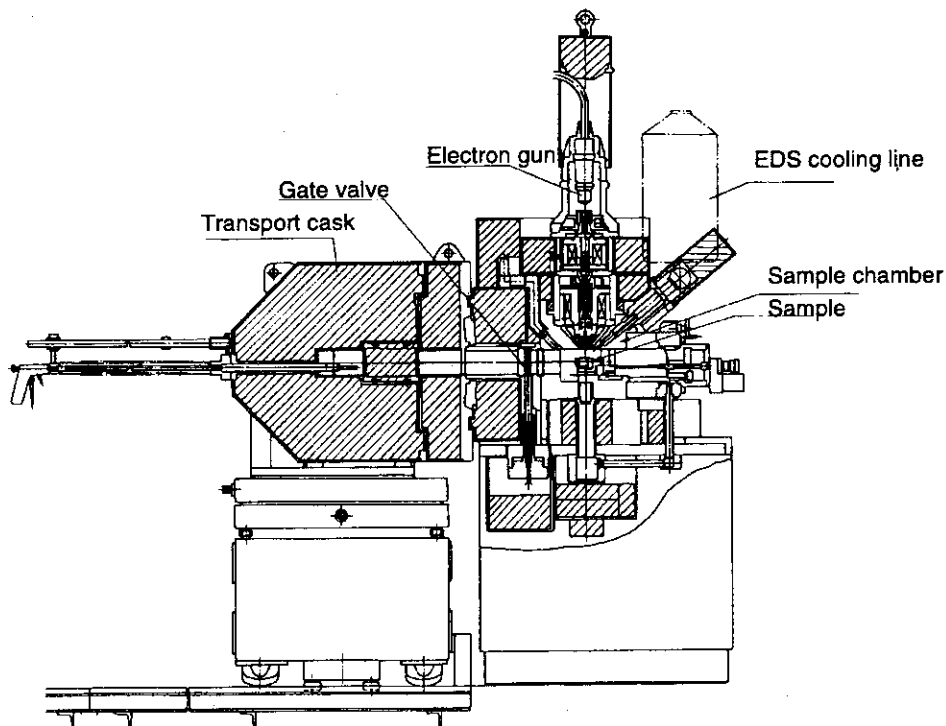
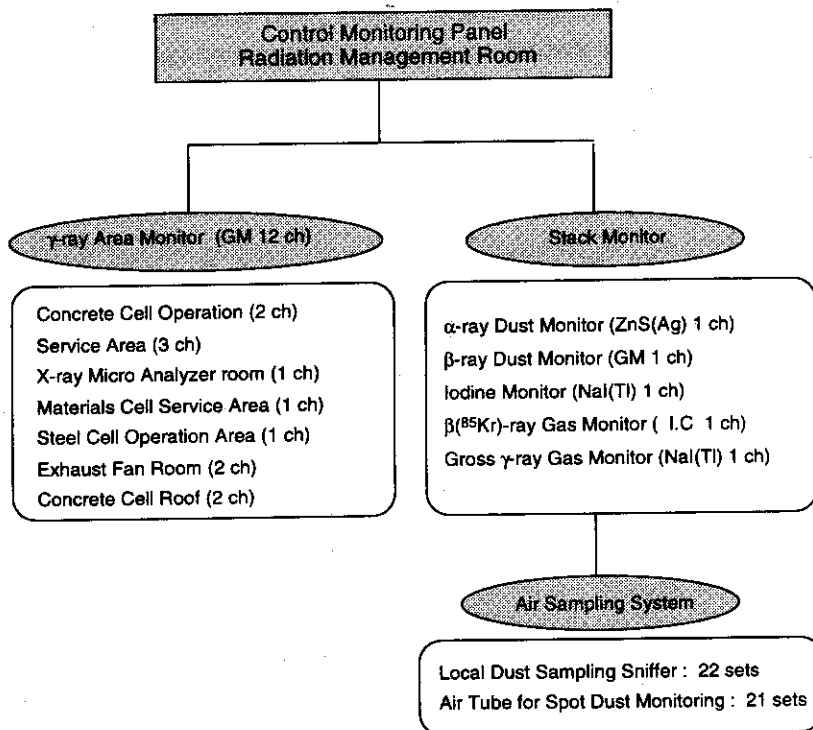


Fig. 2.3.6
X-ray Micro-Analyzer (XMA)

Radiation monitoring system

Radiation monitoring in the Hot Laboratory is carried out continuously by the radiation monitoring systems as shown in Fig. 2.3.7. The central monitoring panel of this system is located in the radiation management room of the Hot Laboratory.

Fig. 2.3.7
Radiation monitoring system in
the Hot Laboratory



3. Activities in FY1994

3.1. Reactor operation

JMTR has been operated with a Low Enriched Uranium (LEU) fuel core since its 108th operation cycle in 1993. The operation cycles operated during FY1994 were the last half of Cycle 109, 110 through 112 and the first 70% of Cycle 113. It is shown in Table 3.1.1. During the operation of Cycle 109, an unscheduled shutdown took place with the item "output voltage of diesel power generator lowered" due to mechanical trouble with one of the two diesel engines for power supply. The trouble took place in FY1993, and recovered to restart the normal operations in the next fiscal year. The operation of Cycles 110 through 112 was completed on schedule. At the beginning of the operation of Cycle 113, the reactor scrambled due to a failure in the control system indicating "CRD over speed" that was due to a failure in the power range switching of the two-out-of-three nuclear power indicator systems. Therefore, the operation of Cycle 113 finished with a 8 day delay from the scheduled date. The integrated reactor power of Cycle 1 through Cycle 113 attained 105,486MWd. The nuclear properties of each operation cycle are obtained at a low-power level of 20 kW prior to the high-power operation for irradiation. The obtained values of excess reactivity, shutdown margin and the worths of the two automatic control rods (SR-1, 2) are listed in Table 3.1.2.

The reactor cooling water is chemically analyzed. During reactor operation, the analysis is performed once a day, which detects ^{24}Na , ^{27}Mg , some radioactive isotopes of iodine, etc. The concentration of the radioactive isotopes are indicated in Fig. 3.1.1 and Fig. 3.1.2 ranging from operation cycles 109 through 113. As observed in the presented figures, no significant changes took place during the operation term. The detected radioactive iodines are considered to be produced by the fission of impure uranium included in beryllium

Table 3.1.1
Operation summary
of FY1994

Cycle No.	Period *1	Integral power	Operation time *2	Operating	Cumulative integral power (MWd)
		(MWd)	(hours:minutes)	efficiency(%)*3	
109	94. 3. 19 - 94. 4. 23	1097.7	536:00	88.5	100,499.2
110	94. 6. 8 - 94. 7. 3	1243.8	602:30	100.2	101,743.0
111	94.11.16 - 94.12.11	1242.8	602:28	100.1	102,985.8
112	95. 1.18 - 95. 2.12	1242.0	602:22	100.0	104,227.8
113	95. 3.6 - 95. 4. 8	1249.6	606:00	100.7	105,486.4

Note *1 Period indicates the startup and shutdown dates for 50MW operation.
*2 Operation time excludes the time to get the nuclear properties of the reactor.
*3 Operation efficiency = Actual integral power / Scheduled integral power(1241MWd).

Table 3.1.2
Nuclear properties of
each operation cycle

Cycle No.	Excess*1 (%Δk/k)	Shutdown margin		Rod worth of automatic control rods	
		(%Δk/k)	keff	SR-1 (%Δk/k)	SR-2 (%Δk/k)
109	11.3	36.0	0.74	0.26	0.24
110	11.4	25.1	0.80	0.21	0.22
111	11.0	22.5	0.82	0.23	0.22
112	11.1	27.5	0.78	0.24	0.24
113	11.6	33.7	0.75	0.22	0.24

Note *1 Fuel addition method was used for Cycle 109 and 111.
Comparison method was used for the other cycles.

reflector elements. High-purity demineralized water of 4,800 m³ was supplied to the primary cooling channel, the pool-canal and the cooling system of the irradiation facility in FY 1994. Filtered water of 336,000m³ was supplied to the secondary cooling channel and to some other utility systems.

Fig.3.1.1
Radioactive nuclide concentration in primary coolant

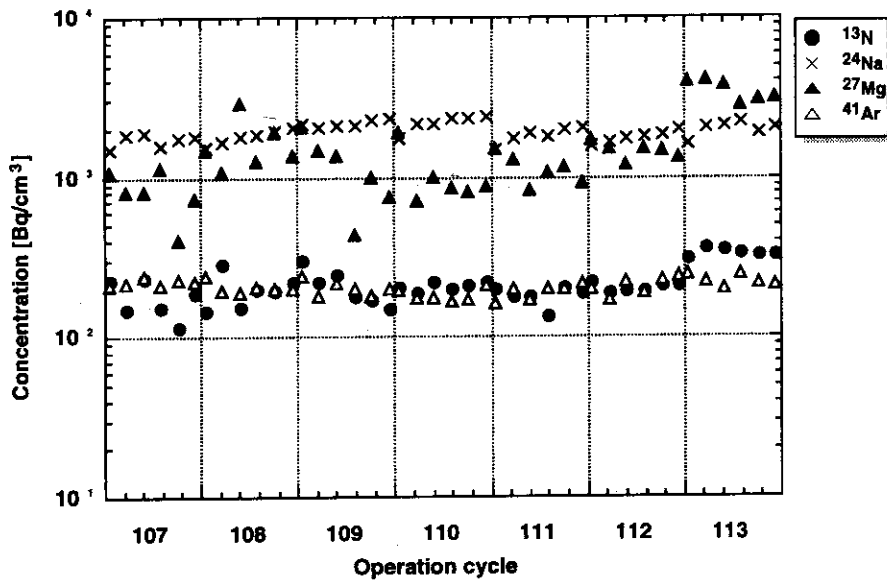
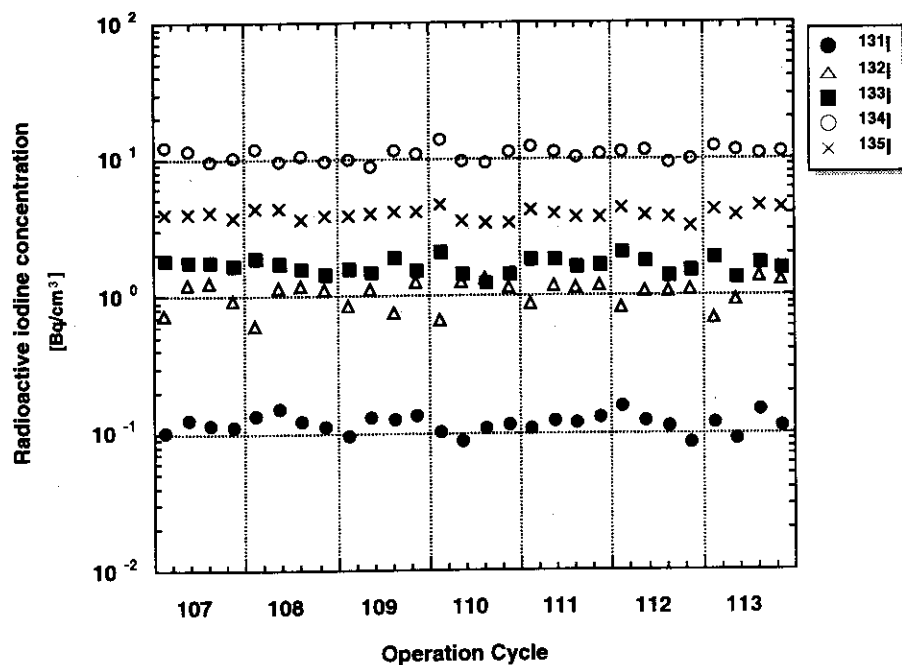


Fig.3.1.2
Radioactive iodine concentration in primary coolant



Fuel management

The fuel elements using LEU were manufactured by CERCA (France) and B&W (U.S.A.). Thirty-eight standard fuel elements and 15 fuel follower elements were supplied for JMTR in FY1994. The spent fuel could not be shipped to reprocessing plants in U.S.A. due to some political reason in that country. To increase storage capacity for spent fuel, JMTR prepared new two spent fuel racks in the year. Twelve times of the safeguard inspection measures were carried out on the basis of the inspection agreement between Japanese Government and IAEA.

Personnel exposure and release of radioactive waste

(1) Personnel exposure

At JMTR, there has been no occupational exposure exceeding the prescribed effective dose equivalent limit as shown in Table 3.1.3.

(2) Release of radioactive gaseous and liquid waste

At JMTR, neither radioactive gaseous nor liquid waste was released exceeding the release limit specified in the relevant regulations as shown in Table 3.1.4.

Table 3.1.3
Annual effective dose equivalent of personnel at JMTR

Contents	No. of personnel	No. of personnel with accumulated dose (mSv) of each range			Collective dose equivalent (person*mSv) **1)
		Undetectable	0.2 ≤ D < 1	1 ≤ D < 5	
JAERI personnel	151	151	0	0	0
Visiting researchers	14	14	0	0	0
Consigned employees	239	235	4	0	1.4

*1) Not detect according to internal exposure.

Table 3.1.4
Gaseous and liquid waste released from JMTR

Gaseous (TBq)	3.8×10^1 (⁴¹ Ar)
Iodine-131	Undetectable
Gross β- emitter	Undetectable
Volume of liquid Wastes * (m ³)	2.7×10^3
Main nuclide	³ H, ⁵¹ Cr, ⁶⁰ Co

* Those liquid wastes were transported to Radioactive Waste Management Facilities and there were treated.

3.2. Irradiations in the reactor

JMTR is equipped with various irradiation facilities such as capsule irradiation facility, OGL-1, BOCA/OSF-1 and hydraulic rabbits to perform various irradiation tests of fuel and materials to be used for LWR, FBR, HTTR and fusion reactor, and the production of RIs.

Irradiation tests performed using these facilities in FY1994 are given in Table 3.2.1. Sixty-six capsules (123 cycle×item), one specimen (4 cycle×item) in OGL-1, eight BOCA's (10 cycle×item) and 72 rabbits (5287.4 hours×items) were irradiated during operation of cycles 110 to 113 in FY1994.

Irradiations in JMTR in FY1994 are summarized according to users and purposes in Table 3.2.2 and Table 3.2.3, respectively. The utilization status of capsules, OGL-1 and BOCA are shown in Fig. 3.2.1. The utilization status of hydraulic rabbits can be seen in Fig. 3.2.2.

Table 3.2.1
JMTR Irradiation Results in FY1994

Irradiation Facilities	110cy	111cy	112cy	113cy	Total		
					(cycle×item)	(item)	
Capsule	37	31	31	24	123	(66)	
BOCA	4	3	3	0	10	(8)	
OGL-1	1	1	1	1	4	(1)	
Subtotal	42	35	35	25	137	(75)	
Rabbit						72	
Number	21	15	15	21			
hour×rabbit	1000.4	1128.4	1062.0	2096.7	5287.4		
Details of Capsule							
Capsule	110cy	111cy	112cy	113cy	Total		
					(cycle×item)	(item)	
Instrumented	11	14	14	8	47	(23)	
Non-instrumented	26	17	17	16	76	(43)	
Fuel	5	5	4	2	16	(7)	
Material	32	26	27	22	107	(59)	
FGS	1	1	1	1	4	(1)	

Table 3.2.2
Purposes of JMTR utilization in FY1994 (Capsule, OGL-1, BOCA and Hydraulic Rabbit)

Purposes of the utilization	Capsule, OGL-1, BOCA				Hydraulic Rabbit			
	item	ratio	cycle/item	ratio	item	ratio	hour/item	ratio
Research at Universities	10	13.3%	27	19.7%	67	93.1%	4314.5	81.6%
Fusion	13	17.3%	25	18.2%				
Irradiation Technique	13	17.3%	25	18.2%	2	2.8%	287.9	5.4%
LWR	14	18.7%	21	15.3%				
RI Production	18	24.0%	20	14.6%	1	1.4%	432	8.2%
HTTR	2	2.7%	8	5.8%				
Basic Research(JAERI)	3	4.0%	7	5.1%	2	2.8%	253	4.8%
FBR	2	2.7%	4	2.9%				
Total	75		137		72		5287.4	

Table 3.2.3
Users of JMTR utilization in FY1994 (Capsule, OGL-1, BOCA and Hydraulic Rabbit)

Users of the utilization	Capsule, OGL-1, BOCA				Hydraulic Rabbit			
	item	ratio	cycle/item	ratio	item	ratio	hour/item	ratio
JAERI(JMTR)	24	32.0%	44	32.1%	3	4.2%	444.9	8.4%
JAERI(Laboratory)	16	21.3%	39	28.5%				
JAERI(Isotope)	18	24.0%	20	14.6%	2	2.8%	528	10.0%
Universities	10	13.3%	27	19.7%	67	93.1%	4314.5	81.6%
NUPEC	6	8.0%	6	4.4%				
PNC	1	1.3%	1	0.7%				
Total	75		137		72		5287.4	

RI production

JMTR constantly carries out irradiation for producing various kinds of radioisotopes such as ^{32}P , ^{51}Cr , ^{35}S , ^{192}Ir , ^{169}Yb . In FY1994, 18 capsules (20 cycle×item) and one rabbit were irradiated for radioisotope production shown in Table 3.2.4. The nuclides and their uses are shown in Table 3.2.5.

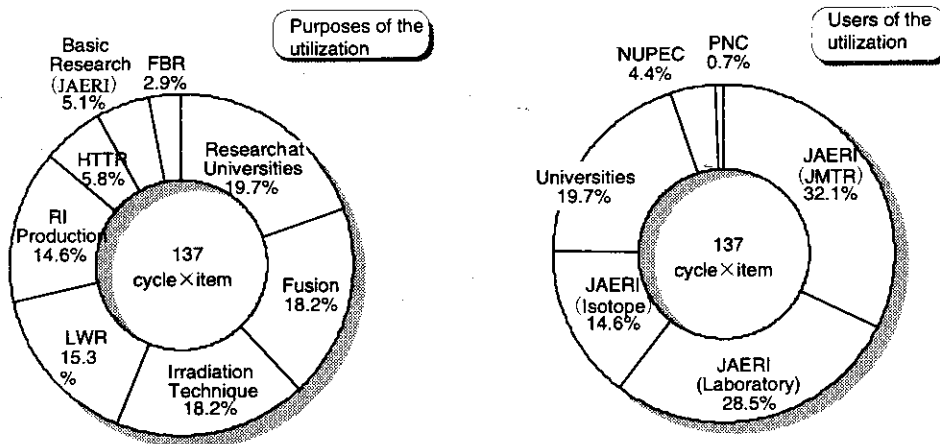


Fig. 3.2.1
Utilization of JMTR in FY1994
(Capsule, OGL-1,BOCA)

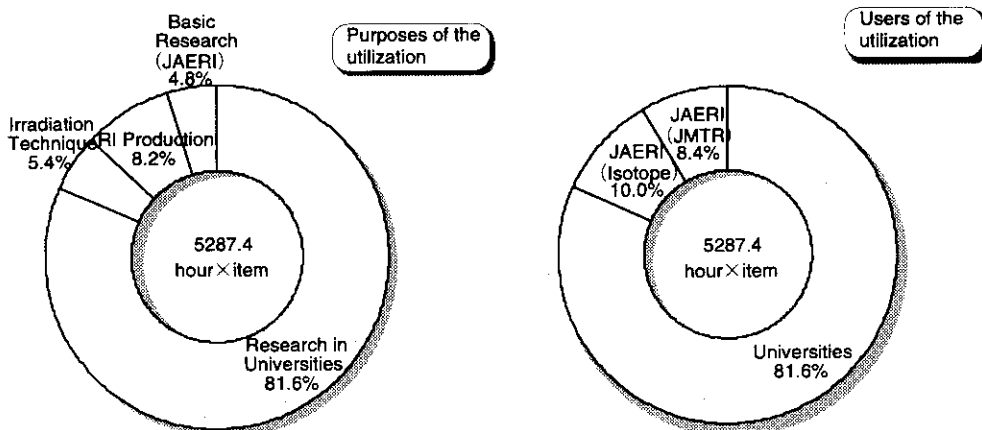


Fig. 3.2.2
Utilization of JMTR in FY1994
(Hydraulic rabbit)

Table 3.2.4
Utilization of the Isotope Division
of JAERI in FY1994

Capsule		cycle				Irradiation hole	Dia. (mm)	User	Type	Specimens
No	Name	110cy	111cy	112cy	113cy					
1	92 M-25RS	1				L-11	41	RI production	Al basket	Ir
2	92 M-27RS			1		D-6	41	RI production	Al basket	Ir
3	92 M-28RS				1	M-10	41	RI production	Al basket	Ir
4	93 M-19RS	1				I-5	41	RI production	Al basket	Ir(medical)
5	93 M-20RS		1			I-5	41	RI production	Al basket	Ir(medical), Cr ₂ O ₃ , KCl
6	93 M-21RS			1		I-5	41	RI production	Al basket	Ir(medical), Cr ₂ O ₃
7	93 M-22RS				1	I-5	41	RI production	Al basket	Ir(medical), Cr ₂ O ₃ , KCl
8	92 M-19RS	1				H-5	41	RI production	Al basket	Cr ₂ O ₃ , KCl
9	93 M-8R		1			H7-1	31.4	RI production	Al basket	S
10	93 M-9R			1		H7-1	31.4	RI production	Al basket	S
11	93 M-10R				1	H7-1	31.4	RI production	Al basket	S
12	93 M-7R	1				H7-1	31.4	RI production	Al basket	S, ¹⁸⁶ WO ₃
13	94 M-40RS			1	1	H-5	41	RI production	Al basket	SrCO ₃ , ¹⁸⁶ WO ₃
14	93 M-24R	1				J9-4	31.4	RI production	Al basket	Yb ₂ O ₃
15	93 M-25R		1			J9-4	31.4	RI production	Al basket	Yb ₂ O ₃
16	93 M-26R			1		J9-4	31.4	RI production	Al basket	Yb ₂ O ₃
17	93 M-27R				1	J9-4	31.4	RI production	Al basket	Yb ₂ O ₃
18	94 M-21R			1	1	L-11	41	laboratory	Al basket	LiAl
Total		5	3	6	6					

Hydraulic rabbit

No	Name	cycle	Irradiation time	Irradiation hole	Dia. (mm)	User	type	Specimens
1	R257	113	432 hour	M-11	32	RI production	Rabbit (HR-2)	Gd ₂ O ₃
2	R258	111	96 hour	M-11	32	laboratory	Rabbit (HR-2)	Am-241

Purpose of R258 is the basic research on actinide, not RI production.

Table 3.2.5
List of capsules and rabbits irradiated
for RI production in FY1994

RI	Target	Reaction	Uses	Capsule or rabbit	Production (TBq)
³² P	S powder	³² S(n,p)	Tracer in medical and agriculture field	93M-7R	2.3
				93M-8R	3.2
				93M-9R	3.2
				93M-10R	2.6
⁵¹ Cr	Cr ₂ O ₃ powder	⁵⁰ Cr(n, γ)	Diagnostic of blood disease in medical field	92M-19RS	0.34
				93M-20RS	0.17
				93M-21RS	0.29
				93M-22RS	0.25
³⁵ S	KCl powder	³⁵ Cl(n,p)	Tracer in agriculture and industry field	92M-19RS	0.65
				93M-20RS	0.65
				93M-22RS	0.65
¹⁹² Ir	Ir pellet (φ 2×2mm)	¹⁹¹ Ir(n, γ)	Radiation source of non-destructive inspection	92M-25RS	180
				92M-27RS	190
				92M-28RS	210
	Ir pellet (φ 1.1×1.2mm)	¹⁹¹ Ir(n, γ)	Radiation source for treatment of cancer	93M-19RS	11
				93M-20RS	21
				93M-21RS	22
¹⁸⁶ Yb	Yb ₂ O ₃ pellet (φ 1×1mm)	¹⁸⁶ Yb(n, γ)	Radiation source of non-destructive inspection for thin welded tube	93M-24R	0.36
				93M-25R	0.36
				93M-26R	0.32
				93M-27R	0.31
³ H	LiAl plate	⁶ Li(n, α)	Fuel of fusion reactor (under development)	94M-21R	-
⁸⁹ Sr	SrCO ₃ powder	⁸⁹ Sr(n, γ)	A labeled compound for medical purposes	94M-40RS	1.5 × 10 ⁻⁴
¹⁸⁸ Re	¹⁸⁶ WO ₃ powder	¹⁸⁶ W(n, γ)	A labeled compound for treatment of cancer (under development)	93M-7R	3.8 × 10 ⁻⁴
				94M-40RS	6.9 × 10 ⁻⁴
					¹⁸⁷ W(n, γ)
¹⁵³ Gd	Gd ₂ O ₃ pellet	¹⁵² Gd(n, γ)	Measuring of bone density (under development)	94M-40RS	6.9 × 10 ⁻⁴
				R257	0.012

Basic research

In the field of the basic research at JAERI, irradiation tests of the shape memory alloy, ^{241}Am , composite material and ceramics were performed using three capsules (7 cycle×item) and two rabbits in FY1994.

Research in Universities

JMTR is utilized by researchers of universities in Japan through the Oarai Branch Institute for Materials Research, Tohoku University. Ten capsules (27 cycle×item) and 67 rabbits (4314.5 hour×item) were irradiated for research at universities in FY1994.

Irradiation technique

Irradiation tests for R&D on irradiation technique were performed using 13 capsules (25 cycle×item) and two rabbits, such as the capsule 94M-23A containing Cd to evaluate the shielding performance for thermal neutron flux, capsules containing various fluence monitors (93M-41J,-42J,-43J,-44J,-45J), the capsule 92F-50A of silicide fuel plates for research reactors and the capsule 91*M-22J of the inner cooling type. Irradiation of surveillance test-pieces for reactor vessel(67M-RJ-4) and Be reflector(74M-52J) of JMTR were continued.

Letter (*) reads a
instrumented capsule

Irradiations of stainless steel were also performed using the capsules 91M-7J and 89M-42J. In the power ramp tests at the BOCA/OSF-1, a heater BOCA(91BM-5J) was used for evaluating the heat rate of the segmented fuel rod in BOCA. Two dummy rabbits were irradiated for evaluating the defect of the outer tube head in the hydraulic rabbit.

LWR

Fourteen capsules (21 cycle×item) were irradiated for the R&D of the LWR in FY1994.

1) Power ramping tests on LWR fuels

Seven BOCAs were irradiated for power ramping test in FY1994.

2) Base irradiation of LWR fuels for the NSRR experiments

Three capsules (7 cycle×item) were irradiated for base irradiation of LWR fuel rods for the NSRR experiments.

3) Irradiation tests on materials for LWR

Four capsules (7 cycle×item) were irradiated for the R&D of the materials on LWR. These specimens were concrete, stainless steel, cladding of fuel rod and ferro alloy.

HTTR

For HTTR, one specimen (4 cycle×item) of OGL-1 and one FGS capsule (4 cycle×item) were irradiated in FY1994.

1) Irradiation test in OGL-1

OGL-1 has been used for irradiation tests of fuel for research and development of HTTR since May 1977. The R&D of the HTTR fuel using OGL-1 reached the final stage. HTTR will reach criticality in FY1997.

In FY1994, the irradiation tests of the 15th fuel specimen (92LF-29A) were carried out from the 107th operation cycle and will be continued until the 115th operation cycle in 1995. This specimen was made according to specifications of the fuel element initially loaded in HTTR. The purpose of the test is to confirm the integrity of the fuel at 1,350°C.

2) Fission Gas Sweep (FGS) Capsule

One FGS capsule, the purpose of which was to measure the FP release rate from the HTTR fuel, was irradiated in FY1994. The 91*F-1A capsule was irradiated from the 104th operation cycle and will be irradiated until the 123th operation cycle. The purposes of the test are to investigate the FP gas release rate, integrity and endurance limit of the fuel made by the double over-coating method for improved fuel for HTTR.

FBR

For a fast breeder reactor, two capsules (4 cycle×item) were irradiated in FY1994. Irradiation of the 89*F-3A capsule, of which specimens were two fuel pins containing uranium-plutonium mixed nitride pellets, started in the 94th operation cycle and was completed in the 112th operation cycle to study the irradiation behavior and demonstrate the feasibility of the mixed nitride as an advanced fuel for FBRs.

The capsule 93*M-46P, of which specimens are materials of core components for FBRs, was irradiated in the 112th operation cycle.

Fusion

Thirteen capsules (25 cycle×item) were irradiated for the R&D of the fusion reactor in FY1994. These specimens were of various kinds of materials for the fusion reactor.

3.3. Utilization of Hot Laboratory

In FY1994, PIEs were performed mainly on LWR fuel subjected to power ramping tests, NSRR test fuel, uranium silicide fuel, structural materials of LWR, HTTR and the fusion reactor, and shape memory alloys. Remote recapsuling of BOCAs for the power ramping tests at JMTR and their remote dismantling after the power ramping tests were performed at the Hot Laboratory. Re-instrumentation of the pre-irradiated LWR fuel was also performed for the power ramping tests at JMTR.

The number of capsules treated at the Hot Laboratory is classified on purpose of the PIEs as shown in Fig. 3.3.1.

PIEs of nuclear fuels

(1) Fuel rods for power ramping test

In FY1994, 17 segment fuel rods irradiated in power reactors were mantled or dismantled to/from BOCA at the C-2 cell in the concrete cells. Some of fuel rods were transferred to the Nuclear Fuel Development Co. (NFD) hot laboratory in shipping casks, after being dismantled from BOCA. Their PIEs were performed in the NFD hot laboratory. On the fuel rods irradiated for JAERI's users, the PIEs were carried out in concrete cells. On the other hand, FP gas pressure gauges were re-instrumented on some fuel rods in the concrete cells for the power ramping test.

And, on a segmented fuel rod pre-irradiated in power reactor, FP gas pressure gauge thermocouples were dual re-instrumented in the same facilities.

(2) Nuclear Safety research Reactor (NSRR) test fuel rods

Nondestructive tests on the test fuel rods of NSRR were carried out such as visual inspections, X-ray radiography, gamma-scannings, profilometry and eddy-current tests after pre-irradiation at JMTR for pulse irradiation at NSRR. A few of the fuel rods were examined with destructive tests such as pellet/ cladding gap measurements, FP gas collections and analyses, X-ray microanalysis and density measurements after the nondestructive tests. Some were transported to the Tokai Hot Laboratory for pulse irradiation tests at NSRR.

(3) Nuclear fuel for research reactors

Mini-plates, hot-pressing disks and pellets of uranium silicides and uranium alloy(U-Fe,Ni,Mn) were irradiated at JMTR to study the irradiation behavior of research reactor fuel. The PIEs were carried out primarily by visual inspections, X-ray radiography, gamma-scannings and dimensional measurements.

PIEs of materials

(1) Structural materials of LWR

Test pieces of stainless steel for the reactor core were irradiated to study the life estimation of LWR. The PIEs on these test pieces were performed primarily using a slow-strain-rate tensile test, fracture toughness test, metallography and scanning electron microscopy.

(2) Structural materials of HTTR

Test pieces of the control rod cladding material were irradiated to study the irradiation

characteristics. Creep rupture tests and creep deformation tests were carried out in the steel cells.

(3) Structural materials of the fusion reactor

Test pieces of the stainless steel (SUS316) and Inconel 625 for a vacuum vessel of fusion reactor were irradiated to study the re-welding characteristics. The PIEs such as welding tests, mealing machines, dimension measurements, visual inspections, tensile tests and metallography were carried out.

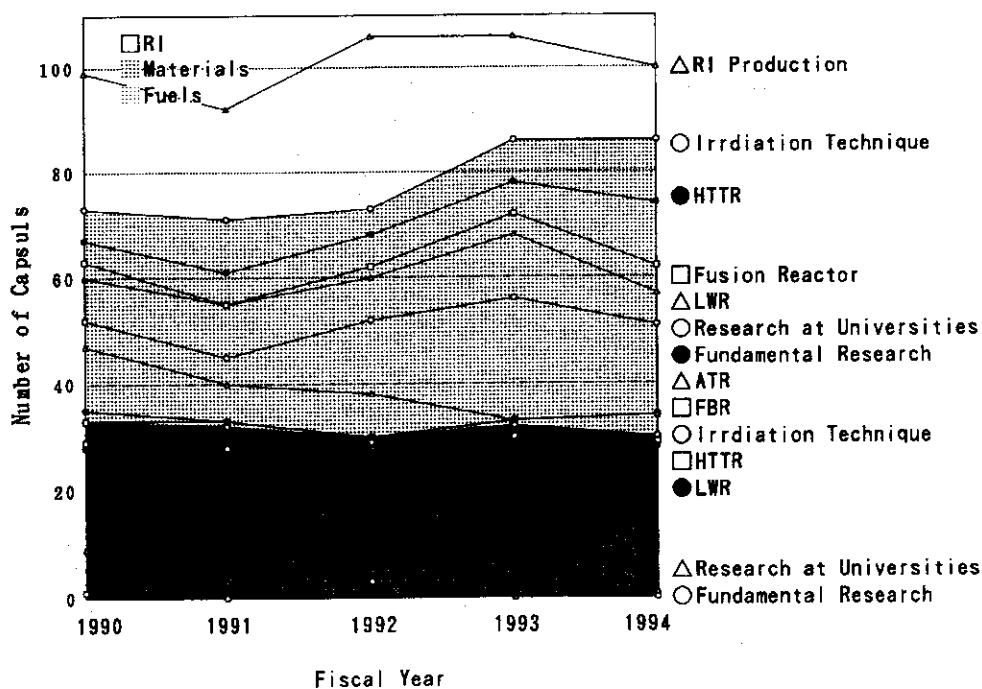
(4) Structural materials of capsules

Test pieces of shape memory alloys were irradiated to study the neutron irradiation effect. PIEs such as the Charpy impact test, high temperature tensile test, constant-load deformation test, fracture toughness test, fractography and metallography were carried out. And, test pieces of friction welding materials (Nb-1Zr/SUS304) for capsules were irradiated to study the irradiation characteristics. PIEs such as tensile tests, hardness tests, metallography and X-ray microanalysis were carried out.

(5) Radioisotope production

In FY1994, 14 radioisotope production capsules were treated at the Hot Laboratory and dismantled in the C-2 cell of the concrete cells. The radioisotopes produced: 756TBq of ¹⁹²Ir, 10TBq of ³²P, 1.4TBq of ⁵¹Cr and 0.74TBq of ³⁵S were transported to the Department of Radioisotope Production, JAERI-Tokai.

Fig. 3.3.1
Number of capsules treated
(FY1990 - FY1994)



Personnel exposure and release of radioactive waste

(1) Personnel exposure

At the Hot Laboratory, there was no occupational exposure exceeding the prescribed effective dose equivalent limit as shown in Table 3.3.1.

(2) Release of radioactive gaseous and liquid waste

At the Hot Laboratory, neither radioactive gaseous nor liquid waste was released exceeding the release limit specified by the relevant regulations as shown in Table 3.3.2.

Table 3.3.1
Annual effective dose equivalent of personnel at the Hot Laboratory

Contents	No. of personnel	No. of personnel with Accumulated dose (mSv) of each range			Collective dose equivalent (person·mSv) *1)
		Undetectable	0.2 ≤ D < 1	1 ≤ D < 5	
JAERI personnel	25	20	4	1	2.3
Visiting researcher	4	4	0	0	0
Consigned employee	190	178	12	0	4.2

*1) Not detected from internal exposure.

Table 3.3.2
Gaseous and liquid waste released from the Hot Laboratory

Gaseous	(TBq)	1.1×10^{-1} (⁸⁵ Kr)
Iodine-131	(MBq)	5.6×10^{-2}
Gross α - emitter		Undetectable
Gross β - emitter		Undetectable
Volume of liquid Wastes *	(m ³)	7.4×10^1
Main nuclide		⁶⁰ Co, ¹³⁴ Cs, ¹³⁷ Cs

* Those liquid wastes were transported to Radioactive Waste Management Facilities and they were treated.

3.4. Design of capsules and irradiation facilities

Power ramping tests on LWR fuels

The seven power ramping tests using the Boiling Water Capsule / Oarai Shroud Facility No.1(BOCA/OSF-1) were carried out this year. In the power ramping test, a fuel rod is inserted into BOCA, and BOCA is inserted into OSF-1 and irradiated.

A refabricated fuel rod with radioactivity, which was cut from a full length BWR high burnup spent fuel rod to a 360 mm active fuel length, was used in the power ramping test and irradiated in the 110th operation cycle. And in the same way, the five refabricated fuel rods with radioactivity were also provided to the power ramping test of the 110th, 111th and 112th operation cycles.

Especially, in the 112th operation cycle, the power ramping test was performed on a refabricated and re-instrumented BWR fuel rod (287.5 mm in active fuel length). The fuel rod were cut from a full length BWR spent fuel rod. And after that a thermocouple measuring the fuel centerline temperature and a FP gas pressure gauge were installed to the fuel rod, it was irradiated. The pressure gauge has successfully monitored fission gas release continuously under various power ramping test conditions. The structure of the capsule is shown in Fig.3.4.1. One of the test results of pressure change induced by power altering can be seen in Fig. 3.4.2.

Fig. 3.4.1
Boiling Water Capsule (BOCA) with a dual instrumented fuel rod

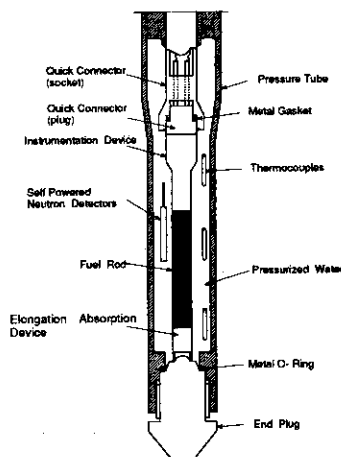
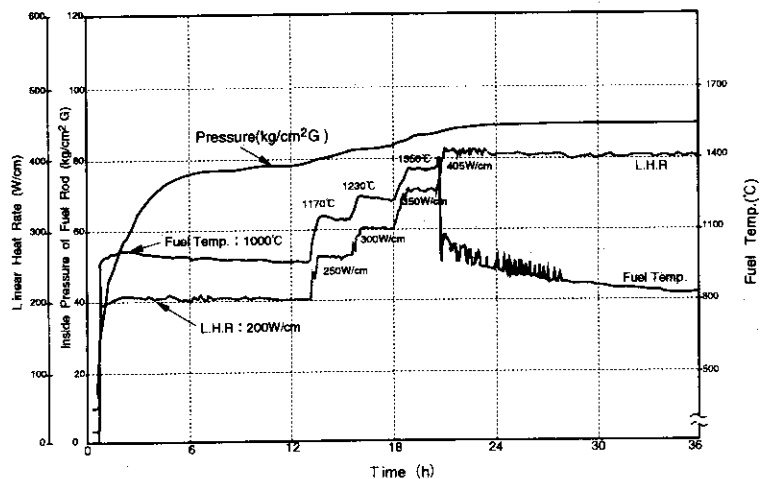


Fig. 3.4.2
Results of irradiation test for a fuel rod with a thermocouple and a FPgas pressure gauge



The power ramping tests on the BWR high burnup fuel carried out in FY1994 are shown in Table 3.4.1.

Irradiation tests on materials for LWR & JMTR

A study of radiation-induced embrittlement and irradiation assisted stress corrosion cracking (IASCC) was carried out for assessment of integrity of the core components of LWR and JMTR. The study was carried out in collaboration with Central Research Institute of Electric Power Industries. The temperature of the core components on LWR was about 300°C under normal operating conditions. The boiling water capsule for the materials, where the temperature of specimen is maintained at a saturated temperature corresponding with the water pressure of 7.5 MPa, and the capsule controlled temperature by electric heaters power were used for the irradiation tests of the core components for LWR. The unsealed capsule was used for the irradiation tests of the core components for LWR & JMTR (Table 3.4.2).

Irradiation tests on HTTR fuels and materials

1) Irradiation test by OGL-1

The irradiation tests of the fuel in OGL-1 have been carried out for the research and the development of HTTR since May 1977. The R&D of the HTTR fuel using OGL-1 reached its final stage.

In FY1994, the 15th fuel specimen (92LF-29A) has been irradiated since the 107th operation cycle and will be irradiated until the 115th operation cycle. This specimen was made according to the specifications of the fuel element to be initially loaded in HTTR. The purpose of the test is to confirm the integrity of the fuel at 1,350 °C.

Table 3.4.1 BOCAs irradiated in FY1994

Operation Cycle	Identification Number	Remarks
110th	93BF-74GO	BWR high burnup fuel
	93BF-75GP	BWR high burnup fuel
	93BF-76GQ	BWR high burnup fuel
111th	93BF-77GM	BWR high burnup fuel
	93BF-78GN	BWR high burnup fuel
112th	93BF-79GO	BWR high burnup fuel
	92BF-67JK	BWR fuel with a FP gas pressure gauge & a center fuel thermocouple
Total	7	

Table 3.4.1
BOCAs irradiated in
FY1994

Table 3.4.2 Irradiation test on materials for LWR & JMTR in FY1994

Identification Number	Operation Cycle	Remarks
86M - 42J	80th - 109th	unsealed capsule assessment of integrity of the core components of JMTR
89M - 42J	94th - 124th	unsealed capsule assessment of integrity of the core components of LWR

Table 3.4.2
Irradiation test on
materials for LWR & JMTR
in FY1994

2) Fission Gas Sweep (FGS) Capsule

In FY1994, one FGS capsule, which was to measure the FP release rate from HTTR fuel, was irradiated.

91F-1A: The irradiation of the 91F-1A capsule started in the 104th operation cycle and will be completed the 123th operation cycle. The purposes of the test are to investigate the FP gas release rate, integrity and endurance limit of the fuel made by the double over-coating method to improve the fuel for HTTR.

Irradiation tests on FBR fuels and materials

For the fast breeder reactor, two capsules were irradiated in FY1994. Irradiation of the 89F-3A capsule, of which specimens are two fuel pins containing uranium-plutonium mixed nitride pellets, started in the 94th operation cycle and was completed in the 112th operation cycle to study the irradiation behavior and demonstrate the feasibility of the mixed nitride as an advanced fuel for FBRs.

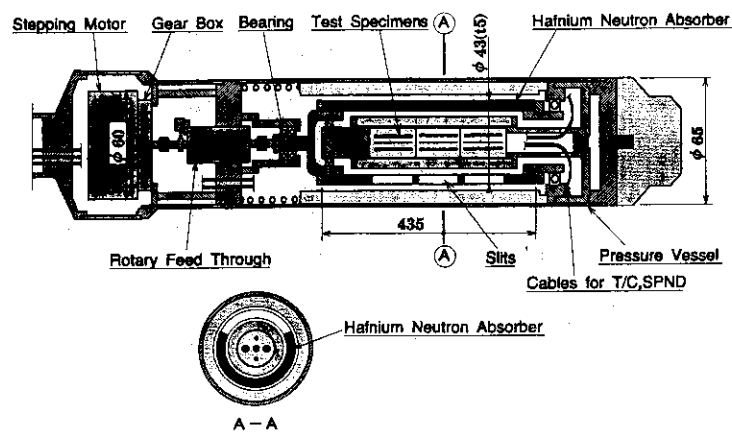
The 93M-46P capsule, of which specimens are the materials of the core components for FBRs, was irradiated in the 112th operation cycle.

Irradiation test for fundamental research

Forty irradiation capsules were designed and the 48 irradiation capsules were fabricated in FY 1994. Two newly developed capsules were irradiated.

One is a capsule for a simulated pulse operation test which is one of the R&Ds for the fusion blanket irradiation tests. The capsule contains a cylindrical rotatable hafnium absorber with a slit for simulating pulse operation. To confirm the simulated pulse operation, several new type Self-Powered Neutron Detectors (SPND), which are combined with the Co type SPND and the Rh type one, are inserted into some holders located inside of the hafnium absorber. As the intensity of neutrons irradiated into the SPNDs is altered by the rotating the hafnium absorber with slit, the sensitivity and response of the neutron density under the simulated pulse operation can be detected by the SPNDs. The capsule was irradiated in the 109th operation cycle. The structure of the capsule is shown in Fig. 3.4.3. The results

Fig. 3.4.3
Structure of the capsule



of the irradiation test are shown in Fig.3.4.4.

The other one was developed to study the mechanism of the defect structure of materials by neutron irradiation. To improve the irradiation conditions for a mechanism study, the irradiation temperature of specimens is constantly maintained at the desired one during transient condition, i.e., reactor start-up and shutdown, and steady-state operation. This type of capsule was developed in 1991. For further improvement, the functions to change the irradiation mode was added to the capsule. That is, the specimens being irradiating under a desired temperature, can be removed from the upside from the reactor core by the lifting devices at a desired irradiation time. The capsule was also irradiated in the 109th operation cycle. The structure of the capsule is shown in Fig.3.4.5.

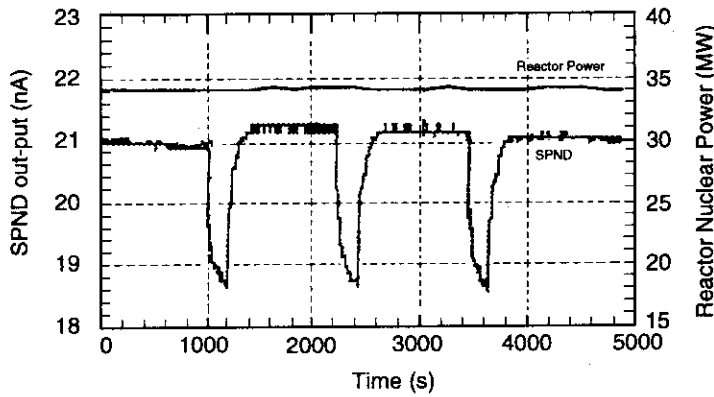


Fig. 3.4.4
Results of the irradiation test (SPND output)

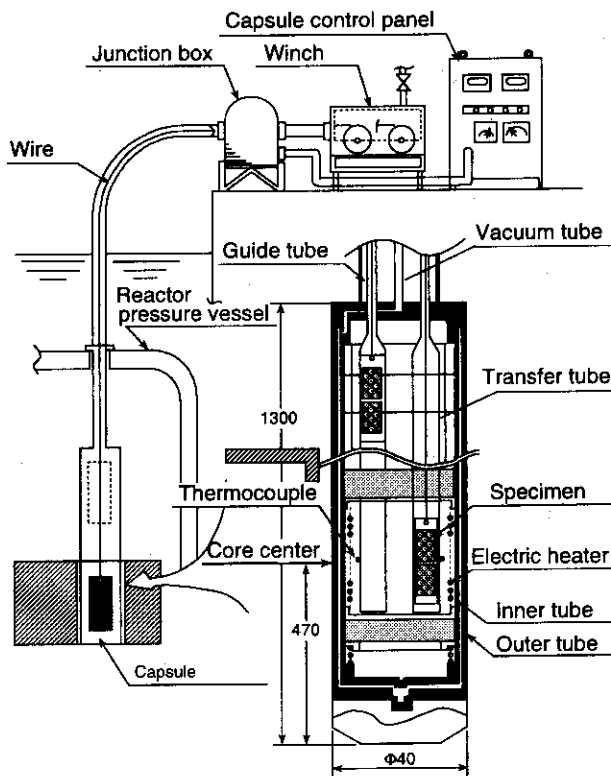


Fig. 3.4.5
Neutron fluence and temperature control capsule

De-calibration of Tungsten-Rhenium thermocouple

To evaluate a de-calibration of Tungsten-Rhenium thermocouple measuring a fuel centerline temperature on a nuclear transmutation, the electromotive force of a post-irradiated thermocouple was measured in the hot cell at Oarai Hot laboratory. And the measured results and the calculation code developing for the de-calibration was compared.

In the results of the examination, there was about a 30% reduction in the electromotive force at the neutron fluence 10^{21} n/cm² in the JMTR core. The measured value corresponded exactly with the value in the calculation.

Results of the test are shown in Fig. 3.4.6.

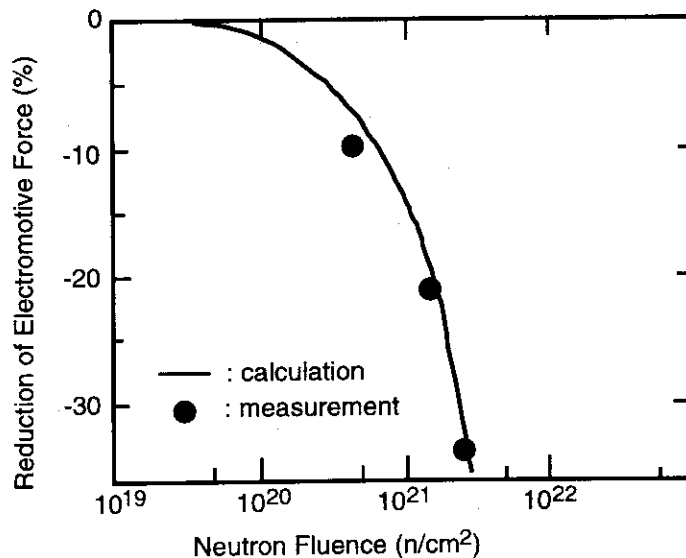
The inside cooling type capsule

Regarding an irradiation test of reactor structural materials, the specimen must be irradiated in the high neutron flux field of JMTR so as to get the high neutron fluence over a short time. However, this field is a high gamma heat generation area. Consequently, the irradiated temperature is higher in this area than the 300°C under the LWR condition, if an irradiation test is carried out by using a conventional capsule which is cooled only at the outside of the outer tube.

The inside cooling-type capsule, which is not only cooled at the outside but also at the inside of a capsule, was developed to get a lower temperature even in the high gamma heat generation area, and the irradiation test was carried out.

In the results of the irradiation test, an irradiated temperature for the tensile specimen of a rod type ($\phi 10 \times 55$ Lmm) was 200°C using the inside cooling-type from 400°C using a conventional capsule. As a result, the availability of the inside cooling-type capsule could be verified.

Fig. 3.4.6
Reduction of electromotive
force for a neutron dose



Re-utilization on the basket-type capsule

The basket-type capsule has been used to produce radio isotopes. This basket is scrapped after irradiation. If the handle of the upper end plug has a mechanism of the clip-type spring, the basket can be reused, and it is easy to manipulate in the hot cell. Now, the new type end plug has been developed. An outline of the capsule can be seen in Fig. 3.4.7.

Consequently, in the new type capsule, it is easy to take out the irradiation specimens from the basket without cutting the basket in the hot cell. Also, the radioactive waste can be reduced if the basket is reused.

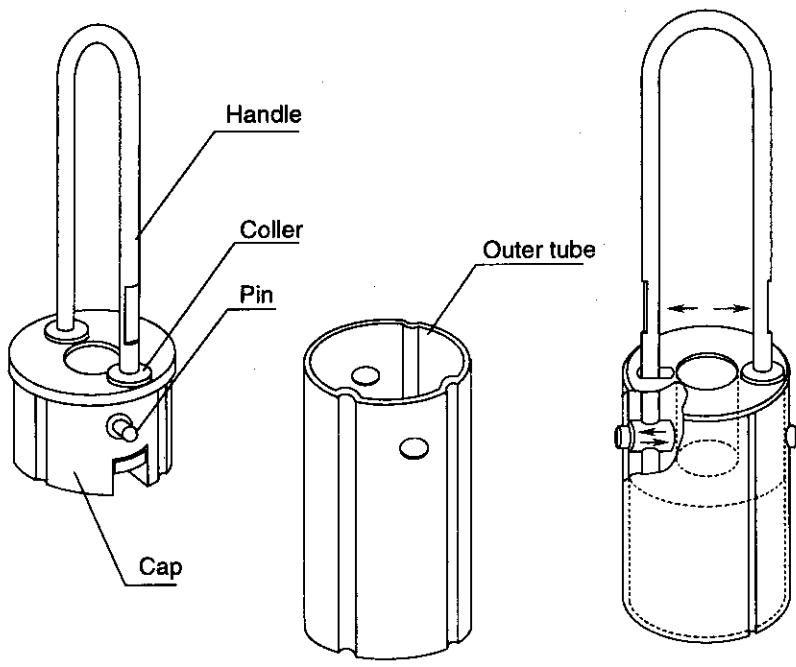


Fig. 3.4.7
Structure of an end plug
and an outer tube

3.5. Technological Development for a Fusion Reactor Blanket

In addition to demonstrating the physics of burning D-T plasma, an experimental reactor such as ITER will also be used to conduct a verification test of a blanket design. Therefore, it is essential for the design of the blanket to obtain engineering data, and several kinds of studies on blanket materials being continued in the JMTR project. The activities of irradiation studies on a fusion blanket for 1994 are shown in this section.

In-pile Functional Test at JMTR

1) Design study

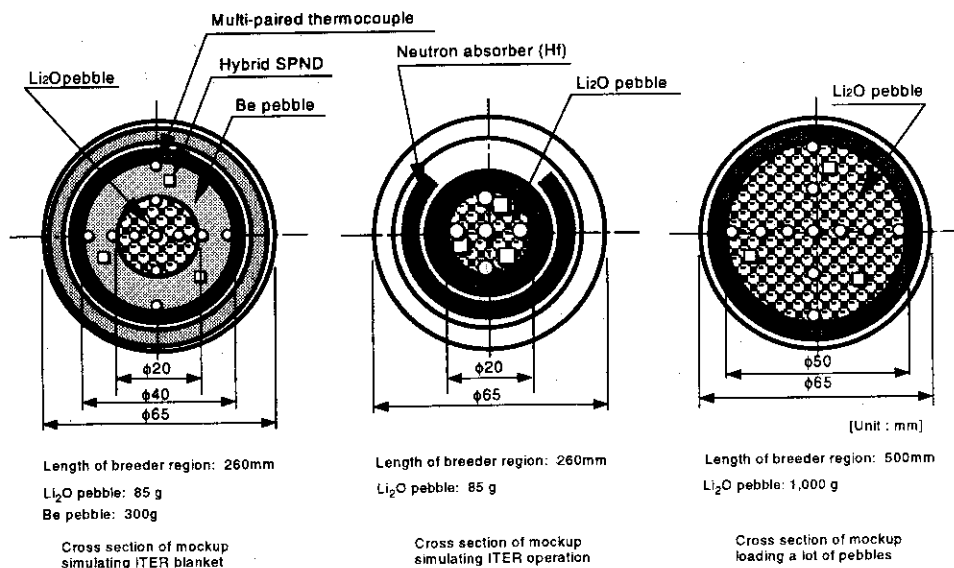
An in-pile functional test facility has been considered to obtain engineering data since 1991. The facility consists of a blanket mockup and a sweep gas system.

There are three types of mockups which are considered in the in-pile functional test : a mockup simulating the ITER blanket structure which has proposed by Japan, a mockup which can simulate the ITER operation pattern and a mockup loading a lot of breeder material pebbles. The cross sections of these mockups are shown in Fig. 3.5.1. The length of the breeder material region is about 40 cm which is determined so that the maximum tritium release from the mockup becomes 1.8×10^{11} Bq/d. Of these mockups, neutronic and thermal calculations were carried out for a mockup simulating the ITER blanket structure. The tritium production rate was about 2.8×10^{11} Bq/d and the temperature in the breeder region was in the range of 380-660°C which is suitable for a tritium release.

The sweep gas system is a system to measure and recover tritium released from the blanket mockup in order to acquire engineering data such as the temperature control characteristics in the breeder material region, nuclear properties and characteristic of tritium release and recovery rates. The detail design activity has been carried out and the followings were determined:

- specification of each component in the sweep gas system,
- construction drawings of an oxidation bed, a molecular sieve unit, an ceramic

Fig. 3.5.1
Cross sections of
three type mockups



electrolytic cell and a glove box,

- arrangement plan of each component in the glove box.

2) Development of instruments

Instruments such as a magnetic probe, a hybrid self-powered neutron detector, a sweep gas sensor, a multi-paired thermocouple and so on have been developed at JMTR. Of these instruments, the development of the sweep gas sensor is described here.

To obtain the engineering data for a design of a fusion blanket, it is necessary to purge the tritium produced in the mockup by sweep gas and to measure the tritium concentration in the sweep gas on line. In considering the tritium measuring system, the tritium release from the mockup is introduced to an ionization chamber to measure the tritium concentration in the sweep gas with a stainless steel pipe about 20m in length. However, bad effects such as tritium adsorption on the inner surface of the pipe and tritium diffusion from the pipe can be observed. Therefore, it is necessary to develop a sweep gas sensor which can measure the tritium concentration in a mockup directly without the above problem.

The sweep gas sensor has been fabricated on a trial basis. The perovskite-type oxide ($\text{CaZr}_{0.9}\text{In}_{0.1}\text{O}_{3-a}$) was selected as the solid electrolyte because it has good proton conduction at high temperatures in the range of 600-700°C. The mixture of $\text{AlPO}_4 \cdot x\text{H}_2\text{O}$ and $\text{La}_{0.4}\text{Sr}_{0.6}\text{CrO}_{3-a}$ was used as the solid standard material and its optimum mixture ratio was 1:9 in weight. The porous platinum electrodes were attached on the outer and inner surface of the sensor. The ceramic heater was installed inside the sensor so that this sensor could indicate good proton conduction. The structural drawing of the fabricated sweep gas sensor is shown in Fig. 3.5.2.

Verification tests such as an electromotive force test, a responsibility test and a durability test were carried out for the fabricated sensor with parameters of the hydrogen concentrations and temperatures. Furthermore, a γ -ray irradiation test was also carried out up to 2.2×10^6 Gy.

From the results of these tests, this sensor can be used at high temperatures from 600-700°C and has good response (about 20 s). Furthermore, there was no effect due to γ -ray irradiation up to 2.2×10^6 Gy. However, it was found that special care had to be taken in assembling the sensor because this sensor is very sensitive to contamination due to hydrogen.

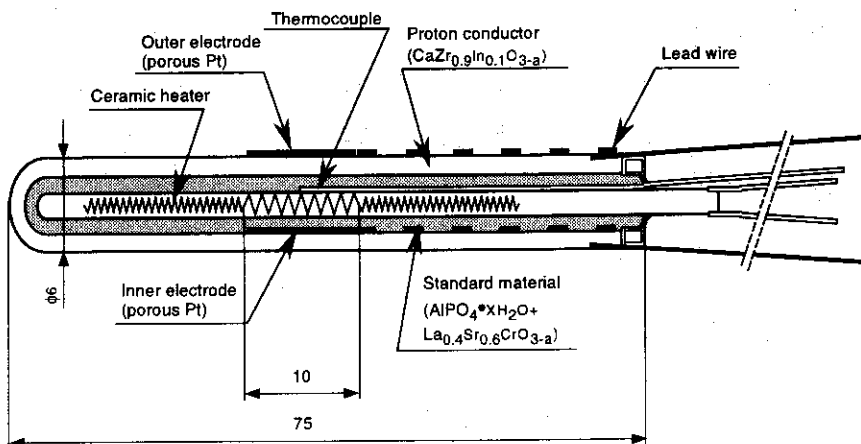


Fig. 3.5.2
Sweep gas sensor

If hydrogen exists inside the sensor except for the solid standard material, it can have an influence on the electromotive force. From now on, the irradiation test, with a fission reactor will be planned so as to evaluate the soundness in the neutron irradiation field.

Research and development on the tritium breeder and neutron multiplier materials

1) Development of the fabrication technology for tritium breeder materials

Lithium-contained ceramics have been considered as candidates for solid breeder materials for fusion reactors. In lithium ceramics, lithium oxide (Li_2O) is one of the best tritium breeders from the standpoint of high lithium density and high thermal conductivity. Several studies have been carried out on the fabrication of spherical Li_2O forms to reduce the induced thermal stress in the breeder. The melting granulation method and rotated granulation method have already established for the fabrication of ϕ 1mm Li_2O spheres. From the point of Li reprocessing, new fabrication methods are being studied by using the sol-gel method. The sol-gel method is best for fabrication of small Li_2O spheres from the reprocessing solution with lithium. The cost of the fabrication of small spheres will also decrease through the use of this method. The characteristics of lithium ceramics pebbles fabricated by these method are shown in Table 3.5.1. In the present work, preliminary fabrication tests of small Li_2O spheres are carried out using the sol-gel method.

The fabrication process is shown as follows:

- a) Fabrication of gel-spheres: The liquid mixture of Li_2CO_3 and polyvinyl alcohol (PVA) is dropped in cooled acetone through a nozzle and the gel-spheres are fabricated.
- b) Calcination of gel-spheres: PVA in the gel-spheres is removed and the Li_2CO_3 spheres are fabricated in this process.
- c) Thermal decomposition and sintering: The Li_2CO_3 spheres are heated in vacuum and then transformed to Li_2O spheres and sintered.

The main results obtained from preliminary fabrication test are as follows. It is obviously that the gel-spheres with high sphericity can be fabricated when the ratio of Li_2CO_3 and PVA in the mixture liquid is about 30 wt%. It was confirmed that Li_2CO_3 changed completely to Li_2O after thermal decomposition. From the results of this test, bright prospects are obtained concerning the basic fabrication process of small Li_2O spheres using the sol-gel method.

2) Characterization of beryllium (neutron multiplier materials)

For the beryllium studies as a neutron multiplier, the new apparatus for the tritium release and thermal constants measurements could be carried out in the glove boxes of the

Table 5.3.1
Characteristics of lithium
ceramics pebbles

	Melting granulated method	Rotated granulation method	Sol-Gel method
Sphericity	superior	good	(cultivating now)
Impurities	good	good	(good)
Mass production	possible	good	(superior)
Cost performance	difficult	good	(superior)
Reprocess	difficult	difficult	possible

new facility. The details of this new facility is shown in the section.

In the compatibility studies, the reaction between beryllium and copper alloy (OFC and beryllium-copper alloy) was studied by a diffusion couple test. It is summarized as follows:

- a) The reaction layer which consisted of a few layers was formed above 400°C, and the thickness became remarkable at 700°C.
- b) The reaction products which were formed by the reaction were the Be₂Cu phase and BeCu phase above 400°C, and the Be-Cu(B) phase was identified at 700°C in addition to the Be₂Cu phase and BeCu phase. The reaction products between cobalt and beryllium, and between cobalt and copper could not be identified.
- c) The thickness of the BeCu phase was linear to a square root of annealing time.

Compatibility between beryllium and ferritic stainless steel (F82H) under helium sweep gas (moisture: 100 ppm) was also studied. Oxidation of the beryllium surface was observed at 400-600°C. The reaction layer with beryllium in F82H was 10 μm at 600°C.

Technology Development related to the Fusion Blanket

1) Development of joint technology

High-strength, high-conductivity copper alloys are being considered for several magnetic fusion energy applications such as the first wall in high-power-density devices, resistive magnetic coils, and high-heat flux components. Cu-Cr-Zr alloy is an attractive candidate that possesses good room-temperature strength, ductility and conductivity, and maintains its best strength at temperatures up to 450 °C.

Recently, joint technology between Cu-Cr-Zr alloy and stainless steel(SS316) have been investigated for the solid-state diffusion bonding, the brazing joints, and so on. Friction welding is one of the most popular welding methods for jointing different materials. This welding method can be applied to join this copper alloy to SS316. A schematic diagram and the conditions of the friction welding method of Cu-alloy and SS316 are shown in Fig. 3.5.3. In the present work, a joint of Cu-alloy(Cu-1%Cr-1%Zr)/SS316 is examined by the

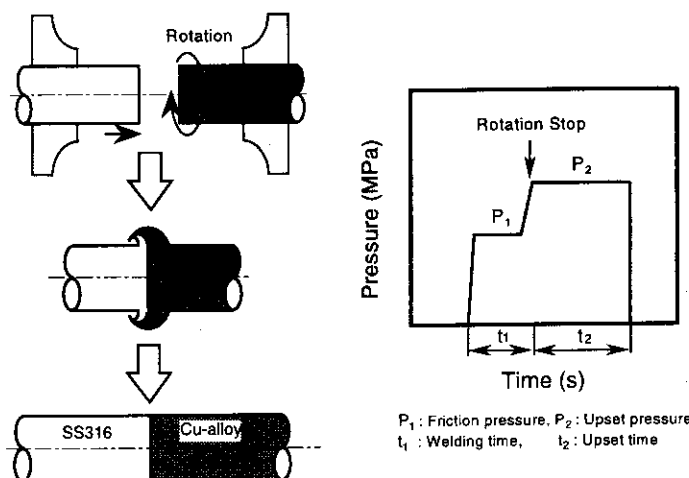


Fig. 3.5.3
Schematic draw and condition of friction welding method

friction welding method, and mechanical properties on the joint of Cu-alloy/SS316 was evaluated.

The results obtained are as follows. The optimum fabricating condition by friction welding has been obtained for joint of Cu-alloys/SS316 in these experiments. As for the friction condition, the rotational speed was 2200 rpm, and the friction pressure was 353 MPa. It was evident from a liquid penetrate test that good results were obtained for joint of Cu-Cr-Zr alloy/SS316 fabricated by friction welding. The tensile strength of Cu-Cr-Zr alloy/SS316 joint was 544 MPa and similar to the strength of base material (Cu-Cr-Zr alloy). These specimens broke on the base material side. It was found that a very narrow inter metallic compound layer was generated at this joint from metallographic observation and SEM/EPMA analysis. Therefore, useful data on the several characteristics of joints of Cu-Cr-Zr alloy/SS316 fabricated by friction welding were obtained for the design of a potential fusion reactor.

2) Reweldability test

Stainless steel is one of the candidate materials for fusion reactors. Rewelding of irradiated materials has a large influence on the design and maintenance scheme of in-vessel components from the point of helium accumulation in structural material. In the present work, rewelding joints of un-irradiated and/or irradiated stainless steel are examined using the tungsten inert gas (TIG) welding method for evaluation of the mechanical properties of their joints. The details will be shown later (see section 4.6).

3) Development of ceramic coating technology

Ceramic coating on the surface of structural materials such as SS316 is being considered for an electrical insulator and a tritium permeation barrier for fusion reactors. Y_2O_3 is one of the most promising materials as a coating material. However, cracks and peeling occur due to the difference in thermal expansion between SS316 substrate and Y_2O_3 coating. Therefore, undercoating between SS316 substrate and Y_2O_3 coating is indispensable to prevent cracks and peeling of the Y_2O_3 coating. From this point, the effect of the undercoating regarding the properties of the Y_2O_3 coating was investigated.

For the undercoating, SS410 was selected because the thermal expansion coefficient of 410SS was close to that of Y_2O_3 . Thickness of SS410 undercoating was about 150 μ m. Y_2O_3 was coated by an atmospheric plasma spray and densified by impregnation with a $Y(NO_3)_3$ solution and sintered at 500°C to close the pores. Densification treatment of the Y_2O_3 coating was set at 6 cycles.

The undercoating was performed using two plasma spray methods (atmospheric plasma spray (APS) and vacuum plasma spray (VPS)) and with two 410SS particle sizes (10-45 μ m and 10-74 μ m).

Case 1 : APS using 10-45 μ m 410SS particle size

Case 2 : APS using 10-75 μ m 410SS particle size

Case 3 : VPS using 10-45 μ m 410SS particle size

Case 4 : VPS using 10-75 μ m 410SS particle size

The optimum fabrication condition was selected on the basis of the results from the

thermal shock tests. Thermal shock tests were performed by water quenching from 500, 600, 700 and 800°C. The results of the thermal shock tests are shown in Fig. 3.5.4.

In the thermal shock tests at 500°C, the Y₂O₃ coating undercoated by Case 1 and 2 was inferior in thermal shock resistivity more than Y₂O₃ coating undercoated by Case 3 and 4. In the thermal shock tests above 600°C, Y₂O₃ coating undercoated by Case 3 was superior in thermal shock resistivity more than Y₂O₃ coating undercoated by Case 1, 2 and 4.

Surface roughness of the SS410 undercoat fabricated by the same spray method using a different particle size of SS410 showed that the roughness of SS410 using a 10-74 μm particle size was greater than that using a 10-45 μm particle size. Surface roughness of the SS410 undercoat fabricated by different spray methods using the same particle size of SS410 showed that the roughness of SS410 by VPS was larger than that by APS. Pores in the region of the SS410 undercoat by VPS were found to coat unmelted SS410 particles. It was considered that the thermal stress due to the thermal shock test was lessened by the roughness on the surface of SS410 undercoat and by the pores in SS410 undercoat.

From the results of the thermal shock test of the Y₂O₃ coating, it was obvious that the thermal shock resistivity of the Y₂O₃ coating could be improved for the SS410 undercoat fabricated by VPS using a 10-45 μm SS410 particle size.

4) Thermal shock tests of plasma facing materials

Plasma facing components such as the first wall and the divertor plate are exposed to a high heat load and high energy particles generated by the plasma, and it is necessary to develop plasma facing components which can withstand the heat load, etc. Therefore, electron beam heating facility ("OHBS", Oarai Hot-cell electron Beam Irradiating System) have established at hot cell at the JMTR hot laboratory in order to estimate thermal shock resistivity of plasma facing materials and heat removal capabilities of divertor element under a steady-state heat load. The details will be given later (see section 4.6).

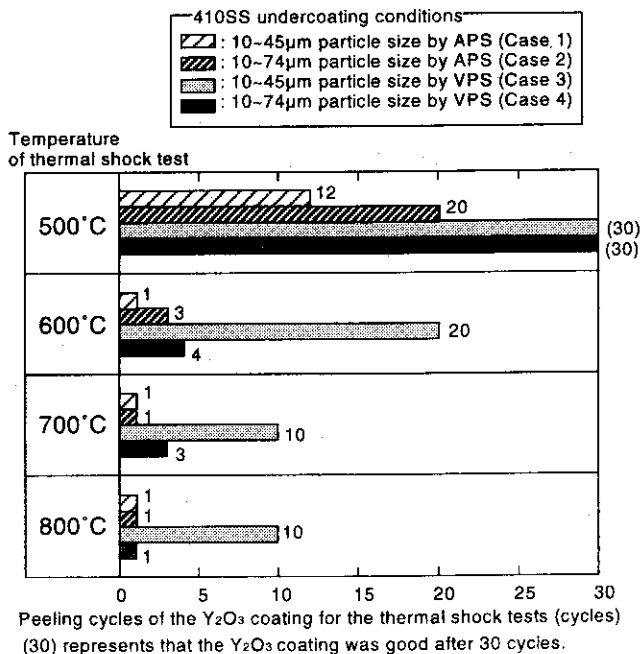


Fig. 3.5.4 Results of thermal shock tests

3.6. Experimental study on advanced irradiation field

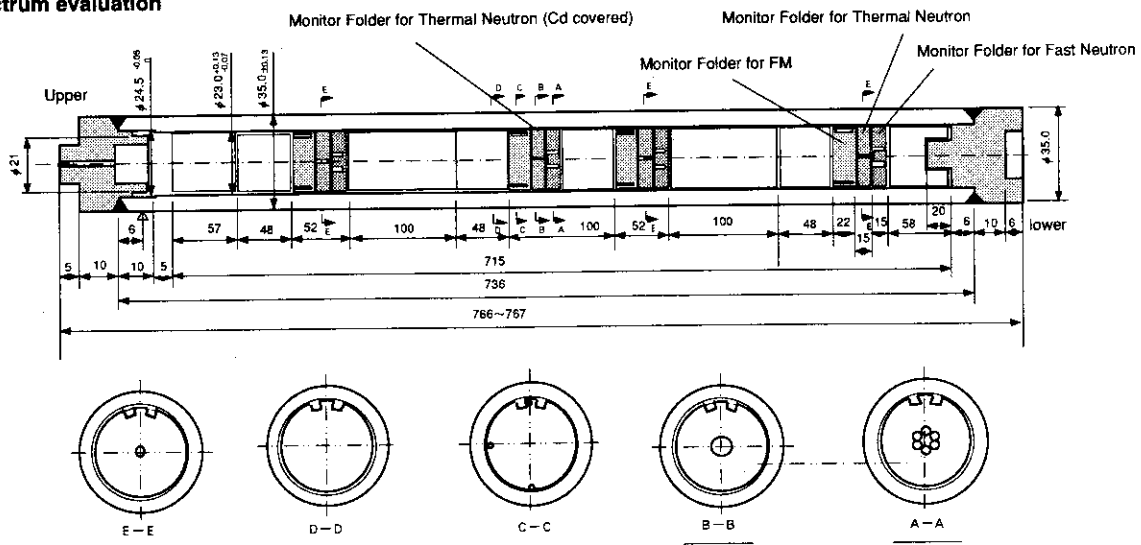
Outline

With the progress in nuclear material development, the needs regarding irradiation test has shifted to high quality and high precision. Since effect of neutron energy spectrum on the irradiation damage is regarded as important from the viewpoint of irradiation correlation, detailed spectrum information and neutron spectrum adjustment are needed in irradiation tests for R&D of light water reactors or fusion reactor materials. The technology development to positively respond to these irradiation needs was started at JMTR since 1992.

Development of neutron spectrum evaluation technology

On irradiation tests at JMTR, neutron energy spectra evaluated at each layer in reactor core of JMTRC (JMTR Critical Facility) by the multi-foil method were provided to the users. These layer-dependent spectra have been predicted with satisfactory precision for the fast neutron range, the precision in thermal neutron range of the spectra is however has not been confirmed. It is difficult to evaluate thermal neutrons at the local position like at a sample position due to the strong dependence on capsule structure materials. The development of whole energy spectra evaluation technology is therefore still being conducted. The spectrum measurement experiments with multiple activation wires were started from 1994, and the irradiation at JMTR with the wires was finished. Wires of Ag, Au and Co were used as thermal neutron range monitor, and wires of Ti, Mn, Cu, Ni, Fe and Nb were used as the fast neutron range monitor. A schematic of the capsule used for irradiation is shown in Fig. 3.6.1. The dismantling work of the irradiated wires for activation measurement was started and preparation of NEUPAC code for spectrum adjustment was continued. The data on the adjustment of neutron spectrum will be obtained at an end in FY1995.

Fig. 3.6.1
A schematic of the capsule
used for neutron energy
spectrum evaluation



Development of neutron spectrum adjustment irradiation technology

In recent studies on the irradiation behavior of fusion reactor materials, a demand has risen for irradiation tests under an adjusted neutron energy spectrum by the controlling thermal to fast neutron flux ratio. Neutronics calculations have been performed to obtain the spectrum adjusting ability for a method of arranging neutron absorption materials or neutron slowdown materials in an irradiation capsule at JMTR. For this technology development, a new calculation code was developed in FY1993 to evaluate the helium production due to a nickel two-step reaction, which was one of the important irradiation parameters for spectrum adjusted irradiation. Using this code, the spectrum adjusting ability to irradiate austenitic stainless steel under a simulating fusion reactor condition ($\text{He appm/dpa} = 15$) was studied, and it was made clear that He(appm)/dpa could be in the range of 13 ~ 15. In FY1994, as a comprehensive study on neutron spectrum adjustment, a neutronics analysis was carried out for a possible helium production range in austenitic stainless steel under constant neutron fluence represented by dpa. The analytical results are shown in Fig. 3.6.2. This figure shows that helium production could be controlled in the range of 1.4 to 12 appm at 2 dpa with the thermal neutron adjustment element being made of cadmium or graphite. The calculation precision of the helium production is to be evaluated experimentally.

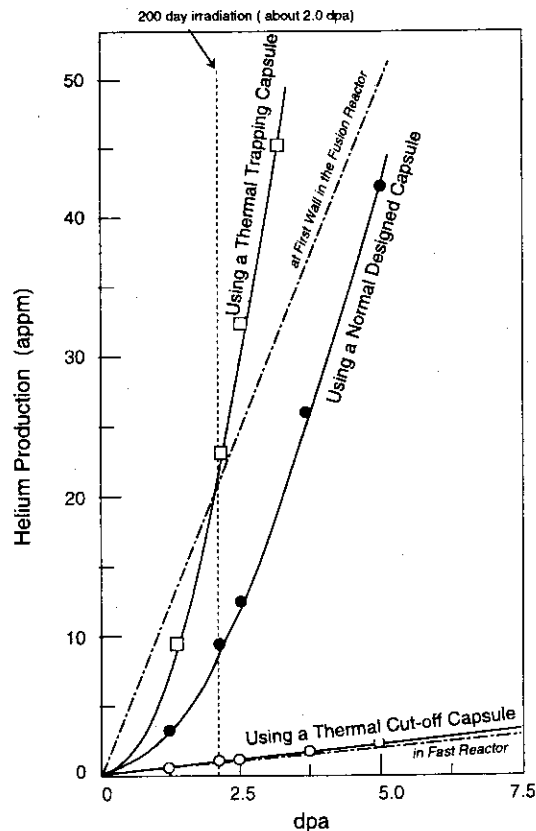


Fig. 3.6.2
Analytical results of
Helium production in
304 stainless steel

4. R&D and Major Achievements in Recent Years

4.1. Present situation and future plans for the LWR fuel tests

To study the safety of the LWR fuel and confirm the integrity of the high performance fuel for BWR at JMTR, the design and fabrication of a power ramping test facility was started in 1978, and the facility has been operating ever since 1981. The investigation into the safety of the LWR fuel is being carried out according to "The Yearly Program for Safety Research of the Reactor Facilities" promoted by the Atomic Energy Safety Commission, and includes the following :

- (1) Study of the fuel failure mechanism caused by mechanical and chemical interaction, i.e., PCI/SCC.
- (2) Evaluation and verification of the computing code for irradiation behavior analysis developed on the basis of data from both inside and outside the country.
- (3) Study of the fuel failure correlation under various power ramping conditions for determining the fuel failure threshold.

The high performance fuel, zirconium-liner cladding, have been developed according to "The Verification Program for High Performance LWR Fuels" (this program was changed to "The Verification Program for High Performance and High Burnup LWR Fuel" in 1988) enforced by Ministry of International Trade and Industry. And in order to confirm the integrity of these types of fuel the following tests should be conducted:

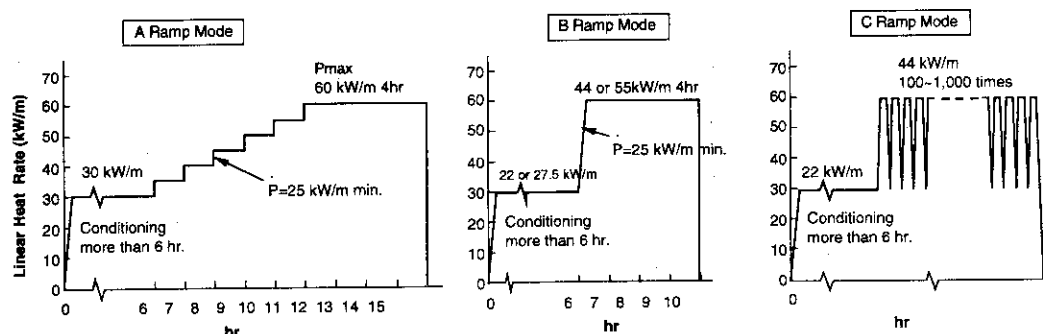
- (1) Test specifying the fuel failure threshold.
- (2) Verification test for integrity of the fuel adjacent to control rods against a rapid power increase caused by control rods movement.
- (3) A power cycling test for confirming integrity under flexible power operation required to meet daily, weekly and seasonal variations in power demand.

Power ramping test modes

There are various kinds of power ramping test modes according to the with testing purpose, however, one test mode for a fuel rod to be tested is generally selected out of the three typical modes shown in Fig. 4.1.1.

The first one is a multi-step ramp mode called the A ramp mode by which the fuel failure threshold is obtained. In this case, the linear heat rate of the fuel rod is increased

Fig. 4.1.1
Power ramping test modes



from 30 kW/m to 60 kW/m at interval increases of 5 kW/m. This ramp mode is also used for obtaining the relationship between He-3 gas pressure and linear heat rate of fuel rod as shown in Fig. 4.1.2.

The second one is a single step ramp mode called the B ramp mode which is used for confirming the integrity of fuel rods under similar conditions of a rapid power change caused by the movement of the adjacent control rods. In this mode, the power level is rapidly doubled, such as 22 kW/m to 44 kW/m or 27.5 kW/m to 55 kW/m. This ramp mode is also used to confirm the safety margin under abnormal power transients.

The last is a cycling ramp mode called the C ramp mode in which the power level is changed cyclically for confirming the integrity of fuel rods under flexible power operational conditions. The power level is generally changed from 22 to 44 kW/m, and the number of cycles is usually set up from 100 to 1,000 times for testing purposes and taking account of the operational conditions of JMTR.

Present situation and future plans of the power ramping test

For a safety study of LWR fuel, fresh LWR fuel rods had been subjected to various kinds of power ramping tests in the early stage. To study the fission gas release behavior during the power ramping tests, re-instrumented fuel rods which were individually welded with a pressure gauge to the refabricated LWR fuel rods have been carried out for the power ramping tests ever since 1990. These refabricated fuel rods were cut from full length spent LWR fuels.

For measuring both the fission gas pressure and the centerline temperature of fuel pellets during power ramping tests, a dual re-instrumentation technique has been developed. This technique involves installing a pressure gauge and a thermocouple onto a fuel rod.

The power ramping tests for the BWR high performance fuel were started in 1987 and finished in 1992. The tests were performed on 26 segmented fuel rods. As the following step of the BWR high performance fuel, the BWR high burnup fuel is being developed, and their power ramping tests were started from February 1994.

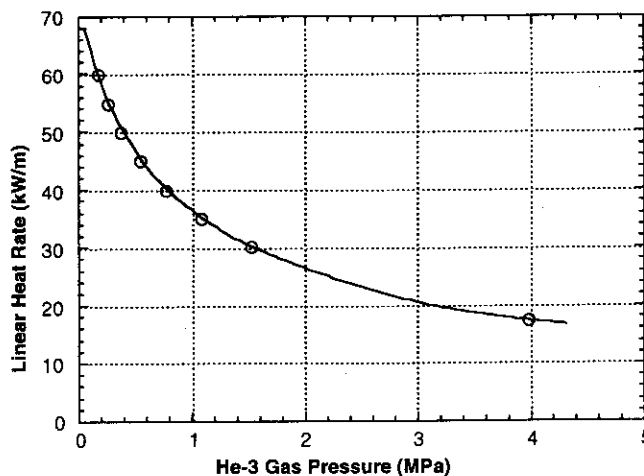


Fig. 4.1.2
Relationship between
He-3 gas pressure and
linear heat rate

4.2. Irradiation effect of stainless steel at a high exposure by neutrons

Purpose

The in-pile tubes which were developed at JMTR were made of stainless steel called SUS 316TP under the Japanese Industrial Standard (JIS). This stainless steel had little data regarding the mechanical properties of the irradiation effect at a high neutron fluence at JMTR. The assessment on the irradiation damage of the in-pile tube has been carried out by using data of the surveillance of test pieces which had been done in JMTR under a neutron fluence of $3 \times 10^{25} \text{ n/m}^2 (>1\text{MeV})$. For getting the data of mechanical properties at a high neutron fluence $1 \times 10^{26} \text{ n/m}^2 (>1\text{MeV})$, the stainless steel had been irradiated in JMTR. In order to extend the operating life of in-pile tubes installed at JMTR core, tensile test and charpy impact test were conducted at the JMTR Hot Laboratory. The results of these tests are shown below.

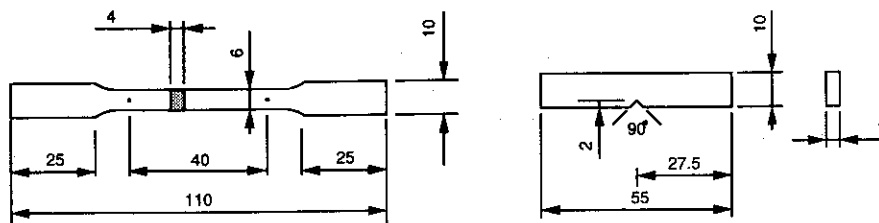
Test specimens

The test specimens and the OWL-2 in-pile tube were cut out of a stainless steel tube. The analysis report is shown in Table 4.2.1. The tensile test specimens and the charpy impact test specimens are shown in Fig. 4.2.1. These test specimens were cut out along the axis.

Table 4.2.1
Analysis report

Article : Seamless Stainless Steel Pipe (Cold drawn)													
Specification : JIS G3459 (SUS316)													
Size : 117.8mm ^φ O.D. x 4.8mm													
Hydrostatic Test	Surface and Dimensions		Description of Tests	Remarks									
13.7 MPa			Flattening	Liquid Penetrant Examination..... good									
good	good		good	Ultrasonic Test..... good									
				Straightness (1/1500)..... good									
Mechanical Properties			Chemical Compositions										
	Yield Strength (MPa)	Tensile Strength (MPa)	Elongation (%) in 50 mm	C	Si	Mn	P	S	Ta	Ni	Cr	Mo	Co
min.	206	510	31							10.00	16.00	2.00	
Std.				.08	1.00	2.00	.040	.030		14.00	18.00	3.00	
max.													
—	274	559	59	.05	.63	1.80	.024	.007	Trace	13.30	17.00	2.16	.29
	265	578	60	.05	.64	1.77	.024	.006		13.40	17.00	2.15	.29

Fig. 4.2.1
Tensile test specimen (left)
and the charpy impact test specimen (right)



Irradiation conditions

The test specimens which were put in the unsealed capsule were irradiated in the JMTR core. All irradiation holes in the JMTR core have a wide neutron flux by shifting the height of the hole. The neutron fluence of the test specimens had been varied by shifting the height in the capsule. Therefore, the test specimens, which had a wide neutron fluence, were acquired at the irradiation hole in the JMTR core.

The temperatures of the test specimens were between 40 and 50°C which were as much as the temperature of the primary coolant of the reactor, because the test specimens in the unsealed capsule were directly cooled by the primary coolant of the reactor.

Post irradiation test

A post irradiation tests were carried out in the Hot Laboratory adjacent to JMTR. In the post irradiation tests, a tensile test and charpy impact test were conducted. The tensile test was carried out at a specimen strain rate of 0.12 m/h. These tests were held at room temperature.

Results of the post irradiation tests

The effect of fast neutron fluence on the ultimate tensile strength, the yield strength and the fracture strength are shown in Fig. 4.2.2. The effect of fast neutron fluence on the

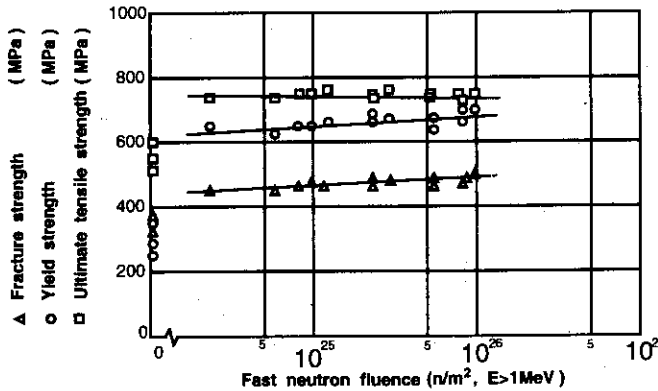


Fig. 4.2.2
Effect of fast neutron fluence on ultimate tensile strength, yield strength and fracture strength

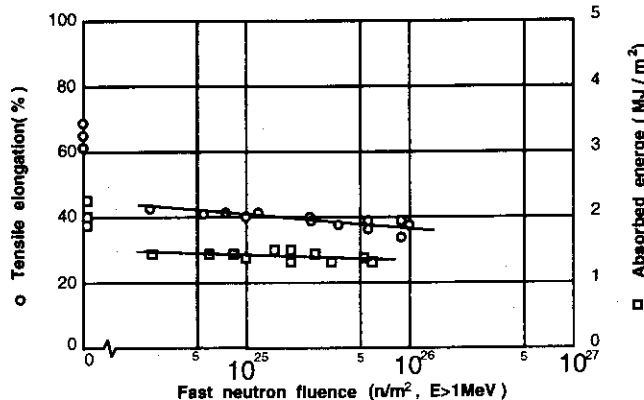


Fig. 4.2.3
Effect of fast neutron fluence on tensile elongation and charpy absorbed energy

tensile elongation and charpy absorbed energy can be seen in Fig. 4.2.3.

It is found that the data of the tensile strength, yield strength and fracture strength increased in comparison with the data of the non-irradiated specimens.

The tensile elongation slightly decreased between 1.0×10^{24} and 1.0×10^{26} n/m², a good elongation was able to remain at 1.0×10^{26} n/m².

The data of the absorbed energy in contrast with the data of non-irradiated specimens decreased. However, the ductility of the test specimens between 1.0×10^{24} and 6.2×10^{25} n/m² decreased slightly. Pictures of the fracture can be seen in Photo 1 through Photo 13.

Conclusion

From the results of the post irradiation tests, when the test specimens were irradiated at 1.0×10^{26} n/m², these test specimens retained their properties in that the tensile strength was 735 MPa, the yield strength was 715 MPa, the fracture strength was 500 MPa, and the tensile elongation was 37 %. When the stainless steel, which is called SUS316TP, was irradiated at 1.0×10^{26} n/m², the SUS316TP had sufficient strength. Therefore, the in-pile tubes which were installed in JMTR could be confirmed that extended time was available.

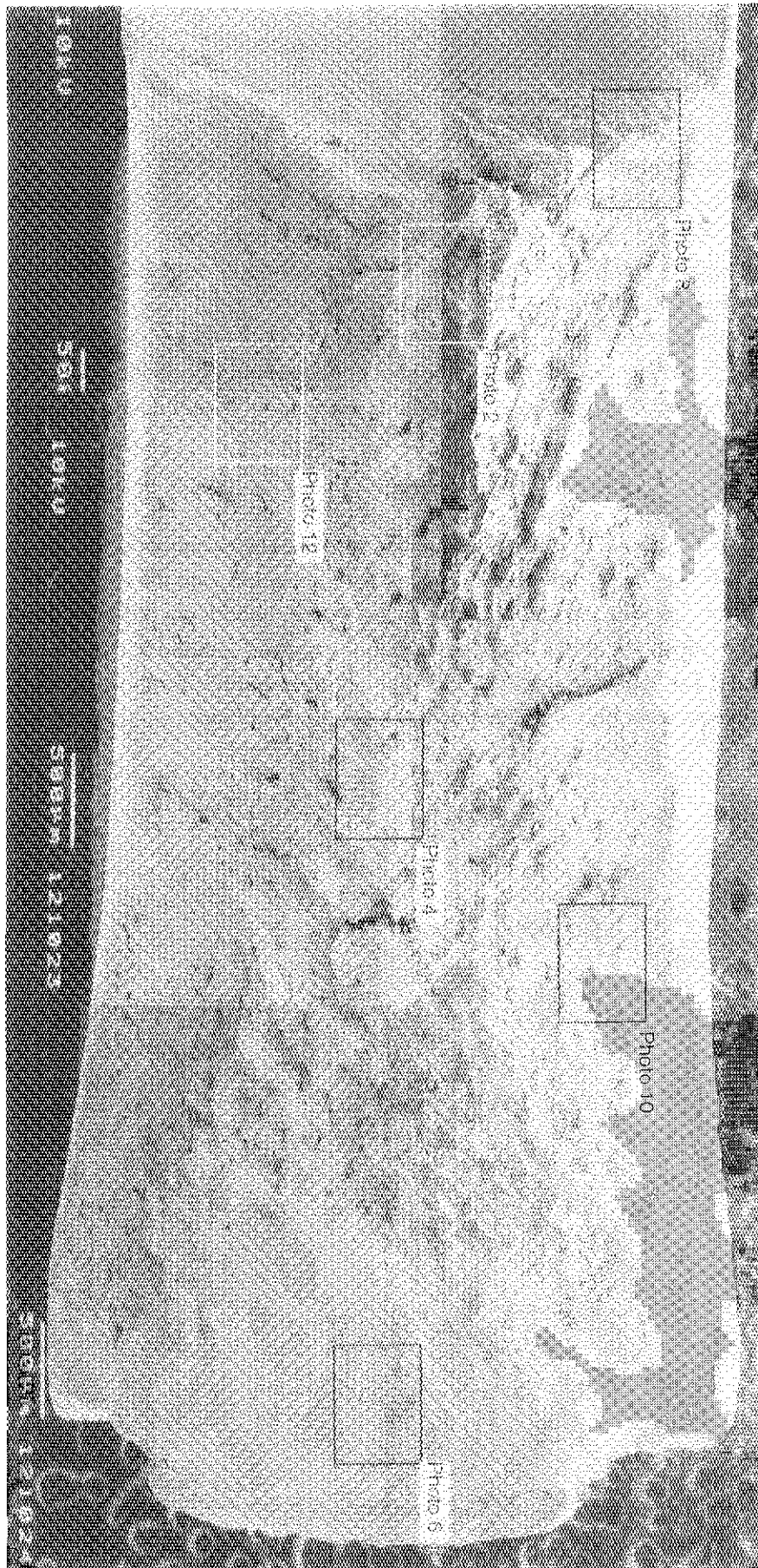


Photo 1

Photo 2 - 7

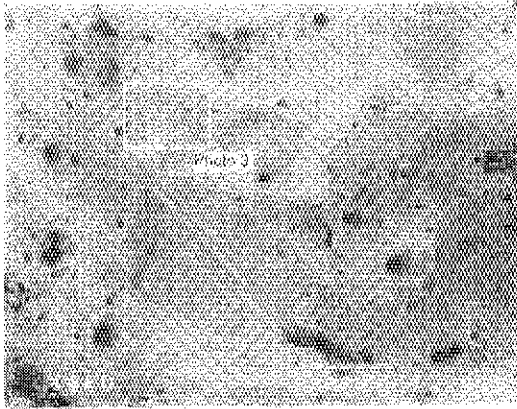


Photo 2

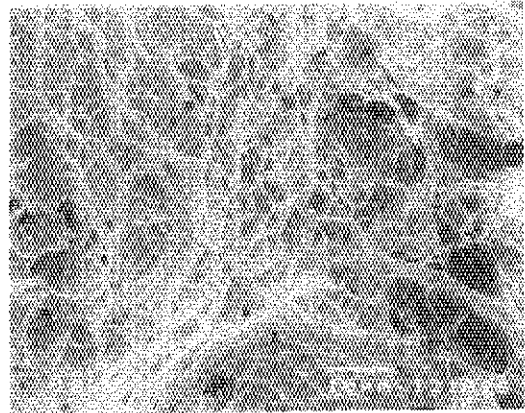


Photo 3

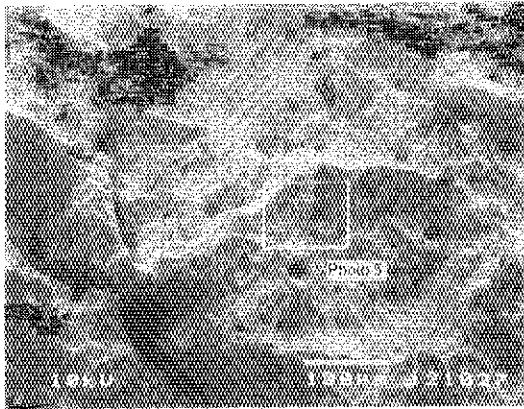


Photo 4

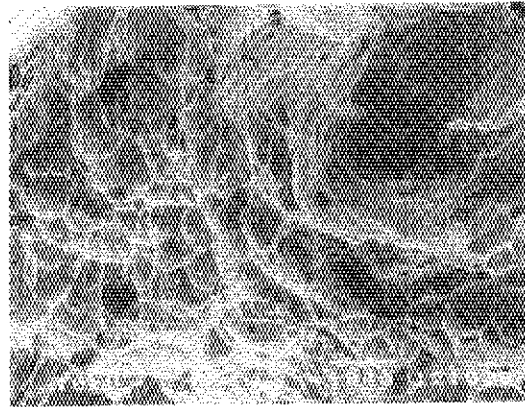


Photo 5

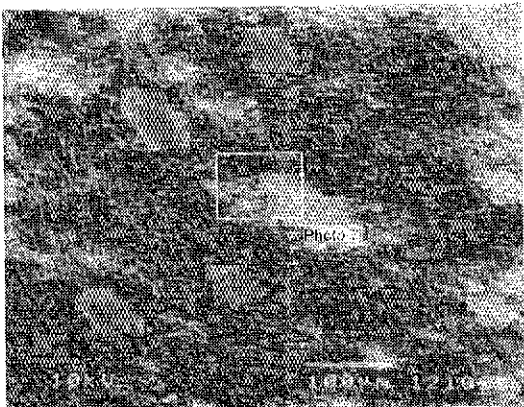


Photo 6

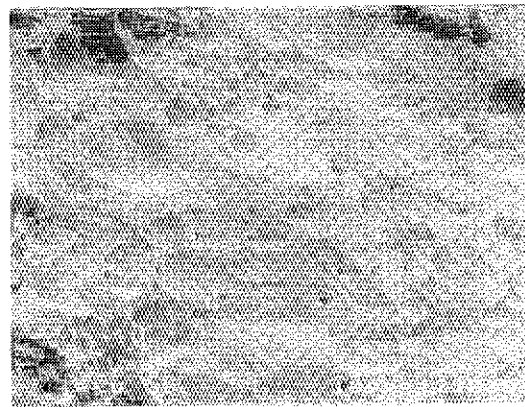


Photo 7

Photo 8 - 13



Photo 8

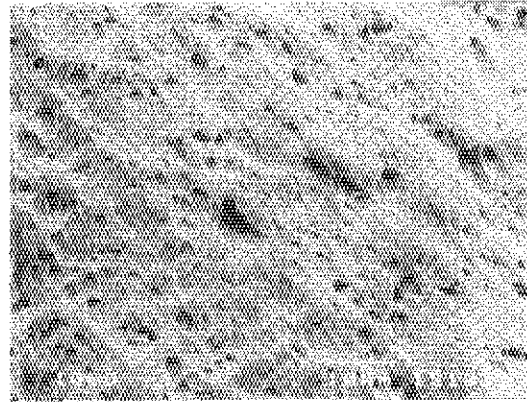


Photo 9

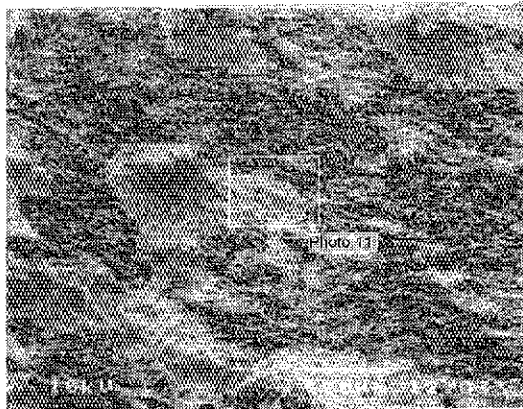


Photo 10

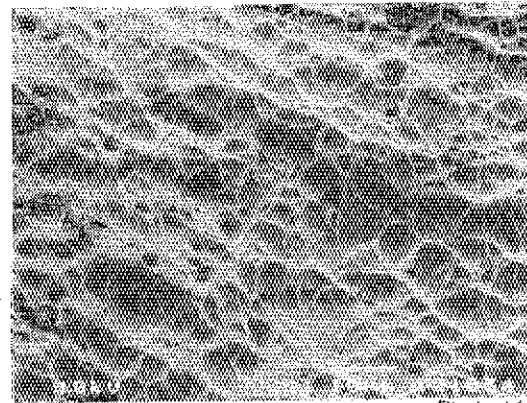


Photo 11

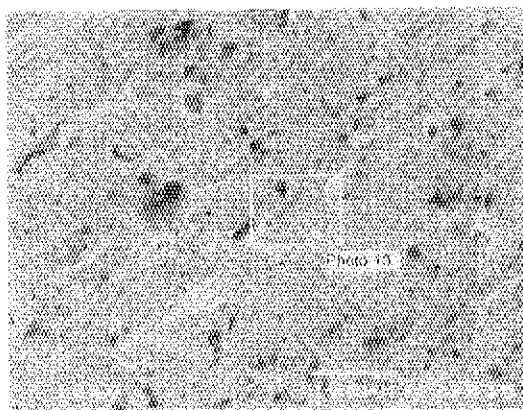


Photo 12

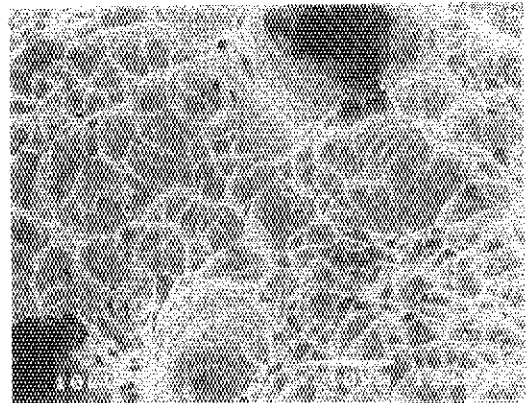


Photo 13

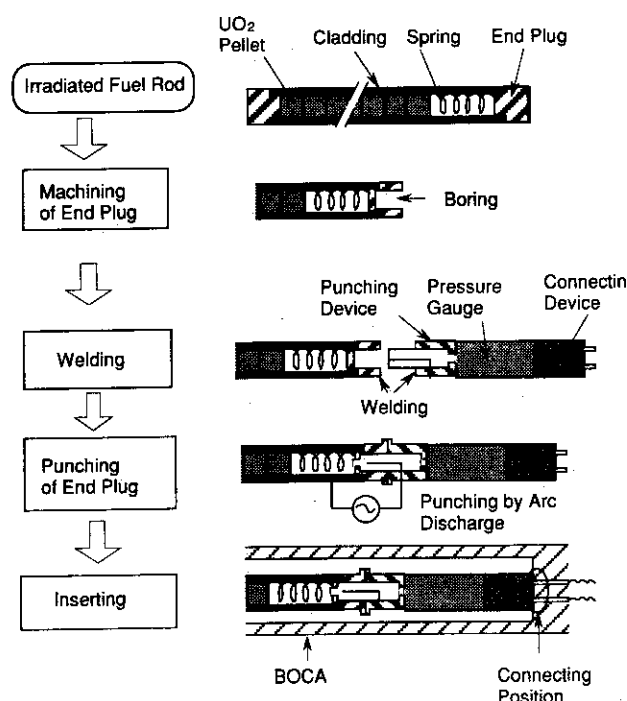
4.3. Re-instrumentation technique for irradiated fuel rod

The extension of the burnup of LWR fuel is one of the current important issues from an economical point of view. The information on fission product (FP) gas release and centerline temperature of fuel pellets during power transient are important to study the PCI mechanism of the LWR fuel rods. To study the irradiation behavior of high burnup LWR fuel, re-instrumentation to LWR fuel irradiated in LWRs of FP gas pressure gauge and thermocouple for center temperature measurement has been developed in the JMTR Project.

FP pressure gauge re-instrumentation technique

The re-instrumentation of the FP gas pressure gauge has been under development ever since 1985 at JMTR, and put into actual use currently through a successful demonstration of the test performed in 1990 using power ramping test facility, BOCA. The re-instrumentation procedure of the FP gas pressure gauge to an irradiated fuel rod is shown in Fig. 4.3.1. The fuel rod used for the demonstration test was a segmented fuel rod (length, 412 mm) irradiated up to about 25 GWd/t in a BWR. The FP gas pressure gauge was attached to the end plug of the fuel rod by TIG welding. Then, a perforation with a diameter of about 1.5 mm was made on the end plug by electric arc discharge to bring the FP gas from the inside of the fuel rod to the FP gas pressure gauge without gas leakage. The connector allows to bring the electric signal of FP gas pressure gauge to a data processing system. The schematic view of BOCA in which a fuel rod with an instrumentation device is loaded is given in Fig. 4.3.2. The FP gas pressure data obtained in the demonstration test is shown in Fig. 4.3.3. It was noted that the pressure increased when the linear heat rate of

Fig. 4.3.1
Re-instrumentation
proceduer of FP gas
pressure gauge to
irradiated fuel rod



the fuel decreased after the power ramping. A possible mechanism for the FP gas release during power reduction is that released (or reversed to tensile) thermal stress in the center part of pellet during power reduction leads to the growth and inter linkage of grain boundary bubbles, and that the fission gas accumulated at the grain boundary is released to a free volume through the open porosity formed by the inter linkage of grain boundary bubbles.

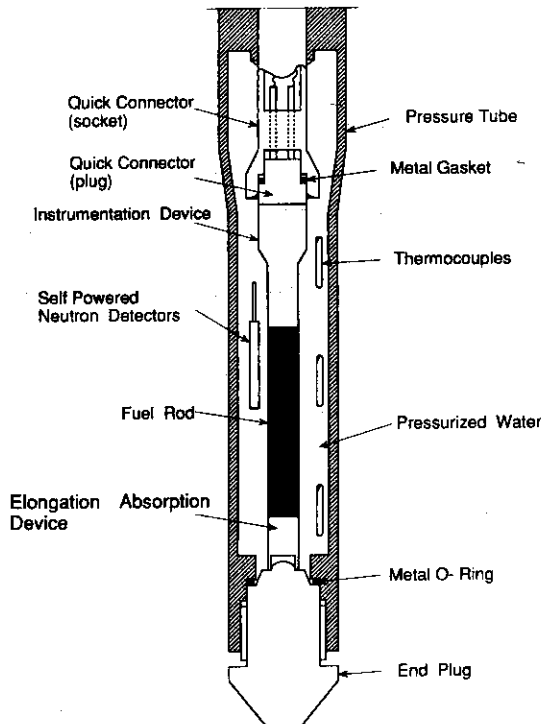


Fig. 4.3.2
Boiling water capsule (BOCA)
with instrumented fuel rod

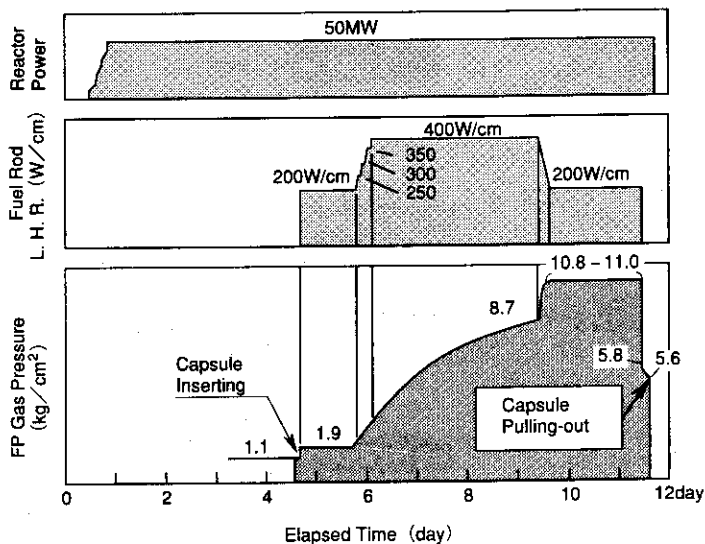


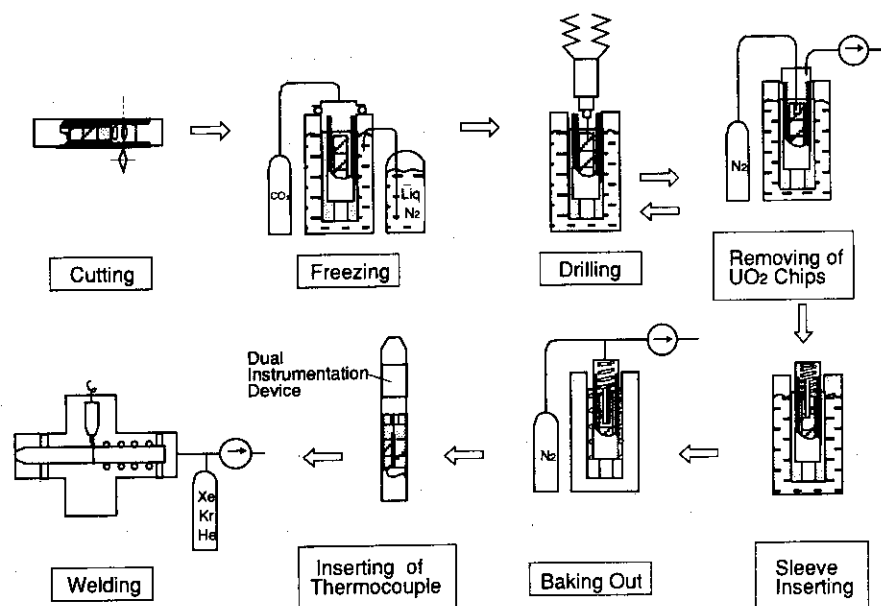
Fig. 4.3.3
FP gas pressure data obtained
in the demonstration test

Thermocouple re-instrumentation technique

In addition to the information of FP gas pressure, the fuel centerline temperature is highly desirable so as to study the irradiation behavior. Therefore, thermocouple re-instrumentation techniques have been developed since 1988. The re-instrumentation procedure of a thermocouple to irradiated fuel rod is shown in Fig. 4.3.4. A shortened fuel rod is used in the Hot Laboratory. Regarding this work, it is important to keep the pellets cracked in the power reactor. Therefore, the pellets are fixed by frozen carbon dioxide (CO_2) during the drilling work, and diamond drills are used to make the center hole. The re-instrumentation procedure of thermocouple to an irradiated fuel rods is performed in the following manner.

- (1) Cut the cladding of irradiated fuel rod.
- (2) Remove the cladding oxides at positions for subsequent welding processing.
- (3) Set the fuel rod into the center of a double container of drilling machine.
- (4) Pressurize the double container having a fuel rod up to 1 MPa with CO_2 gas at room temperature.
- (5) Freeze up the fuel rod with liquid nitrogen filled in the annular space of the double container. This situation is kept according procedures (6)-(9).
- (6) Drill a center hole into the fuel stack by diamond drills.
- (7) Remove the fuel chips from the center hole and top of an end pellet by a cleaning unit.
- (8) Repeat operations (6) and (7) until the depth of the center hole has reached the set

Fig. 4.3.4
Re-instrumentation procedure
of thermocouple to irradiated
fuel rod



value.

- (9) Insert a molybdenum tube into the center hole.
- (10) Heat the fuel rod slowly up to the room temperature.
- (11) Set the fuel rod in a drying unit with a transfer jig.
- (12) Bake out the remnant of CO₂ gas in vacuum, 573K for 24 hr.
- (13) Move the fuel rod with a transfer jig to another hot cell for thermocouple re-instrumentation.
- (14) Insert a thermocouple of dual instrumentation device into the center hole.
- (15) Weld the dual instrumentation device to the fuel rod.
- (16) Evacuate the fuel rod through a small hole of the end plug, then fill with the gas of the same composition and pressure as FP gas.
- (17) Seal the small hole by welding.

Various drilling tests were carried out using dummy fuel rods consisting of Zry-2 cladding and Ba₂FeO₃ pellets. These tests were completed successfully. A center hole, 54 mm in depth and 2.5 mm in diameter, was realized by these methods.

Dual re-instrumentation technique

The schematic drawing of the dual instrumentation device is shown in Fig. 4.3.5. The device consists of a thermocouple for the fuel centerline temperature measurement, a pressure gauge for the fuel rod inner pressure measurement and a quick connector for connecting the signal wires of the dual instrumentation device in BOCA. Design and manufacturing of the dual instrumentation device has been completed. The comprehensive demonstration test for dual re-instrumentation technique has been successfully carried out in FY1994. The fuel rod used for the demonstration test was a shortened fuel rod irradiated up to about 25 GWd/tU in a BWR. The irradiated fuel rod was instrumented with a dual instrumentation device according to the re-instrumentation procedure described above. In this work, it was realized to make a center hole with about 35 mm depth and 2.5 mm diameter into the irradiated fuel pellets. Figure 4.3.6 shows a photograph of the butt welding work of the dual instrumentation device to the fuel rod. As the last of the in-cell work, the dual instrumented fuel rod was inserted into BOCA. The in-cell demonstration test was

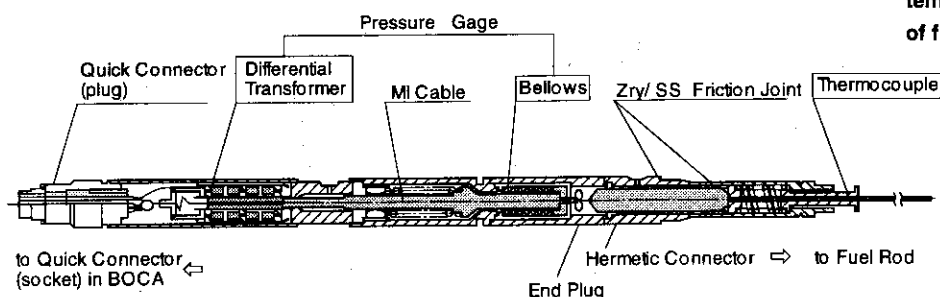


Fig. 4.3.5
Dual instrumentation device for measurements of centerline temperature and internal pressure of fuel rod

successfully completed. The BOCA in which the fuel rod with the dual instrumentation device was transported from the JMTR hot laboratory to the BOCA depository in the reactor pool of JMTR through the water canal. Then, BOCA was inserted into the reactor core of JMTR (in the 112th operation cycle) as the in-pile demonstration test in January 1995. In this test, the linear heat rate of the fuel rod was increased from 20 to 40 kW/m by intervals of 5 kW/m. Figure 4.3.7 shows the data of centerline temperature of the fuel rod by the W/Re type thermocouple of instrumentation device. The data of the centerline temperature showed good agreement with the calculated value. Using this technique, it is expected to carry out comprehensive experiments concerning the irradiation behavior of LWR fuel.

Fig. 4.3.6
A photo of welding the dual instrumentation to irradiated fuel rod

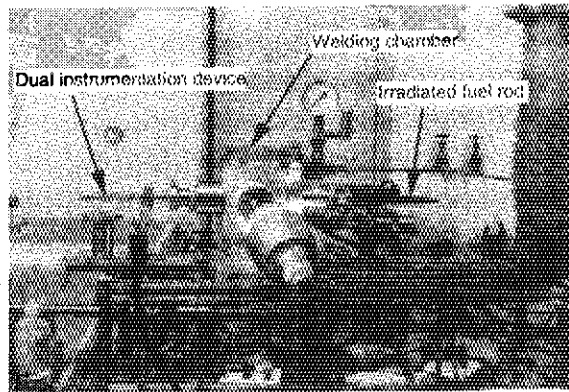
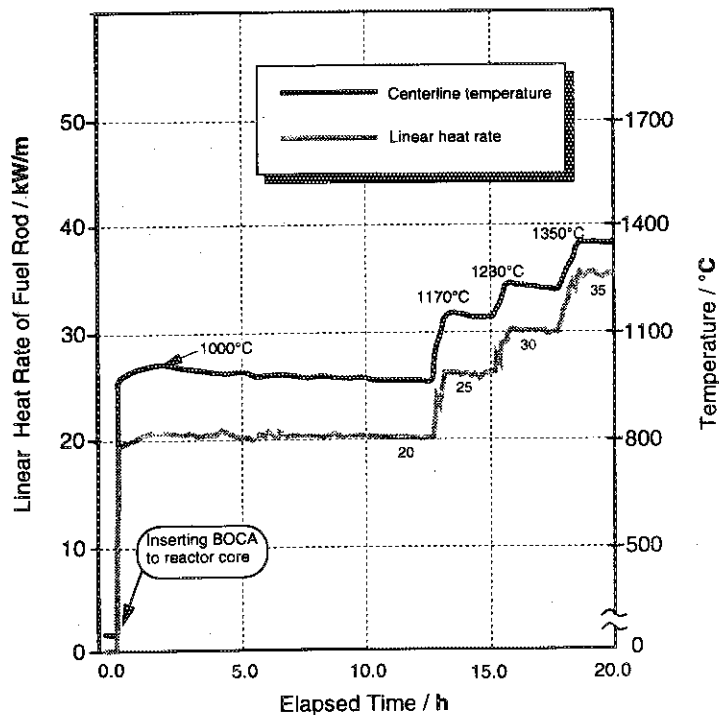


Fig. 4.3.7
Centerline temperature data of the fuel rod obtained in the demonstration test



4.4. Remote Controlled Scanning Electron Microscope (SEM)

It is very important for fractography after mechanical testing to study the mechanical properties on the fracture of irradiated materials. To carry out fractography, the remote controlled SEM apparatus has been developed and installed in a hot cell (lead #7 cell) in 1994. The apparatus consists of a main body, a sample stage, an operation console, vacuum system and so on. Figure 4.4.1 shows a schematic drawing of the apparatus. Also, Table 4.4.1 shows the specification and performance of the apparatus.

The improvements for the SEM apparatus concerning the influence of sample radio activities and manipulation were performed in the following manner.

- 1) To protect the γ -ray from the samples, the second electron detector was housed in a shielded box.
- 2) To examine the radioactive samples, the main body was installed in a hot cell.
- 3) To allow for easy operation and maintenance, the main parts were made as separable as possible.
- 4) To set the sample into the sample stage by remote operation, a variety of sample holders were prepared.

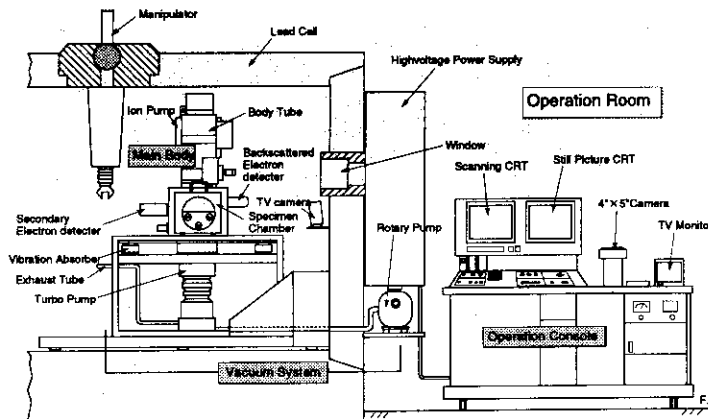


Fig. 4.4.1
Remote controlled scanning electron microscope

Table 1 Specification and Performance of the Remote Controlled SEM Apparatus

Part of Apparatus	Specifications and Performance
SEM Main Body	Resolution : 4.0nm(SEI 30kV,WD-8mm)
	Acceleration Voltage : 0.5 to 30 kV
	Probe Current : 10^{-12} to 10^{-6} A
	Signal Detector : Secondary Electron and Back scattered Electron Detector
	Gun Filament : LaB ₆
Sample Stage	Maximum available sample's diameter : 125mm ϕ
	Specimen Tilt Correction : -10 to +90°
	Drive Device : Motor Drive
Operation Console	Kind of image : Secondary Electron and Back scattered Electron Image
	Magnification : X15 to 200000
	Camera : 4"X5" size
Vacuum System	Automatic Regulation Function : Brightness/Contrast,Focus,Stigmator
	Vacuum System : Automatic
	Vacuum Pump(specimen Chamber) : Rotary and Turbo pump
	Vacuum Pump(Gun Filament Chamber) : Ion Pump

Table 4.4.1
Specifications and performance of the remote controlled SEM apparatus

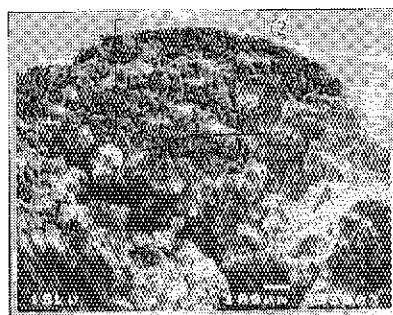
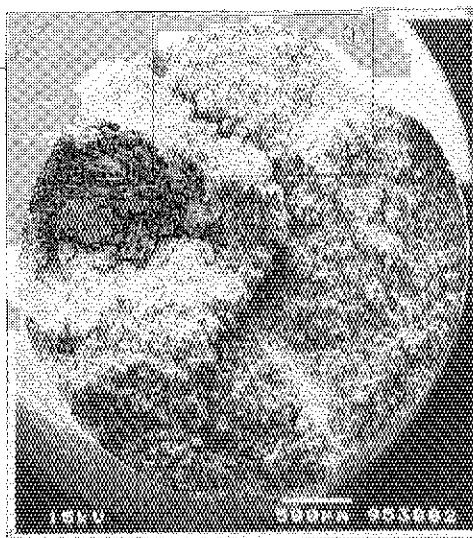
**SSRT:
Slow Strain Rate Test**

Typical SEM images of the fracture surface for the irradiated SSRT specimen are shown in Fig. 4.4.2.

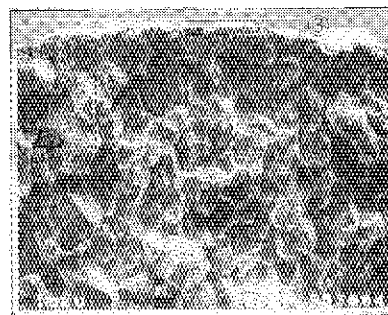
The fractographies of irradiated specimens with the SEM apparatus were carried out over for 140 hr in total, and the maximum dose rate of these samples was 20 mSv/h. Through these fractographies, the SEM apparatus has greatly contributed to the study of fracture mechanism of the irradiated materials.

Moreover, this apparatus has been installed in FY1994 as STA commissioned research.

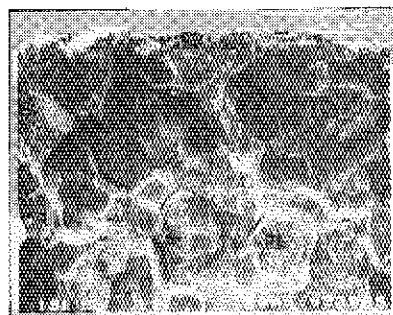
Fig. 4.4.2
SEM images of fracture surface
of SSRT specimen



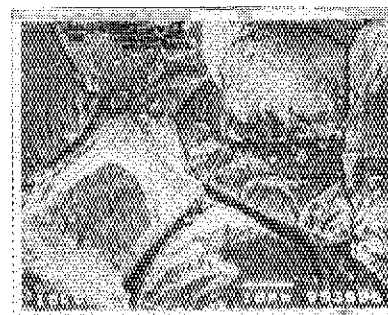
Enlarged photograph of the part ①



Enlarged photograph of the part ②



Enlarged photograph of the part ③



Enlarged photograph of the part ④

4.5. Examination technology with miniaturized specimens

To research and develop the materials for fusion reactor, small specimens will be irradiated in an accelerator which provides high energy neutron.

Therefore, the examination of miniaturized specimens are indispensable for evaluating mechanical property of materials. Also, the technical developments of miniaturized specimen test become important to evaluate mechanical properties of specimens which are manufactured from a small part of LWR structural materials. The technical development of tests has been pursued in cooperation with JAERI Tokai since 1987. In this framework, a small punch (SP) testing equipment and an electric discharge fabricating machine were installed in the hot cell in 1990.

The SP equipment shown in Fig. 4.5.1 is used for SP test of irradiated TEM (Transmission Electron Microscope) specimens and has an automatic specimen exchanger with a turntable which can test 12 specimens in one batch, under a vacuum condition and at temperature ranging from -160 to 750 °C.

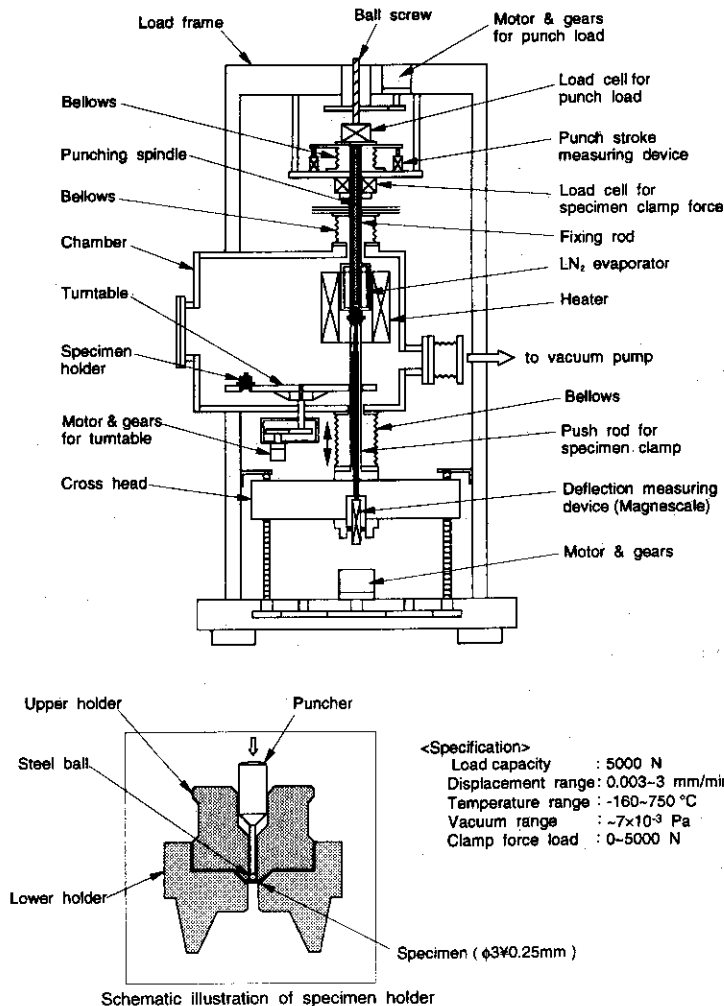


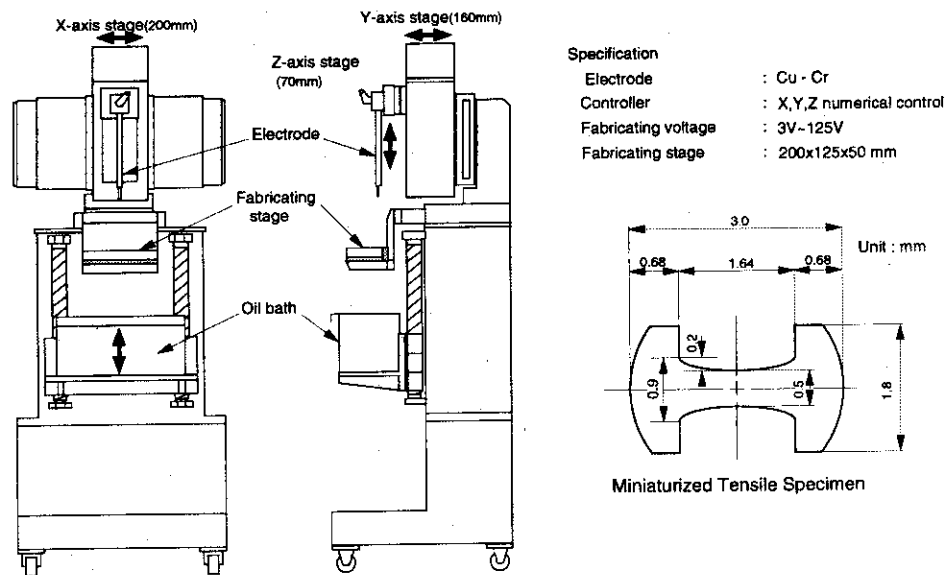
Fig. 4.5.1
Remote-type small punch testing machine

In FY1994, the temperature control system of the SP equipment was established for practical use, temperature ranging -160 °C to 750 °C.

The electric discharge fabricating machine shown in Fig. 4.5.2 is used to fabricate micro-tensile specimens from TEM specimens with $\phi 3 \times 0.25$ mm and SP specimens from Charpy impact specimens after testing. The machine consists of an electrode mechanism with X, Y and Z axes numerical control, a fabricating stage, an oil bath, a fabricating oil circulation pump, a filter and a controller.

For electric discharge fabricating machine, the manufacturing of an electrode and a fabricating stage were completed.

Fig. 4.5.2
Remote electrical discharge
fabricating machine



4.6. New PIE Facilities for the Fusion Reactor Development

In 1994, new facilities for the post irradiation examination of neutron irradiated fusion materials were constructed at the JMTR hot laboratory to get engineering data. Three kinds of new facilities; beryllium PIE facility, reweldability testing facility and electron beam heating facility (OHBIS) have been already installed in the hot laboratory, new-type tests are started in this year. Each position of new facilities is shown in Fig. 4.6.1.

Beryllium PIE facility

An outline of the beryllium PIE facility is shown in Fig. 4.6.2. This facility consists of the five glove boxes, dry air supplier, tritium monitoring and removal system, storage box of neutron irradiated beryllium. The exhaust of the normal mode (V1 and V3 open, V2 and V4 close) is conducted in the duct by That does this mean. The tritium removal system is operated by closed mode (V1 and V3 close, V2 and V4 open) when the detection of tritium concentration level is high.

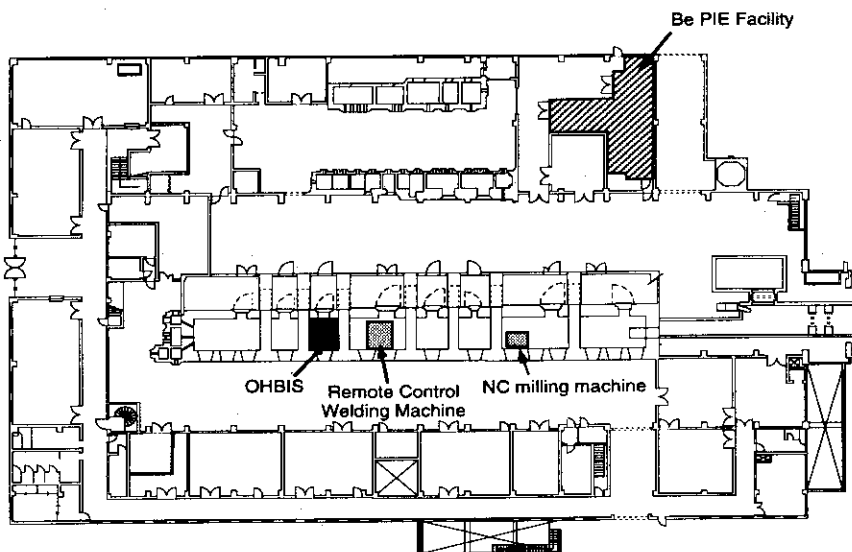


Fig. 4.6.1
Position of new facilities

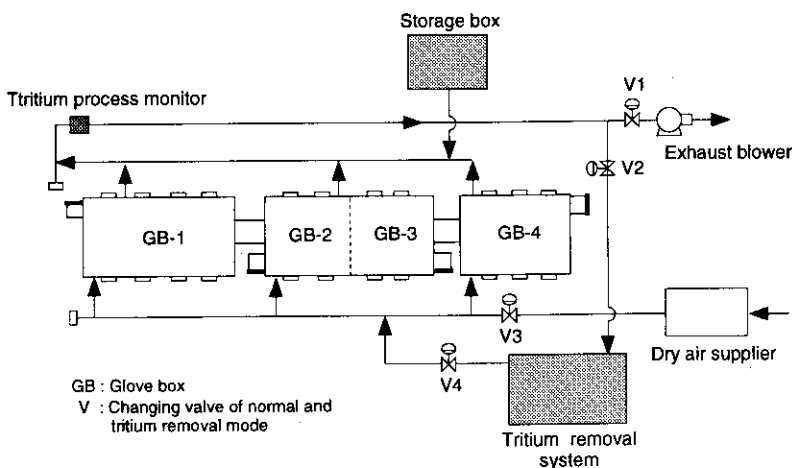


Fig. 4.6.2
Beryllium PIE facility

Samples handling are restricted by the amount of tritium; 7.4 GBq/day (200 mCi/day) and γ dose; 7.4 MBq/day in ^{60}Co equivalence.

At this new facility, the apparatus of tritium release and thermal constants measurement are equipped with glove boxes. The equipment for the mechanical test will be installed in 1996.

1) Tritium release apparatus

The new tritium release equipment with the function of pulse mode heating was developed by using the infrared ray furnace to demonstrate the pulse mode heating of tritium breeder blanket for the fusion reactor. This apparatus was installed in the glove box No.1. Tritium release apparatus consists of a carrier gas supplying system, a tritium release system, a tritium measurement system and a tritium removal system. The performance of a tritium release part is that the minimum time of rapid heating up to 1015 °C is about 119s and maximum heating rate reached at 1000 °C/min under helium sweep gas condition. The maximum temperature depends on the crucible materials due to the differences in infrared ray absorption. The conversion efficiency of the gaseous water by ceramic electrolysis cell for the tritium measurement part is more than 99.99 %. The pulse mode heating of the tritium breeder and neutron multiplier materials of the blanket could be demonstrated by using this apparatus. A vacuum heating equipment is also incorporated into tritium release to enable tritium and helium measurements.

2) Apparatus for thermal constant measurements

Equipment for the thermal constant measurement with the laser flush method was installed in the glove box No.4. This apparatus consists of a Nd glass laser, an electric furnace, a vacuum system and a tritium removal system. Thermal constant measurements are possible under the condition of RT.-1300 °C in vacuum. ($< 1 \times 10^{-7}$ Torr).

Reweldability test of irradiated materials by TIG welding method

Stainless steel and Inconel alloy are the candidate materials in a fusion reactor. Rewelding of irradiated materials has large impact on the design and the maintenance scheme of in-vessel components from the point of helium accumulation in the structural materials. In the present work, rewelding joints of un-irradiated and/or irradiated stainless steel and Inconel 625 are examined by the tungsten inert gas (TIG) welding method for evaluation of mechanical properties of their joints.

A flow chart of a reweldability test is shown in Fig.4.6.3. The rewelding specimens are made of 316 stainless steels (SS316, SS316LN) and Inconel 625 alloy. The irradiation capsules are fabricated and irradiated in JMTR. The rewelding joints of un-irradiated and/or irradiated stainless steels and Inconel 625 are fabricated using the remote control welding machine and milling machine in the hot laboratory of JMTR and characterized by tensile strength (Test Temperature: 20 and 200 °C), hardness, metallographical observation and SEM/XMA analysis.

From the results of the preliminary tests, useful data on several characterizations of reweldability by the TIG welding method were obtained for the design potential of a fusion reactor.

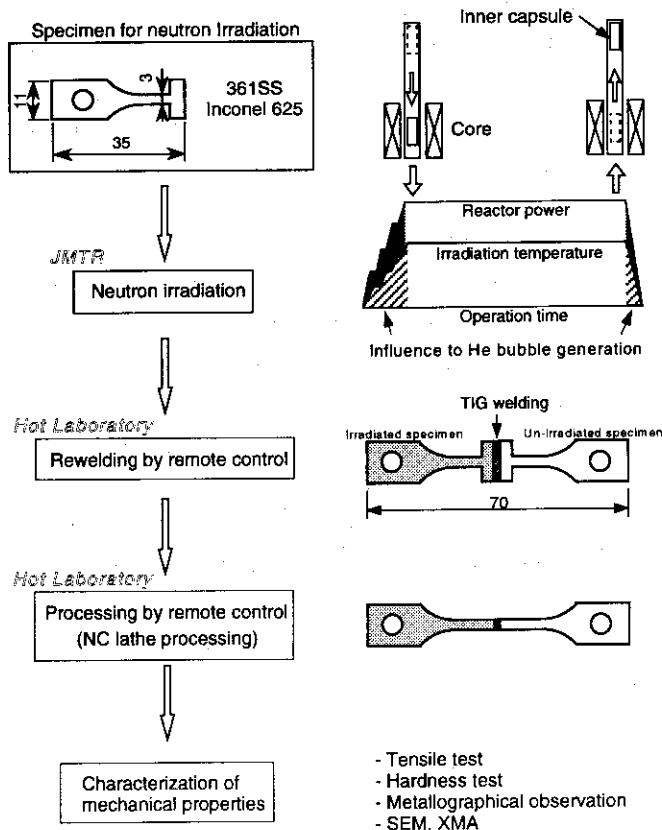
Electron beam heating facility

Since plasma facing components such as the first wall and the divertor are exposed to high heat load and high energy particles generated by plasma, it is urgent to develop plasma facing components which can with stand the heat load, etc.

Electron beam heating facility ("OHBIS", Orai Hot-cell electron Beam Irradiating System) is being established in a hot cell in JMTR hot laboratory in order to estimate thermal shock resistivity of plasma facing materials and heat removal capabilities of divertor element under a steady-state heat load. In this facility, un-irradiated / irradiated plasma facing materials (beryllium, carbon based materials and so on) and divertor elements can be treated.

A schematic view of OHBIS is shown in Fig. 4.6.4. This facility consists of an electron beam unit with the maximum beam power of 50 kW and the vacuum vessel. The acceleration voltage is 30 kV, and the maximum beam current is 1.7 A. The exposure time of the electron beam is not less than 0.1 ms. The vacuum vessel is made of stainless steel with the dimensions of 4 mm in wall thickness, 500 mm in inner diameter of the base, and 1000 mm

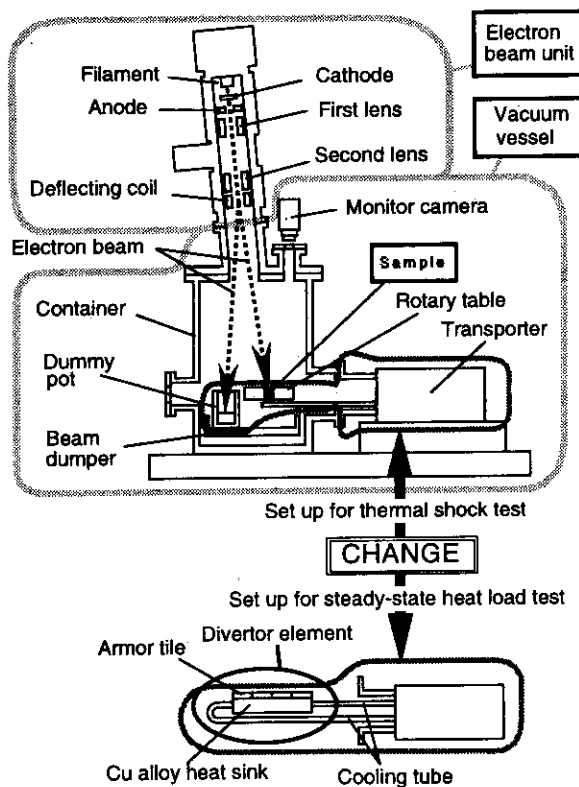
Fig. 4.6.3
Flow chart of reweldability test.



in height . At present, a thermal shock test has been set up for hot cells. The 11 samples for the thermal shock test can be placed on a rotary table in the vacuum vessel using the remote manipulators. The maximum sample dimensions is $\varnothing 25 \times 25 \times 30$ mm. The estimation items for the thermal shock tests are as follows.

- Weight loss of the sample by electron beam irradiation
- Surface morphology of the sample before and after electron beam irradiation
- Eroded or melted area on cross section of the sample after electron beam irradiation

Fig. 4.6.4
A schematic view of
OHBSIS



4.7. Development of high temperature shape memory alloys

TiPd based alloys are well known to be one of the hopeful high-temperature shape memory alloys (HTSMA)^[1,2]. Recently, transformation properties of these alloys have been extensively studied by electrical resistivity measurement^[3]. In our previous work, it is confirmed that the transformation temperatures vary in the wide temperature range by substituting palladium by transition metal such as chromium and that internal structure of the B19 (2H) martensite is characterized by {111}2H type twins^[4]. When the chromium content is less than 4at.% in Ti50Pd50-XCrX alloys, B2 to B19 (2H) transformation was found to exist^[3,4]. To develop the high-temperature shape memory alloys using TiPd based alloys, the detailed information is not yet obtained on deformation behavior at high temperatures. The effect of chromium addition on the deformation behavior at high temperatures is quite an important item to establish how to use these promising alloys in a high-temperature environment.

Mechanical tests were carried out to study the deformation behavior of HTSMA which can be used at temperatures above 573K. Furthermore, preliminary tests were also made to apply HTSMA to practical sealing plug for heat exchanger pipe of PWRs. From the experimental results, TiPd-Cr HTSMA reveals the high performance of shape recovery and pseudoelasticity. HTSMA can be useful by improvement of appropriate heat treatments and addition of the third element.

Experimental procedures are follows: ingots were prepared by arc melting under an argon atmosphere. The nominal composition of the alloys used is Ti50Pd50-XCrX (X = 0, 1, 2, 3, 4 at.%Cr). Specimens for DSC measurements and for tensile test were cut by spark-cut from the sheets at a thickness of 1.0mm, and then, were homogenized at 1373K for 600s and quenched into iced water without a crashing argon filled quartz capsule. Transformation temperatures were determined by DSC measurements. High-temperature

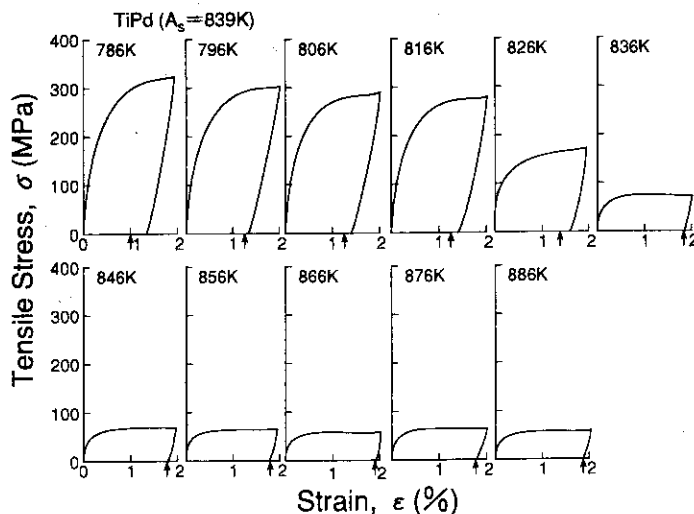


Fig. 4.7.1
Stress-strain curves
of TiPd alloy at
temperatures between
786K and 886K

tensile tests were carried out in a temperature range between (A_s-50K) and (A_s+50K) by using an MTS tensile machine. Specimens were heated by a conventional electric furnace with the argon flow system. Tensile stress was loaded until a strain of 2% was attained, and then, was unloaded and heated up to a temperature of (A_f+100K). Residual strain was determined after heating. Strain at high temperatures was measured by using an MTS type 632 High Temperature Extensometer.

Figure 4.7.1 shows stress-strain curves of TiPd alloy at temperatures between 786K and 886K. Specimens were heated about 100K above A_f ($A_f=869K$) after unloading. In the temperature region below A_s ($A_s=839K$), apparent yield stress decreased with increasing temperature. This negative temperature dependence of yield stress is due to the reorientation of several kinds of variants in martensites or the twinning deformation. At temperatures above 826K, the yield stresses abruptly fell down to about 80MPa and no positive temperature dependence of yield stress was observed at any temperatures above A_s . After unloading, it was seen that a substantial amount of the residual strain above 1.0% was found to exist as shown by arrow marks in Fig. 4.7.1. This may be attributed to a sort of stabilization of martensitic phase by recrystallization process at grain boundaries of parent phase.

Figure 4.7.2 shows stress-strain curves of the TiPd-2Cr alloy at temperatures between 716 and 816K. At temperatures of (A_s-40K) ($A_s=764K$), apparent yield stress showed a minimum of 100MPa. This minimum may not be due to the martensitic deformation. In a TiPd-2Cr alloy, the yield drop was pronounced at temperatures of 726K. Stress began to decrease and showed a typical high temperature deformation behavior, which was characterized by the negative temperature dependence of yield stress. The residual strain of a 2at.%Cr alloy decreased below 1% as compared with that of a 0 at.%Cr alloy (TiPd alloy). The yield stress showed around 120MPa above A_s ($A_s=766K$).

Fig. 4.7.2
Stress-strain curves
of TiPd-2Cr alloy at
temperatures between
716 and 816K

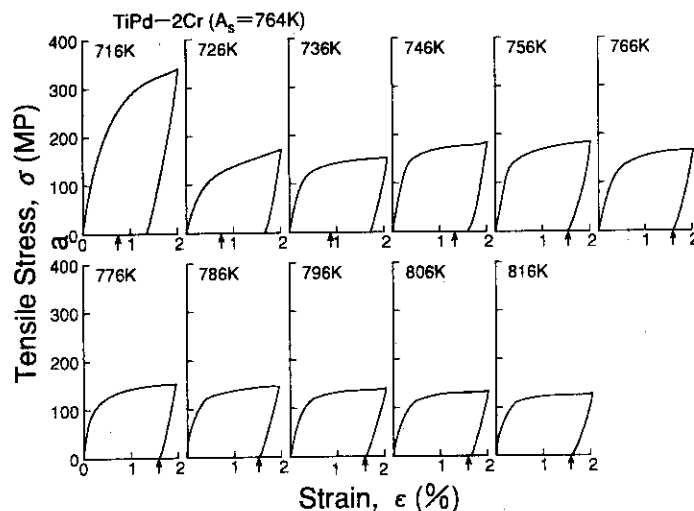


Figure 4.7.3 shows the stress-strain curves of the TiPd-4Cr alloy at temperatures between 546 and 645K. When the chromium content was increased to 4at.%, the positive temperature dependence of yield stress was confirmed at temperatures above A_s ($A_s=600K$). This temperature dependence was due to the formation of stress induced martensites. A slight amount of the residual strain around 0.3% was observed as shown in the figure. A small amount of the residual strain was reported in the solution treated TiNi alloys^[5]. In the present study, specimens were solution treated at 1373K. This residual strain can be explained by the stabilization of martensitic phase. This suggests that some kinds of thermomechanical treatments for TiPd based alloy are effective to improve the shape memory capabilities. No pseudoelasticity was observed during the tensile testing. In the preliminary study, it was considered that this was due to the artifact of the extensometer system of measurement of the strain at high temperature used. Thick specimens with a thickness of 6.0mm were used in compression tests and that a sort of retardation effect of pseudoelasticity was observed^[6]. It was thought that TiPd based alloys have a pseudoelastic effect at temperatures above A_f . In the present study, recoverable strain due to pseudoelasticity seem to exist, and may be counterbalanced out by the plastic strain which were caused by slip deformation at high temperatures.

Temperature dependence of the 0.2% offset stress in a TiPd based alloy is shown in Fig. 4.7.4. It is seen that TiPd-1Cr and TiPd-2Cr alloys are harder than TiPd-3Cr and TiPd-4Cr alloys below A_s . This indicates that reorientation of martensite variants does not occur for 1Cr and 2Cr alloys at these temperature region. In lower chromium content alloys (1Cr and 2Cr alloy), offset stresses abruptly decreased at temperatures between (A_s-20K) and A_s . This phenomenon is due to the slip deformation at high temperatures. In higher chromium content alloys (3Cr and 4Cr alloy), typical deformation process may take place on twinning deformation or reorientation of martensite variants.

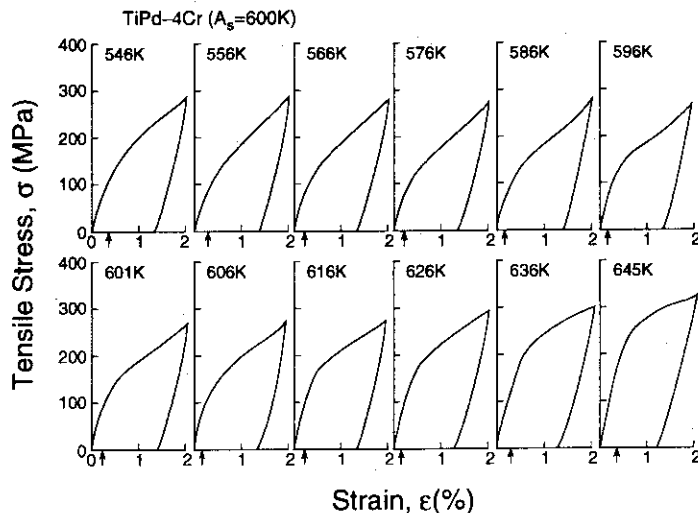


Fig. 4.7.3
Stress-strain curves
of TiPd-4Cr alloy at
temperatures between
546 and 645K

Above A_s , higher chromium content alloys showed a quite similar behavior in the temperature range of the offset stress as in the case of shape memory alloys. Whereas, lower chromium content alloys revealed the negative temperature dependence of offset stress and behaved plastically as in the case of high temperature slip deformation. These results suggest that the higher chromium content alloys have good properties regarding stress-induced transformation even at high temperatures above 600K. Solid solution hardening effect was observed with increasing chromium content up to 3at.%Cr. With further increasing to 4at.%Cr, offset stress decreases by a slight amount of stress. This would be attributed to structural changes in martensitic phase of 2H to (2H+9R) around 4at.%Cr content [4].

Recoverable strains as a function of (testing temperature- A_s) for Ti50Pd50-xCrX alloy are shown in Fig. 4.7.5. From the view point of the residual strain, recoverable strain depends on the amount of deformation. In the previous paper, a residual strain over 2% for TiPd based alloy did not recover completely when the specimen was heated up to A_f [6]. This may be due to the stabilization of martensites caused by heavy deformation in the thick specimens. In the present study, relative recoverable strain was determined as the ratio of amount of recovered strain divided by amount of applied initial strain (2%) that were measured after unloading and heating. Relative recoverable strains increased with

Fig. 4.7.4
0.2% offset stress versus (testing temperature- A_s) for Ti50Pd50-xCrX alloy

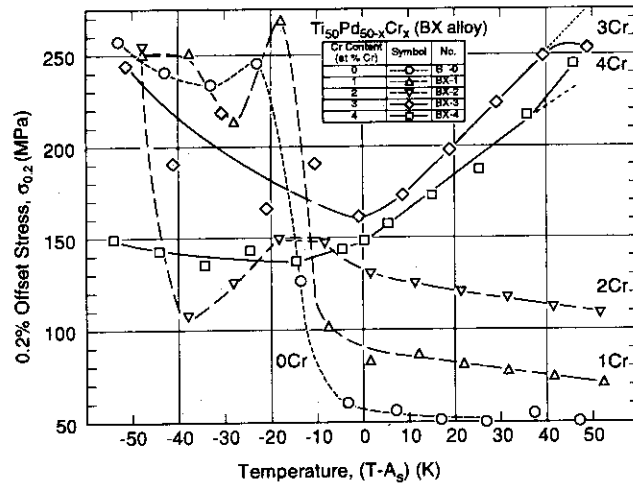
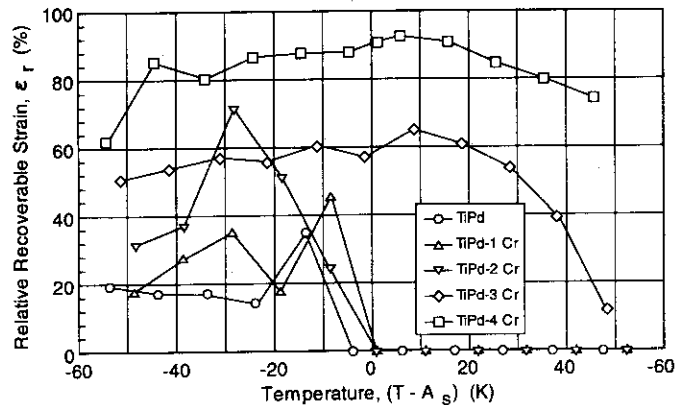


Fig. 4.7.5
Relative recoverable strain versus (testing temperature- A_s) for the Ti50Pd50-xCrX alloy



increasing chromium content.

At temperatures below A_s , the amount of shape recovery due to shape memory effect depends on chromium content. For higher chromium content alloys, relative recoverable strain attained a maximum of 60%. On the other hand, relative recoverable strains were lowered to values of 15 to 50% in the lower chromium alloys. Then, recoverable strain decreased suddenly at temperatures around A_s . When the temperature was increased over A_s , the higher chromium content alloy (TiPd-3Cr and TiPd-4Cr) behaved pseudoelastically. The recoverable strain due to pseudoelasticity began to fall from 60 to 45% (for TiPd-4Cr alloy) and from 52 to 15% (for TiPd-3Cr alloy) in a case that the temperature difference of $(T-A_s)$ was attained at 40K.

The above results suggest that the TiPd-Cr alloys reveal good properties of shape recovery although the additional thermo-mechanical treatment such as aging and rolling would be needed for improving the shape recovery due to shape memory effect and pseudoelasticity. It was concluded that the TiPd-Cr alloy has enough possibility as high temperature shape memory alloy if we choose a proper chromium content and a thermo-mechanical treatment.

REFERENCES

- [1] H. C. Donkersloot and J. H. N. Vucht, *J. Less Com. Met.*, 20(1970) 83.
- [2] K. Enami, K. Yoshida and S. Nenno, *Proc. Int. Conf. on Martensitic Transformations (ICOMAT-86)*, Japan Inst. Met., Nara, Japan, 1986, pp.103.
- [3] K. Enami, K. Kitano and K. Horii, *Proc. MRS Int. Mtg. on Advanced Materials*, Mater. Res. Soc., Tokyo, Japan, 1988, Vol.9, pp.117.
- [4] K. Enami, K. Horii and J. Takahashi, *ISIJ (Iron Steel Inst. Jap.) Int.*, 29(1989) 430.
- [5] T. Saburi, T. Tatsumi and S. Nenno, *J. de Phys (Suppl.)*, 43(1982) 261.
- [6] K. Enami, Y. Miyasaka and H. Takakura, *Proc. MRS Int. Mtg. on Advanced Materials*, Mater. Res. Soc., Tokyo, Japan, 1988, Vol. 9, pp.135.

5. Summary

This report describes the activities of the project of JMTR performed in the FY 1994. During this fiscal year, JMTR was operated nominally for 4 cycles. This is the first year in which all the operation cycles were carried out with the full installation of low enriched uranium fuel (LEU) core. LEU is the latest driver fuel of JMTR that has been developed to operate the reactor with the enrichment down to 20% under the circumstances of the non-proliferation policy of the country who supplies enriched uranium. The LEU manufacturing is running successfully employing two manufacturers.

The irradiation service was made mainly for satisfying the requirements from the laboratories inside JAERI. Nuclear fuels and materials were irradiated for the developments of LWR, FBR, HTTR and fusion reactor. Irradiation for RI production was performed constantly.

R&D works on irradiation and PIE technologies have been extensively carried out.

They are:

- Power ramping tests for LWR fuels for the studies of safety and high performance integrity.
- Assessment on the irradiation damage of an in-pile tube was performed by taking advantage of the surveillance test pieces that had been located in JMTR under irradiation fast neutron with fluence of 3×10^{25} n/m².
- Re-instrumentation technique has progressed by performing re-instrumentation of FP gas pressure gauge and thermocouple, then a dual re-instrumentation technique was demonstrated in a BOCA experiment.
- To study the mechanical properties on fracture of irradiated materials, a remote controlled SEM apparatus has been developed and installed in a hot cell. It greatly contributed to observe and analyze the broken surface of the test pieces.
- An examination technology with miniaturized specimens is under development taking irradiation by accelerator in scope. In this fiscal year, the SP (small punch) testing equipment was installed in a vacuum chamber to confirm the controllable temperature range on SP.
- New PIE facilities for fusion reactor development such as beryllium PIE facilities, reweldability testing facility and electron beam heating facility were installed in the Hot Laboratory, and the respective testing of a new type became enable.

6. Publications

REPORTS

1. Jun-94, Fission product behavior in Triso-coated UO₂ fuel particles, Shimizu, Tayama et al, Journal of Nuclear Materials 208(1994)266-281,
2. Jul-94, BEHAVIOR OF PRE-IRRADIATED FUEL UNDER A SIMULATED RIA CONDITION [RESULTS OF NSRR TEST JM-3], Sakai et al, JAERI-Research 94-006,
3. Sep-94, Development of sweep gas sensor with proton conduction, T.Sagawa et al., Tritium technology in fission, fusion and isotopic application,
4. Sep-94, Characteristics of Li₂O Pebble Fabricated by Melting Granulation Method, Tsuchiya et al., J. Nucl. Materials,
5. Sep-94, Lithium Reprocessing Technology for Ceramic Breeders, Tsuchiya et al., J. Nucl. Materials,
6. Dec-94, Irradiation induced stress relaxation and high temperature deformation behavior of neutron irradiated Ti based shape memory alloy., Hoshiya, Ando, J. Nucl. Mater., 212-215(1994)818,
7. Dec-94, Effects of neutron irradiation on deformation behavior in TiPd-Cr high temperature shape memory alloys., Hoshiya, Ando, Advanced Materials '93, V/B: Shape Memory Materials and Hydrides, edited by K.OTSUKA et al., Trans. Mat. Res. Soc. Jpn., Volume 18B, 1025 ,
8. Dec-94, Deformation behavior of TiPd-Cr high temperature shape memory alloys, Hoshiya, Advanced Materials '93, V/B: Shape Memory Materials and Hydrides, edited by K.OTSUKA et al et al., Trans. Mat. Res. Soc. Jpn., Volume 18B, 1013 ,
9. Dec-94, Development of controlled temperature-cycle irradiation technique in JMTR, T.Sagawa et al., J. Nucl. Mater. 212-215(1994)1665. ,
10. Dec-94, Development of experimental rigs for temperature-controlled reactor irradiations for fundamental study of radiation effects on fusion materials, T.Sagawa et al., J. Nucl. Mater. 212-215(1994)1645. ,,
11. Dec-94, Irradiation induced stress relaxation and high temperature deformation behavior of neutron irradiated Ti based shape memory alloys, Goto, Journal of Nuclear Materials 212-215 818-822 (1994),,
12. Dec-94, Annual report of JMTR, 1993, Dept. of JMTR, JAERI-Review 94-012 ,,
13. Mar-95, Trial fabrication and pre-liminary characterization of electrical insulator for liquid metal system, Nakamichi et al, JAERI-Tech 95-009,,
14. Mar-95, Joining technology development of advanced materials/SS304 by friction welding, Tsuchiya et al., JAERI-Tech 95-017,,

Contributions to conferences

1. May-93, Effects of Undercoating on Properties of Y₂O₃ Coating, Nakamichi et al, ITSC '95,
2. Apr-94, Irradiation Facilities for IASCC Related Studies at JMTR, Matsui et al, 10th ICG-IASCC Meeting(USA),
3. Aug-94, Shape memory characteristics of TiPd-X high temperature shape memory alloys, Hoshiya, Ando, Int. Conf. on Industrial Applications of Shape Memory Alloys (IA-SMA '94) Shape Memory Alloys Associ-18, Canada ,
4. Sep-94, Development of sweep gas sensor with proton conduction, T.Sagawa et al., Tritium technology in fission, fusion and isotopic application,
5. Sep-94, Tritium release from neutron-irradiated Li-LiAlO_2 pellet fabricated with lithium extracted from sea, Tsuchiya et al., Tritium technology in fission, fusion and isotopic application,
6. Sep-94, Preliminary characterization of Zr₉Ni₁₁ alloy as tritium getter for in-situ irradiation test, Imaizumi et al, Tritium technology in fission, fusion and isotopic application,
7. Sep-94, Trial Fabrication of Y₂O₃ Coating on 316SS, Nakamichi et al, ITSC '95,
8. Sep-94, The whole-core LEU silicide Fuel demonstration in the JMTR, Aso et al, 1994 RERTR,
9. Dec-94, Deformation behavior of TiPd-Cr high temperature shape memory alloys, Hoshiya, Advanced Materials '93, V/B: Shape Memory Materials and Hydrides, edited by K.OTSUKA et al et al., Trans. Mat. Res. Soc. Jpn., Volume 18B, 1013 ,
10. Feb-95, New radiographic testing technique using low energy gamma ray (Yb-169), Ooka et al, 13th Int. Conf. on NDE in the Nuclear and Pressure Vessel Industries,

7. Organization

